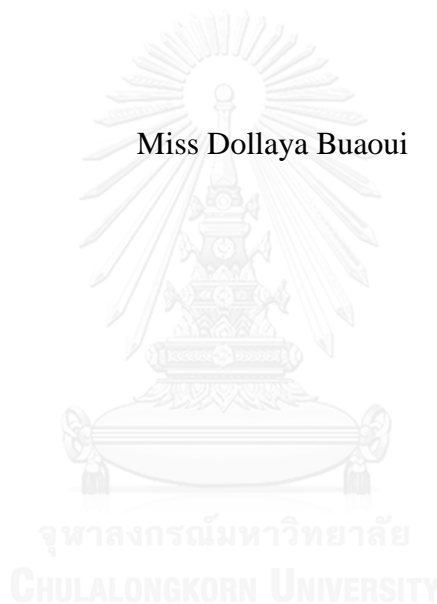


REMOVAL OF DISINFECTION BY-
PRODUCTS IN WATER BY ADSORPTION ON THIOL-
FUNCTIONALIZED MESOPOROUS MATERIAL CONTAINING IN ALGINATE
BEAD

Miss Dollaya Buaoui



บทคัดย่อและแฟ้มข้อมูลฉบับเต็มของวิทยานิพนธ์ตั้งแต่ปีการศึกษา 2554 ที่ให้บริการในคลังปัญญาจุฬาฯ (CUIR)
เป็นแฟ้มข้อมูลของนิสิตเจ้าของวิทยานิพนธ์ ที่ส่งผ่านทางบัณฑิตวิทยาลัย

The abstract and full text of theses from the academic year 2011 in Chulalongkorn University Intellectual Repository (CUIR)
are the thesis authors' files submitted through the University Graduate School.

A Thesis Submitted in Partial Fulfillment of the Requirements
for the Degree of Master of Science Program in Environmental Management
(Interdisciplinary Program)
Graduate School
Chulalongkorn University
Academic Year 2014
Copyright of Chulalongkorn University

การกำจัดสารพลอยได้จากกระบวนการฆ่าเชื้อโรคในน้ำโดยการดูดซับบนอัลจินเตชันชนิดเม็ดที่บรรจุ
ตัวกลางดูดซับชนิดเมโซพอร์สที่ต่อติดหมู่ไทออล



วิทยานิพนธ์นี้เป็นส่วนหนึ่งของการศึกษาตามหลักสูตรปริญญาวิทยาศาสตรมหาบัณฑิต
สาขาวิชาการจัดการสิ่งแวดล้อม (สหสาขาวิชา)
บัณฑิตวิทยาลัย จุฬาลงกรณ์มหาวิทยาลัย
ปีการศึกษา 2557
ลิขสิทธิ์ของจุฬาลงกรณ์มหาวิทยาลัย

Thesis Title	REMOVAL OF DISINFECTION BY-PRODUCTS IN WATER BY ADSORPTION ON THIOL-FUNCTIONALIZED MESOPOROUS MATERIAL CONTAINING IN ALGINATE BEAD
By	Miss Dollaya Buaoui
Field of Study	Environmental Management
Thesis Advisor	Aunnop Wongrueng, Ph.D.
Thesis Co-Advisor	Associate Professor Patiparn Punyapalakul, Ph.D.

Accepted by the Graduate School, Chulalongkorn University in Partial Fulfillment of the Requirements for the Master's Degree

..... Dean of the Graduate School
(Associate Professor Sunait Chutintaranond, Ph.D.)

THESIS COMMITTEE

..... Chairman
(Assistant Professor Srilert Chotpantarat, Ph.D.)

..... Thesis Advisor
(Aunnop Wongrueng, Ph.D.)

..... Thesis Co-Advisor
(Associate Professor Patiparn Punyapalakul, Ph.D.)

..... Examiner
(Associate Professor Chawalit Ngamcharussrivichai, Ph.D.)

..... External Examiner
(Panida Prarat, Ph.D.)

คลญา บัวอูย : การกำจัดสารพลอยได้จากกระบวนการฆ่าเชื้อโรคในน้ำโดยการดูดซับบนอัลจินตชนิดเม็ดที่บรรจุตัวกลางดูดซับชนิดเมโซพอร์รัสที่ต่อติดหมู่ไทออล (REMOVAL OF DISINFECTION BY-PRODUCTS IN WATER BY ADSORPTION ON THIOL-FUNCTIONALIZED MESOPOROUS MATERIAL CONTAINING IN ALGINATE BEAD) อ.ที่ปริกษาวิทยานิพนธ์หลัก: อ. ดร. อรรณพ วงศ์เรือง, อ.ที่ปริกษาวิทยานิพนธ์ร่วม: รศ. ดร. ปฎิภาณ ปัญญาพลกุล, 100 หน้า.

งานวิจัยนี้มีจุดประสงค์เพื่อศึกษากลไกการดูดซับสารพลอยได้จากกระบวนการกำจัดสารพลอยได้จากกระบวนการฆ่าเชื้อโรคในน้ำ (DBPs) ประกอบด้วยสารกลุ่มฮาโลอะซิโตไนไตรล์ (HANs), ไตรฮาโลมีเทน (TCM), ฮาโลคีโตน(HK), และฮาโลอะซิติกแอซิด (HAAs) โดยการดูดซับบนอัลจินตชนิดเม็ดที่บรรจุตัวกลางดูดซับชนิดเมโซพอร์รัสที่ต่อติดหมู่ไทออล(AL:NR/HMS-SH) เปรียบเทียบกับถ่านกัมมันต์ชนิดเกล็ด (GAC) ในงานวิจัยนี้ได้ทำการสังเคราะห์ตัวกลางดูดซับโดยผ่านกระบวนการโซเจลและตรวจสอบคุณสมบัติทางกายภาพของตัวดูดซับด้วยเทคนิคต่างๆ เช่น XRD และ FT-IR จากนั้นทำการศึกษากลไกการดูดซับแบบจลนพลศาสตร์และไอโซเทอมของ DBPs ผลที่ได้นำไปศึกษากลไกที่เกิดขึ้นโดยอาศัยแบบจำลองการดูดซับแบบต่างๆ จากผลการศึกษาการดูดซับแบบโคเนติกของ DBPs บนตัวกลางดูดซับทั้งสองชนิดพบว่าไตรคลอโรมีเทน (TCM) สามารถถูกดูดซับได้ดีกว่าไตรคลอโรอะซิโตไนไตรล์ (DCAN) และไตรคลอโรอะซิโตน (TCA) ตามลำดับ และในการศึกษาการดูดซับแบบไอโซเทอมพบว่าการดูดซับ DBPs ชนิดที่มีความสามารถในการละลายน้ำได้น้อยจะสามารถถูกดูดซับได้ดีกว่าชนิดละลายน้ำได้บนตัวกลางดูดซับทั้งสองชนิด นอกจากนี้ยังพบว่าการดูดซับของ DBPs แต่ละชนิดมีประสิทธิภาพลดลงในระบบที่มีการปรากฏของ DBPs ชนิดอื่นๆรวมอยู่ด้วย

นอกจากนี้งานวิจัยนี้ได้ทำการศึกษาผลกระทบของสารอินทรีย์ที่ปรากฏในน้ำชนิดละลายน้ำได้และชนิดไม่ละลายน้ำที่ต่อประสิทธิภาพการดูดซับของ DBPs ชนิด DCAN พบว่าสารอินทรีย์ชนิดไม่ชอบน้ำจะส่งผลกระทบต่อความสามารถในการดูดซับของ DCAN บนตัวดูดซับที่สังเคราะห์ได้มากกว่าสารอินทรีย์ชนิดที่ชอบน้ำโดยอาจเกิดจากการไปขัดขวางพื้นที่การดูดซับบนพื้นผิวตัวกลางดูดซับทำให้สามารถดูดซับ DCANซึ่งเป็นสารที่ละลายน้ำได้น้อยมีประสิทธิภาพการดูดซับลดลง จากนั้นได้ทำการศึกษากลไกการดูดซับของ DCAN บนตัวดูดซับที่สังเคราะห์ได้ในระบบคอลัมน์พบว่าในระบบที่มีปริมาตรของตัวการดูดซับมากกว่าจะมีค่าความสามารถในการดูดซับและเวลาที่เบรคทลูเพิ่มขึ้น

สาขาวิชา การจัดการสิ่งแวดล้อม
ปีการศึกษา 2557

ลายมือชื่อนิสิต
ลายมือชื่อ อ.ที่ปริกษาหลัก
ลายมือชื่อ อ.ที่ปริกษาร่วม

5687531220 : MAJOR ENVIRONMENTAL MANAGEMENT

KEYWORDS: ADSORPTION / HEXAGONAL MESOPOROUS SILICATE / DISINFECTION BY PRODUCTS (DBPS)

DOLLAYA BUAOUI: REMOVAL OF DISINFECTION BY-PRODUCTS IN WATER BY ADSORPTION ON THIOL-FUNCTIONALIZED MESOPOROUS MATERIAL CONTAINING IN ALGINATE BEAD. ADVISOR: AUNNOP WONGRUENG, Ph.D., CO-ADVISOR: ASSOC. PROF. PATIPARN PUNYAPALAKUL, Ph.D., 100 pp.

The purpose of this research was to examine adsorption mechanism of DBPs including haloacetonitrile, trihalomethane, halogenated ketone, and haloacetic acid on thiol-functionalized hexagonal mesoporous silicates based on natural rubber containing with alginate bead adsorbent (AL:NR/HMS-SH) comparing with granular activated carbon (GAC). First, NR/HMS-SH was synthesized via in-situ sol-gel method, and then was prepared into beads form in calcium chloride solution. The synthesized material was characterized the physicochemical properties by various techniques such as Fourier-transform infrared spectroscopy (FT-IR), X-ray diffraction (XRD), and N₂ adsorption-desorption isotherm. The adsorption kinetics and adsorption isotherms were studied to examine the adsorption mechanism under batch condition. According to the kinetic study, the adsorption rate and capacity of both adsorbent exhibited the higher amount on trichloromethane (TCM) than dichloroacetonitrile (DCAN) and 1,1,1-trichloroacetone (TCA) respectively. The adsorption isotherm models including Linear, Langmiur, and Fruendlich models were estimated to examine the adsorption mechanism on adsorption isotherm study. It found that the lower water solubility DBPs which had high hydrophobicity showed higher adsorption capacity than the higher water solubility DBPs. In addition, the present of other DBPs species in the solution as mixture affected to the adsorption efficiencies of each DBP.

Moreover, this research investigated the effect of natural organic matter (NOM) including hydrophilic-like (HPI) and hydrophobic-like (HPO) natural organic matter on DCAN adsorption on synthesized adsorbent. The results appeared that the adsorption of DCAN on synthesized adsorbent was affected by HPO NOM more than HPI NOM by reducing the adsorption capacity of DCAN due to the competitive adsorption on adsorbent surface.

The adsorption of DCAN on fixed bed condition was investigated by varying bed depth. It revealed that the breakthrough time at breakthrough concentration increased with increasing of bed volume. This might because the higher of bed volume had more available sorption site for particle to be adsorbed.

Field of Study: Environmental Management

Academic Year: 2014

Student's Signature

Advisor's Signature

Co-Advisor's Signature

ACKNOWLEDGEMENTS

Firstly, I would like to express my sincere gratitude to my advisor and co-advisor; Dr.Aunnop Wongrueng and Assoc.Prof.Dr.Patiparn Punyapalakul for their continuous support and helpful suggestion.

Moreover, I would like to represent my appreciate to Asst.Prof.Dr. Srilert Chotpantarat, Chairman and Assoc.Prof.Dr. Chawalit Ngamcharussrivichai and Dr. Panida Prarat members of my thesis committee for their useful and valuable comments.

I am grateful for the financial support from the Center of Excellence on Hazardous Substance Management, Chulalongkorn University. This research was supported by the National Research University Project, Office of higher Education Commission (WCU-014-FW-57). This work was proceeded as part of the research cluster “Fate and Removal of Emerging Micropollutants in Environment” and conducted under the research program “Control of Residual Hormones and Antimicrobial Agents from Aquacultural and Feedstock Industry” granted by the Center of Excellence on Hazardous Substance Management (HSM) and Special Task Force for Activating Research (STAR), from Chulalongkorn University. I also gratefully acknowledge technician support from Department of Environmental Engineering, Faculty of Engineering and the Center for Petroleum, Petrochemicals and Advanced Materials, Chulalongkorn University. In addition, I would like to be thankful for Department of Environmental Engineering, Faculty of Engineering Chaing Mai University for their technician support.

Finally, I would like to appreciate my family for their support and encouragement. Furthermore, I would like to thanks for my friends and my seniors for their favorable help.

CONTENTS

	Page
THAI ABSTRACT	iv
ENGLISH ABSTRACT.....	v
ACKNOWLEDGEMENTS.....	vi
CONTENTS.....	vii
ABBREVIATION.....	ix
LIST OF FIGURE.....	x
LIST OF TABLE.....	xii
CHAPTER 1 INTRODUCTION	1
1.1 STATE OF PROBLEM.....	1
1.2 OBJECTIVES.....	3
1.3 HYPOTHESIS.....	3
1.4 SCOPE OF THE STUDY.....	4
CHAPTER 2 THEORETICAL BACKGROUND AND LITERATURE REVIEWS.....	7
2.1 NATURAL ORGANIC MATTER.....	7
2.2 DISINFECTION BY PRODUCTS.....	8
2.3 HEXAGONAL MESOPOROUS SILIGATE.....	10
2.4 SURFACE MODIFICATION OF ADSORBENT.....	11
2.5 ADSORPTION THEORY.....	13
2.6 LITERATURE REVIEWS.....	18
CHAPTER 3 METHODOLOGY.....	22
3.1 MATERIALS.....	22
3.2 PREPARATION OF ADSORBENT.....	24
3.3 CHARACTERIZATION OF ADSORBENT.....	25
3.4 ANALYTICAL METHOD.....	25
3.5 FRACTIONATION OF NATURAL ORGANIC MATTER (NOM).....	27
3.6 ADSORPTION EXPERIMENTALS.....	27
CHAPTER 4 RESULTS AND DISCUSSION.....	31

	Page
4.1 MATERIAL CHARACTERIZATION	31
4.1.1 X-Ray Diffraction.....	31
4.1.2 Surface area and pore structure by N ₂ adsorption-desorption isotherm...32	32
4.1.3 Surface functional group by FT-IR	34
4.1.4 CHNS Elemental analyzer.....	35
4.1.5 Scanning electron microscopy (SEM).....	35
4.1.6 Surface charge density.....	36
4.2 ADSORPTION OF DBPs ON NR/HMS-SH CONTAINING ALGINATE BEAD AND GAC	37
4.2.1 Adsorption kinetic	37
4.2.2 Intraparticle diffusion	44
4.2.3 Adsorption isotherm model	48
4.3 SELECTIVITY OF ADSORPTION	60
4.4 EFFECT OF NOM ON DBPS ADSORPTION	61
4.5 ADSORPTION ON FIXED BED CONDITION	64
CHAPTER 5 CONCLUSIONS	66
5.1 CONCLUTIONS	66
5.2 RECOMMENDATIONS.....	67
REFERENCES	68
APPENDIX.....	73
VITA.....	100

ABBREVIATION

AL:NR/HMS-SH	Thiol-functionalized hexagonal mesoporous silicates based on natural rubber containing with alginate bead adsorbent
C-DBPs	Carbonaceous disinfection by product
DBPs	Disinfection by products
DCAA	Dichloroacetic acid
DCAN	Dichloroacetoneitrile
DOC	Dissolve organic carbon
DON	Dissolve organic nitrogen
GAC	Granular activated carbon
HAAs	Haloacetic acids
HANs	Haloacetoneitriles
HKs	Halogenated ketones
HMS	Hexagonal mesoporous silica
HPI NOM	Hydrophilic natural organic matter
HPO NOM	Hydrophobic natural organic matter
IS	Ionic strange
MCAA	Monochloroacetic acid
MCAN	Monochloroacetoneitrile
N-DBPs	Nitrogenous disinfection by products
NOM	Natural organic matter
NR	Natural rubber
NR/HMS-SH	Thiol-functionalized hexagonal mesoporous silicates based on natural rubber
PAC	Powder activated carbon
TCA	1,1,1-trichloroacetone
TCAA	Trichloroacetic acid
TCAN	Trichloroacetoneitrile
TCM	Trichloromethane
THM	Trihalomethane
TOC	Total organic carbon
TW	Tap water

LIST OF FIGURE

Figure 1.1	Scope of this study.....	6
Figure 3.1	The fixed bed adsorption experiment	30
Figure 4.1	XRD pattern of AL:NR/HMS-SH	31
Figure 4.2	N ₂ adsorption-desorption isotherms of NR/HMS-SH, AL:NR/HMS-SH and GAC. Closed and opened symbols presented N ₂ adsorption and N ₂ desorption respectively.....	32
Figure 4.3	Types of isotherm shapes by IUPAC classification	33
Figure 4.4	FTIR spectra of AL:NR/HMS-SH.....	34
Figure 4.5	(A, B) show SEM images of AL: NR/HMS-SH (60x and 500x), and(C, D) show SEM images of cross-sectional view of AL: NR/HMS-SH (500x and 2500x).....	35
Figure 4.6	Surface charge density of AL:NR/HMS-SH and GAC	36
Figure 4.7	Kinetics adsorption of DCAN on AL:NR/HMS-SH and GAC at 200 µg L ⁻¹ (pH 7 and IS 10 mM).....	38
Figure 4.8	Kinetics adsorption of TCM on AL:NR/HMS-SH and GAC at 200 µg L ⁻¹ (pH 7 and IS 10 mM).....	40
Figure 4.9	Kinetics adsorption of TCA on AL:NR/HMS-SH and GAC at 200 µg L ⁻¹ (pH 7 and IS 10 mM).....	41
Figure 4.10	Kinetics adsorption of DCAA on AL:NR/HMS-SH and GAC	43
Figure 4.11	Plot of intraparticle diffusion model of DCAN adsorption on AL:NR/HMS-SH and GAC.....	45
Figure 4.12	Plot of intraparticle diffusion model of TCM adsorption on NR/HMS-SH containing alginate bead and GAC	46
Figure 4.13	Plot of intraparticle diffusion model of TCA adsorption on	47
Figure 4.14	Isotherms adsorption of MCAN, DCAN and TCAN on AL:NR/HMS-SH and GAC (pH 7 and IS 10 mM)	50
Figure 4.15	Comparison of the MCAN, DCAN and TCAN adsorption experimental data and the data from predicted model on AL:NR/HMS-SH and GAC at pH 7 with IS 10 mM.....	51
Figure 4.16	Isotherms adsorption of TCM on AL:NR/HMS-SH and GAC	53

Figure 4.17	Comparison of the TCM adsorption experimental data and the data from predicted model on AL:NR/HMS-SH and GAC at pH 7 with IS 10 mM.....	54
Figure 4.18	Isotherms adsorption of TCA on AL:NR/HMS-SH and GAC (pH 7 and IS 10 mM).....	55
Figure 4.19	Comparison of the TCM adsorption experimental data and the data from predicted model on AL:NR/HMS-SH and GAC at pH 7 with IS 10 mM.....	55
Figure 4.20	Isotherms adsorption of CAA, DCAA and TCAA on AL:NR/HMS-SH and GAC (pH 7 and IS 10 mM)	57
Figure 4.21	Comparison of the HAAs adsorption experimental data and the data from predicted model on AL:NR/HMS-SH and GAC at pH 7 with IS 10 mM.....	59
Figure 4.22	Adsorption isotherms of four-DBPs as a single solute and mixed solute on AL:NR/HMS-SH and GAC at pH 7 with IS 10 mM	60
Figure 4.23	Effect of NOM on DCAN adsorption capacity on AL:NR/HMS-SH	61
Figure 4.24	Concentration of NOM in Tab water before and after adsorption of DCAN on AL:NR/HMS-SH.....	62
Figure 4.25	Concentration of hydrophilic NOM before and after adsorption of DCAN on AL:NR/HMS-SH.....	63
Figure 4.26	Concentration of hydrophobic NOM before and after adsorption of DCAN on AL:NR/HMS-SH.....	63
Figure 4.27	Breakthrough curve of DCAN adsorption on AL:NR/HMS-SH with various bed volume.....	64

LIST OF TABLE

Table 2.1	Physicochemical properties of DBPs that used in this study.....	9
Table 3.1	Characterization of NR/HMS-SH containing alginate bead.....	25
Table 4.1	Mean pore diameter, pore volume, and BET surface area of AL:NR/HMS-SH and GAC.....	33
Table 4.2	Sulfur content of AL:NR/HMS-SH.....	35
Table 4.3	Parameters of dichloroacetonitrile (DCAN) kinetic adsorption on AL:NR/HMS-SH and GAC using the pseudo-first order and pseudo-second order kinetic models	39
Table 4.4	Parameters of TCM kinetic adsorption on AL:NR/HMS-SH and GAC using the pseudo-first order and pseudo-second order kinetic models.....	40
Table 4.5	Parameters of 1, 1, 1-trichloroacetone (TCA) kinetic adsorption on AL:NR/HMS-SH and GAC using the pseudo-first order and pseudo-second order kinetic models	42
Table 4.6	Kinetic parameters of DCAN adsorption on AL:NR/HMS-SH and GAC using the intraparticle diffusion model.	46
Table 4.7	Kinetic parameters of TCM adsorption on AL:NR/HMS-SH and GAC using the intraparticle diffusion model	47
Table 4.8	Kinetic parameters of TCA adsorption on AL:NR/HMS-SH and GAC using the intraparticle diffusion model	48
Table 4.9	Parameters of HANs isotherm adsorption on AL:NR/HMS-SH and GAC.....	52
Table 4.10	Parameters of TCM isotherm adsorption on NR/HMS-SH containing in alginate bead and GAC.....	54
Table 4.11	Parameters of TCA isotherm adsorption on AL:NR/HMS-SH and GAC.....	56
Table 4.12	Parameters of HAAs isotherm adsorption on AL:NR/HMS-SH and GAC.....	58
Table 4.13	Parameters of various bed volume of AL:NR/HMS-SH for DCAN adsorption in fixed bed condition	65

Table 4.14 Parameters of the breakthrough curve models for DCAN adsorption on NR/HMS-SH containing in alginate bead in fixed bed condition65



CHAPTER 1

INTRODUCTION

1.1 STATE OF PROBLEM

Nowadays, water pollution is a major global crisis because water is a basic necessity that human use in their daily life. Moreover, the water pollution can cause the health disease. Dissolve organic matter including organic carbon (DOC) and organic nitrogen (DON) that presented in aquatic system can form disinfection by-products (DBPs) when reacted with disinfectants especially chlorine. These DBPs are classified as genotoxic and carcinogenic compounds that affected to human health. Moreover, the toxicity of nitrogenous-disinfection by products (N-DBPs) was reported that show higher toxicity than carbonaceous disinfection by products (C-DBPs) to mammalian cells. Therefore, N-DBPs are important for researchers to concern about their toxic since the beginning of their formation, for example during the disinfection process of drinking water and wastewater treatment. Halogenated acetonitrile group is one of N-DBPs that are focusing on due to its high toxicity. Moreover, there were some other species of DBPs that were discovered and found that they have high toxic with lower amount, and there was not famous to study such as halogenated ketone. However, trihalomethane and chloroacetic acid are the major types of DBPs that presented in water system and they are regulated into the EPA regulation. Therefore, this research focused on the treatment of these DBPs from water.

The physical and chemical methods were used to treat contaminated water including coagulation, oxidation, membrane filtration and adsorption process. However, the technique which has been popular is adsorption technique due to its simplicity and low cost. There are many adsorbents were used in the treatment process such as activated carbon, mesoporous porous materials. Hexagonal mesoporous silicate (HMS) has been promoted to use because of its high surface area, large pore volume and wide pore size distribution. Moreover, the functionalized modification on surface of mesoporous material has been popular to improve the surface properties such as hydrophilic and hydrophobic properties, and higher selectivity. Furthermore, there are using polymer to support the mesoporous silica material to increase pH stability, hydrophobicity and chemical functional group. Natural rubber (NR) which is a hydrophobic polymer has been attempted to modify the properties of adsorbent. Moreover, the improvement of HMS surface with thiol (-SH) functionalized groups has been applied to enhance the selectivity and adsorption capacity of the adsorbent. Alginate, a component of algae cell wall, is a natural anionic polymer that has been widely used as a biomolecule immobilization and metal chelator. Alginic acid has the hydroxyl and carboxyl groups that can complex with cation such as metal. Alginates are the composite of β -D-mannuronic acid and α -L-guluronic acid which produce viscous hydrogel by association with divalent cation compounds such as Ca^{2+} . Accordingly, NR/HMS-SH immobilized with calcium alginate beads are applied to use for remove the organic pollutants such as disinfection by products.

Therefore, this study investigated the efficiency of DBPs adsorption by NR/HMS-SH containing alginate bead using batch adsorption experiment and be

apply to design the fixed bed adsorption. The adsorption kinetics, adsorption isotherms were studied to examine the adsorption mechanism. Furthermore, it found that natural organic matters (NOM) that occurred in water system might affect to the adsorption capacity for DBPs. The NOM affection on DBPs adsorption was studied by adding hydrophilic and hydrophobic NOM into the solution. However, there were various species of DBPs occurred in the real system. Thus, this research investigated the selectivity adsorption of each DBPs on synthesized material when they are amount other competitive DBPs.

1.2 OBJECTIVES

1. To synthesis and characterize NR/HMS-SH containing in alginate beads adsorbent.
2. To investigate the adsorption efficiency of DBPs on NR/HMS-SH containing alginate adsorbent by batch system.
3. To investigate effect of hydrophilic-like and hydrophobic-like natural organic matters on DBPs adsorption in tap water.
4. To investigate the adsorption selectivity of DBPs on synthesized adsorbent in the competitive encounter of other DBPs species under mixture solution.

1.3 HYPOTHESIS

1. The adsorption efficiency of DBPs on NR/HMS-SH containing alginate bead depend on hydrogen bonding, hydrophobic interaction, or electrostatic interaction between organic functional group of adsorbent or polymer that modified the adsorbent and adsorbate.

2. Hydrophobic and hydrophilic character of natural organic matter that presented in the water affect to the adsorption capacity due to the competition of adsorbent surface.

1.4 SCOPE OF THE STUDY

1.4.1 Synthesis of adsorbent

Adsorbent that used in this study was NR/HMS-SH containing in alginate bead that can synthesis via co-condensation method. The adsorption studies were compared with the adsorption on granular activated carbon (GAC).

1.4.2 Characterization of adsorbent

The physicochemical properties of the synthesized adsorbent such as pore volume, surface area, surface functional group, and surface charge density were characterized by using various physical and chemical techniques.

1.4.3 DBPs that used for this study

Four types of DBPs were used in this research including Haloacetonitriles (HANs), Halogenated methane (THM), Halogenated ketone (HK), and Haloacetic acids (HAAs). Monochloroacetonitrile (MCAN), dichloroacetonitrile (DCAN), and trichloroacetonitrile (TCAN) were used as a model of HANs to examine the adsorption capacity and mechanism. Trichloromethane was used as a model of THMs; Monochloroacetic acid (MCAA), dichloroacetic acid (DCAA), and trichloroacetic acid (TCAA) were used as a model of HAAs; and 1,1,1-Trichloroacetone (TCA) was a model of halogenated ketone to examine the adsorption capacity and mechanism.

1.4.4 Adsorption experiment

The adsorption experiments were investigated under batch condition. Adsorption kinetic experiments were investigated by varying contact time from 0 to 24 hours. The adsorption models including the pseudo-first-order, the pseudo-second-order and the intraparticle diffusion models were applied to analyze the adsorption rate and mechanisms.

Adsorption isotherm studies were investigated by varying concentration of the DBPs solution. The adsorption isotherm models i.e. Linear, Langmuir, and Freundlich isotherm model were calculated to determine the adsorption mechanism.

1.4.5 Selectivity adsorption

The selectivity adsorption of four types of DBPs on synthesized adsorbent in mixed solution was investigated and compared with the adsorption capacity of single solution.

1.4.6 Study of NOM effect on adsorption

The organic matters in water supply system (Bangkok Metropolitan Authority's area) were fractionated into two parts including hydrophilic and hydrophobic group and were studied the effect on adsorption capacity.

1.4.7 Fixed bed adsorption

The adsorptions of DCAN on synthesized adsorbent were investigated under fixed bed condition by varying bed depth. The collected data was calculated and analyzed by Thomas model to determine the adsorption mechanism.

The experiment framework of this study is showed in Figure 1.1

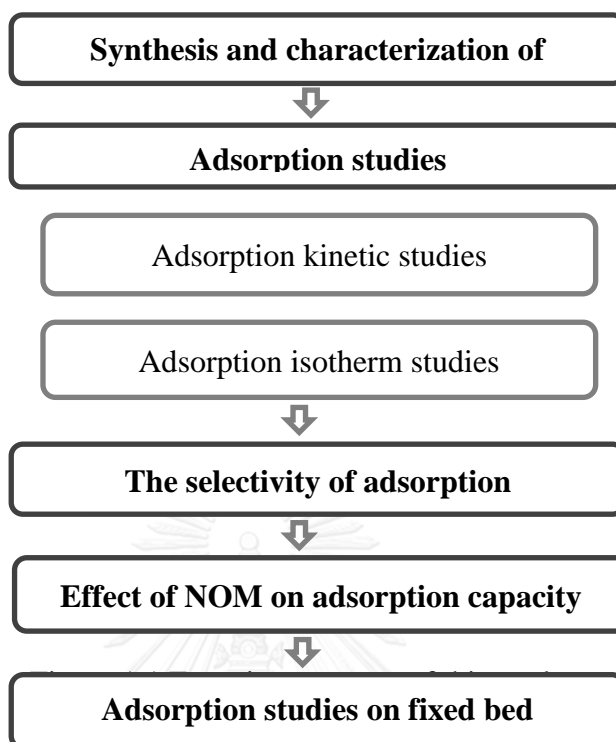


Figure 1.1 Scope of this study

CHAPTER 2

THEORETICAL BACKGROUND AND LITERATURE REVIEWS

2.1 NATURAL ORGANIC MATTER

Natural organic matter (NOM) that appears in water sources result from degradation of some natural materials in watersheds such as products of decomposed plant and animal residues (Water Research Foundation, 2009).

Aquatic NOM that is a mixture of heterogeneous organic compounds was varying in size, structure, and functionality. It can be separated the NOM into more homogeneous groups based on different chemical or physical properties such as hydrophobicity and molecular size (Hua & Reckhow, 2007). It may help water utilities treatment systems to remove these fractions by separating these compounds into group of hydrophilic behaviors based on adsorption relevance for synthetic resins (for example XAD-8 and XAD-4) (Jerry A. Leenheer & Westerhoff, 2007). NOM can be characterized by separating into different fractions that can classify into the hydrophobic-like and hydrophilic-like NOM.

Organic nitrogen compounds are a small fraction (0.5% to 10% by weight) of natural organic matter. There are some problems during their treatment process such as they can cause the growth or regrowth of bacteria, and membrane fouling. Moreover they can form disinfection by products precursors (Jean-Philippe Croue'). Moreover, it can be possible to affect the adsorption capacity of the adsorbate due to its hydrophilic and hydrophobic characters.

2.2 DISINFECTION BY PRODUCTS

Disinfection by products (DBPs) is a group of contaminants in water that was formed during the disinfection process. Several of DBPs are formed by the reactions of NOM precursors and disinfectant such as chlorine and chloramine. DBP formation depends on many factors including the types of disinfectants, disinfectant dosages, and water quality characteristics such as pH and concentration of natural organic material (NOM) that occur in the water (USEPA, 1992). The previous study found that the organic compounds which presented in different water sources displayed in different activities with chlorine, this might affected to the different characteristics for the DBPs formation.

World Health Organization (WHO) reported that close to billion people in the world still defaulted of safe drinking water consumption, and there are some questions about health effects from chlorine by products formed during the disinfection. Human are exposed to DBPs through drinking water and oral, dermal, and inhalation contact with chlorinated water. According to WHO, there are the regulation of THMs and HAAs in drinking water, however there is no about HANs and others. However, HANs have been considered in The US Environmental Protection Agency Information Collection Rules and they might be set on EPA regulation in the future.

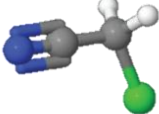
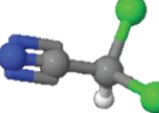
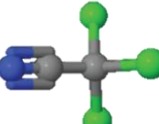
As previously, most researches have focused on carbonaceous disinfection by products (C-DBPs) which resulting from chlorination of natural organic matters (NOM), because carbon based DBPs are the largest fraction (Muellner et al., 2007). However, nitrogenous disinfection by products (N-DBPs) at lower concentration are more toxic than C-DBPs (Muellner et al., 2007; Plewa et al., 2004). The toxicity of N-DBPs was reported that show much cytotoxicity and genotoxicity than C-DBPs to

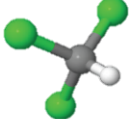
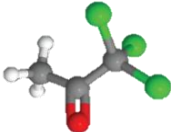
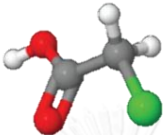
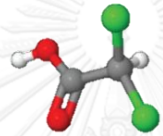
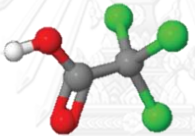
mammalian cells (Hou et al., 2012). Therefore, N-DBPs are important for researchers to concern about their toxic since the beginning of their formation, for example during the disinfection process of drinking water and wastewater treatment (W. Lee et al., 2007).

Several researches has identified the treatment alternatives for control of DBPs by removing of NOM prior to disinfection, use of alternative oxidants or disinfectants that do not create DBP at levels considered adverse to human health, removal of DBPs after they are formation. The alternative techniques were used for remove DBPs such as adsorption on activated carbon (Hsin Hsin Tung, 2006; H. Kim et al., 2002), coagulation (Zehra Yigit, 2009), ozone oxidation (Amy et al., 1991), membrane filtration (Cho et al., 1991), adsorption on functionalized silica-based porous material (Prarat et al., 2011)

2.2.1 Physicochemical properties of DBPs

Table 2. 1Physicochemical properties of DBPs that used in this study

DBPs	Molecular structure	Molecular weight	Water solubility (g/L)	pKa
Monochloroacetonitrile (MCAN)		75.50	> 100	-
Dichloroacetonitrile (DCAN)		109.94	33.5	-
Trichloroacetonitrile (TCAN)		144.39	< 1	-

DBPs	Molecular structure	Molecular weight	Water solubility (g/L)	pKa
Trichloromethane (TCM)		119.37	7.95	-
1,1,1-trichloroacetone (TCA)		161.41	7.45	-
Monochloroacetic acid (MCAA)		94.49	Very soluble	2.86
Dichloroacetic acid (DCAA)		128.94	86.3	1.26
Trichloroacetic acid (TCAA)		163.39	13	0.51

2.3 HEXAGONAL MESOPOROUS SILICATE

In the past decade, the successful synthesis of hexagonal mesoporous silica (HMS) with sponge-like framework structures has been reported. It has been widely used in advanced catalysis, and adsorption application due to its high surface area, large pore volume, and a narrow pore size distribution (Mercier et al., 1997). In addition, HMS has a thicker silica framework comparing with other mesoporous silica materials that represent to a high thermal stability. Moreover, the amine surfactants which used as templates are cheaper, and can be simply removed by extraction using

a solvent, such as acidic water and ethanol. The advantages make HMS attractive for many applications.

Chemical and physical modifications of the HMS surface have been promoted to prepare materials properties for adsorption and catalysis to provide the specific application such as hydrophobicity, thermal and structural stability.

There are two general procedures to chemical modification on the surface properties of mesoporous silica materials, included co-condensation method and post-grafting method. The co-condensation method which is a one-step procedure that has a better control for organic loading and organo-functional groups distribution; however, it can create less ordered of mesoporous structures materials (Athens et al., 2009). The post grafting method can prepare well-ordered functionalized mesoporous materials, but it often results in non-uniformly distribution of organic group. In addition, the functionalized materials by these modification methods receive a loss of surface area, pore size and pore volume.

2.4 SURFACE MODIFICATION OF ADSORBENT

2.4.1 Mesoporous composites based on natural rubber

Polymer and silica composites have been studied to prepare new materials by combining the advantages of silica (e.g. high porosity, surface area and thermal stability) and organic polymers (e.g. pH stability, hydrophobicity and chemical functional group).

Natural rubber (NR) is a hydrophobic polymer of cis 1,4-isoprene monomers. There have been used to modify the properties of NR through various techniques, such as hydrogenation, functionalization and adding nanofillers (Zou et al., 2008).

The combination of rubber and silica became interesting because of its some useful properties, for example high thermal resistant, controlled size of silica particles and enhanced dispersion in rubber matrix (Tang et al., 2013).

According to Sakdinun Nuntang et al. 2014, a series of NR/HMS composites were prepared in tetrahydrofuran via an in situ sol-gel process using tetraethylorthosilicate as a silica source. The surface of NR/HMS composites were covered with NR molecules. The synthesized NR/HMS composite had a high surface area, large pore volume and wide pore size distribution; moreover it has an increasing hydrophobicity.

The important parameters that affect to the preparing of in silica and rubber composite are polymer types, solvent, silica precursor, the molar ratio of base: water: silica, temperature, and pH of the solution.

2.4.2 Alginate gel bead

Alginic acid, a component of algae cell wall, is a natural anionic polymer that has been widely used as a biomolecule immobilization and metal chelator. Alginic acid has hydroxyl and carboxyl groups which can complex with cation such as metal. Alginates are the composite of β -D-mannuronic acid and α -L-guluronic acid which produce viscous hydrogel by association with divalent cation compounds such as Ca^{2+} (T. Y. Kim et al., 2008). There are some research has been combined the alginate bead with activated carbon to remove heavy metal and toxic organic compound (T. Y. Kim et al., 2008; H. G. Park et al., 2007). Accordingly, NR/HMS-SH immobilized with calcium alginate beads are applied to use for remove the organic pollutants such as disinfection by products.

2.5 ADSORPTION THEORY

Adsorption is the adhesion of adsorbate on the surface of the adsorbent by creating adsorbate's film on the surface of the adsorbent. The removals of adsorbates are occurred when be adsorbed on the adsorbents 'surface. Adsorbents with higher specific surface area have more adsorption capacity. Moreover, the adsorbent with small particle size has higher mass transfer efficiency (Tung & Xie, 2006).

There are three steps of adsorption mechanism. The first step is film diffusion step that is adsorbate transported to external surface of adsorbent. The second step is intraparticle diffusion step that is adsorbate diffused to inter part of adsorbent. Final step is adsorption step that is the adsorption of adsorbate to internal surface of adsorbent. Normally, the rate limiting step might be the first or second step because the last step is very rapid represent.

2.5.1 Adsorption capacity

The adsorption capacity of adsorbent can be calculated by following equation

$$q = \frac{(C_0 - C_e)}{M} \times V \quad (2.5.1)$$

where C_0 and C_e is the adsorbate concentration ($\mu\text{g/L}$) at initial and at equilibrium respectively, q is the adsorption capacity ($\mu\text{g/g}$), M is the amount of adsorbent (g), and V is the volume of solution (L).

2.5.2 Adsorption kinetic

Adsorption kinetic is used to describe the adsorption rate of reaction. The pseudo-first-model and pseudo-second-model are usually used to investigate the adsorption kinetic.

2.5.2.1 The pseudo-first order kinetic model

$$q_t = q_e(1 - \exp^{-k_1 t}) \quad (2.5.2)$$

$$\ln(q_e - q_t) = \ln q_e - k_1 t \quad (2.5.3)$$

Where q_t and q_e are the amount of adsorbate (mg/g) at time t (h) and at equilibrium respectively, and k_1 is the pseudo-first order rate constant (mg/g). The value of k_1 and q_e can be calculated from slope and intercept of the plots between $\ln(q_e - q_t)$ and t .

2.5.2.2 The pseudo-second order kinetic model

$$q_t = \frac{q_e^2 k_2 t}{1 + q_e k_2 t} \quad (2.5.4)$$

$$\frac{t}{q_t} = \frac{1}{k_2 q_e^2} + \frac{t}{q_e} \quad (2.5.5)$$

Where k_2 is pseudo-second order rate constant that can calculate from the plot between t/q_t and t .

2.5.3 Adsorption isotherm

Adsorption isotherms are amount of adsorbate on the adsorbent in term of pressure of gas or concentration of liquid at constant temperature. It shows the relationship between adsorption capacity of adsorbent and concentration of the adsorbate at equilibrium. The Linear, Langmuir, and Freundlich models are most commonly used isotherm to investigate the adsorption isotherm modeling.

2.5.3.1 Linear Isotherm

Linear isotherm is the equation of adsorbate concentration and the amount of adsorbate at equilibrium.

$$q = K_p C_e \quad (2.5.6)$$

where q_e is the amount of adsorbate at equilibrium ($\mu\text{g/L}$), K_p is the Linear constant ($\text{L}/\mu\text{g}$), and C_e is the adsorbate concentration at equilibrium.

2.5.3.2 Langmuir Isotherm

Langmuir isotherm is calculate by following equation

$$\frac{1}{q_e} = \frac{1}{K_L q_m C_e} + \frac{1}{q_m} \quad (2.5.7)$$

where q_m is the maximum adsorption capacity ($\mu\text{g/g}$), q_e is the capacity of adsorbate at equilibrium ($\mu\text{g/L}$), and K_L is the Langmuir constant ($\text{L}/\mu\text{g}$).

2.5.3.3 Freundlich Isotherm

Freundlich isotherm is calculate by following equation

$$\ln q_e = \ln k_f + \frac{1}{n} \ln C_e \quad (2.5.8)$$

where k_f is the Freundlich constant and n is the adsorption intensity.

2.5.4 Column adsorption

As column adsorption, determination of breakthrough curve is very important because it leads to the information to design a column adsorption system. There are two approaches that widely used to obtain the breakthrough curve including direct experimental and mathematical modeling.

As the liquid-solid column adsorption, there are four basic steps (1) liquid phase mass transfer, (2) interface diffusion between liquid phase and the external surface of the adsorbent, (3) intrapellet mass transfer involving pore diffusion and surface diffusion, and (4) the adsorption and desorption reaction (Barros et al., 2013).

2.5.5 The breakthrough curve

In a column process, a solution is passed through a bed of adsorbent. The composition of the adsorbate and its change depend on the properties of adsorbent and the operation condition such as flow rate. Plotting between C/C_0 ratio (outlet concentration of adsorbate per its initial concentration) and time are presented in breakthrough curve. According to the experimental, the mass transfer occurs near the inlet zone of the bed, where the solution contacts with the adsorbent. When the zone near the inlet is almost saturated, the mass transfer will take place further from the

inlet. The concentration gradient is presented in S shape. The area where the concentration is changed is called the mass transfer zone.

2.5.6 The breakthrough curve model

The mathematic model that used to describe the dynamic adsorption in column system including

2.5.6.1 Bohart and Adams model

Bohart and Adams model (Bohart & Adams, 1920) assumes that equilibrium is not immediately occur; therefore, the adsorption rate relates to the adsorption capacity. The model equation describes the relationship between C_t/C_0 and t in a continuous system. The Bohart and Adams model is used for describe the initial part of the breakthrough curve. The equation is the following:

$$\ln \frac{C_t}{C_0} = k_{AB} N_0 \frac{Z}{F} - k_{AB} C_0 t \quad (2.5.9)$$

Where, C_0 and C_t (mg/L) are the initial concentration and concentration at time t . k_{AB} (L/mg·min) is the kinetic constant, F (cm/min) is the linear velocity, Z (cm) is the bed depth of column and N_0 (mg/L) is the saturation concentration.

2.5.6.2 Thomas model

Thomas model assume that: (i) axial and radial dispersion in the fixed bed column can be neglected; (ii) the adsorption is described by a pseudo second-order reaction rate principle; (iii) void fraction of the column is constant; (iv) the solid and fluid phase has same physical properties; (v) the process take place under isothermal

and isobaric conditions; (vi) the intra particle diffusion and external resistance during the mass transfer processes can be ignored. The equation of Thomas model is showed as follows:

$$\ln\left(\frac{C_0}{C_t} - 1\right) = \frac{k_{Th}q_0w}{v} - k_{Th}C_0t \quad (2.5.10)$$

Where, k_{Th} (mL/ μ g. min) is the Thomas rate constant; q_0 (μ g/g) is the equilibrium capacity adsorbent; C_0 (μ g/L) is the initial concentration; C_t (mg/L) is the concentration at time t ; w (g) the amount of adsorbent and v (mL min⁻¹) the flow rate. The C_t/C_0 value is the ratio of outlet and inlet concentrations. A linear plot between $\ln[(C_0/C_t)-1]$ and time (t) can determine q_0 and k_{Th} values from the intercept and slope of the plot.

2.6 LITERATURE REVIEWS

2.6.1 Removal of DBPs

As previously, most researches have focused on carbonaceous disinfection by products (C-DBPs) which resulting from chlorination of natural organic matters (NOM), because carbon based DBPs are the largest fraction (Muellner et al., 2007). However, nitrogenous disinfection by products (N-DBPs) at lower concentration are more toxic than C-DBPs (Plewa et al., 2004, 2008; Muellner et al., 2007). The toxicity of N-DBPs was reported that show much cytotoxicity and genotoxicity than C-DBPs to mammalian cells (Hou et al., 2012). Therefore, N-DBPs are important for researchers to concern about their toxic since the beginning of their formation, for example during the disinfection process of drinking water and wastewater treatment (Lee et al., 2007).

Several researches has identified the treatment alternatives for control of DBPs by removing of NOM prior to disinfection, use of alternative oxidants or disinfectants that do not create DBP at levels considered adverse to human health, removal of DBPs after they are formation. The alternative techniques were used for remove DBPs such as adsorption on activated carbon, coagulation, ozone oxidation, membrane filtration, adsorption on functionalized silica-based porous material.

Kleiser et al. (2000) explored the reduction of DBPs formation using pre-oxidation process to remove NOM which is the important role substances to causing DBPs. It showed the reduction of THM and organic halogen formation potential on adsorbed ozone mass was decreased to about 70%.

Udak et al. (2007) studied the removal of DBPs precursors by enhanced coagulation and PAC adsorption technique. They found that removal of DOC using enhanced coagulation by ferric chloride was more appropriate with large organic molecules with negative charged functional group while PAC adsorption are preferable to low molecular weight and uncharged NOM substance. Moreover, they reported that the combination of both techniques can be more effective than alone. Moreover, Yigit et al. (2009) studied the removal of NOM by measuring DOC, UV absorbance, and different trihalomethane formation. They informed that NOM can be disposed from drinking water with 40-50% efficiency through enhanced coagulation by ferric chloride and Alum.

Altes et al. (2009) explored the removal of DBPs precursor in surface water on ultrafiltration (UF) and nanofiltration (NF) membranes. They showed that the higher molecular weight DOC was successfully removed on UF and NF filter than lower molecular weight fraction.

2.6.2 Adsorption of DBPs

Kim and Kang (2008) studied the removal of DBPs on GAC filter adsorber comparing with sand filter. They found that the removal efficiencies of DBPs and DOC on GAC filter was better than sand filter, and the removal of haloacetic acids on GAC filter had higher levels than THM.

Jiun-Horng et al. (2008) investigated the adsorption of chloroform, acetone and acetonitrile on activated carbon comparing with sludge adsorbent. They found that the adsorption on activated carbon filter rate was higher than other adsorbents because of the higher surface area and smaller diameter.

Punyapalukul et al. (2009) investigated the adsorption efficiencies of DCAA on pure framework and difference functionalized surface of hexagonal mesoporous silicate. The results showed that the amino-functionalized material exhibited the high efficiency on DCAA adsorption. Moreover, they found that when combined the mercapto- or thiol group (-SH) with amino- functional groups resulted in the increasing of DCAA adsorption capacity due to its higher active site on the adsorbent surface.

Prarat et al. (2011) studied the adsorption efficiencies of haloacetonitriles on functionalized mesoporous silica materials in aqueous solution. They found that adsorption of DCAN on 3-Mercaptopropyl-grafted HMS had high capacity comparing with PAC. Furthermore, they reveal that the adsorption of HANs on 3-Mercaptopropyl-grafted HMS was more selectivity than PAC adsorption.

Prarat et al. (2013) investigated haloacetonitriles removal by adsorption on polymerizable surfactant-modified mesoporous silica in aqueous solution. It resulted that the less water solubility HANs were effectively adsorbed onto PG surfactant-

modified SBA-CHX due to the hydrophobic interaction between adsorbent and adsorbate characteristics. Moreover, they found that increasing number of substitute halogen in HAN molecule affected the adsorption capacity and selectivity.

According to the previous researches, the adsorption of THM and DCAA has been widely study. However, there were not much research studied about removal of other species of DBPs such as HANs and halogenated ketone with had higher toxic with lower concentration. Moreover, the adsorption process is one of the simple techniques that popular to remove DBPs. In the real situation the DBPs removal usually use GAC as adsorbent due to its granular form was easier to manage. However, GAC had some problem about the regeneration. In the other hand, the mesoporous material has been widely used as adsorbent and can adsorb some types of DBPs with high adsorption capacity. Therefore, this research used functionalized mesoporous silicate as adsorbent and tries to improve their function to remove DBPs from water.

CHAPTER 3

METHODOLOGY

3.1 MATERIALS

3.1.1 Chemical reagents

- Acetic acid	99%	SIGMA-ALDRICH
- Alginic acid		
- Calcium chloride		UNIVAR
- Copper sulfate anhydrous		CARLO ERBA
- Chloroacetonitrile		WAKO
- Dichloroacetic acid	99%	ACROS ORGANICS
- Dichloroacetonitrile	98%	SIGMA-ALDRICH
- Dipotassium hydrogenphosphate	99%	CARLO ERBA
- Dodecylamine	99%	SIGMA-ALDRICH
- Ethanol	99.9%	QRëC
- Ethyl alcohol		Fisher Scientific UK
- Hydrochloric acid	37%	QRëC
- Methanol	HPLC	Fisher Scientific UK
- Methyl-tert butyl ether	HPLC	Fisher Scientific UK
- Natural rubber		Thai Hua Chumporn Natural Rubber Co., Ltd (Thailand)
- Potassium dihydrogenphosphate		QRëC
- Sodium chloride		CARLO ERBA
- Sodium hydrogencarbonate		QRëC

- Sodium hydroxide		CARLO ERBA
- Sodium sulfate	99%	CARLO ERBA
- Sulfuric acid	98%	QRëC
- Sodium bicarbonate		CARLO ERBA
- Tetraethoxysilane	98%	SIGMA-ALDRICH
- Tetrahydrofuran	99.5%	QRëC
- Trichloroacetic acid	≥99%	SIGMA-ALDRICH
- Trichloroacetronitrile	98%	SIGMA-ALDRICH
- Trichloromethane		Fisher Scientific UK
- 1,1,1-trichloroacetone	>95%	TCI
- 2,3-dibromopropionic acid		Fluka
- 3-mercaptopropyltrimethoxysilane	95%	SIGMA-ALDRICH

3.1.2 Analytical Instruments

1. Gas Chromatography with an electron capture detector (GC/ECD)
2. VF-X Column (30 m x 0.32 mm i.d. x 0.10 µm film thickness)
3. HP-1 Column (30 m x 0.32 mm i.d. x 0.25 µm film thickness)
4. UV-Visible spectroscopy
5. TOC analyzer
6. Syringe filter (Nylon 0.45 µm, 13 mm, Chrom tech)
7. Filter papers (Quantitative 1, 90 mm, Whatman)
8. Magnetic stirrer
9. Vacuum filtration apparatus
10. Vacuum pump

11. Oven
12. Thermometer
13. Hot plate
14. Shaker
15. pH meter
16. Glass column with 2.5 cm diameter and 3 cm, 5 cm, and 10 cm length
17. Glass column with 2.5 cm diameter and 1 m length
18. Peristaltic pump

3.2 PREPARATION OF ADSORBENT

3.2.1 NR/HMS-SH

The NR/HMS-SH was prepared via a sol-gel method followed Nuntang et al. procedure (Nuntang et al., 2014). Firstly, 1 gram of natural rubber was dissolved in tetrahydrofuran (THF) for overnight to obtain a homogenous solution. Then dodecylamine (DDA), tetraethoxysilane (TEOS), deionized water and 3-mercaptopropyltrimethoxysilane (MPTMS) were added into the homogenous solution respectively. The mixture was stirred at 40°C for 1 hour and then the gel solution was aged for 3 days. The molar composition of the synthesis mixture was 0.1008 TEOS: 0.0405 DDA: 5.8880 H₂O: 0.0147 NR: 0.3700 TEOS: 0.0240 MPTMS. After that, the mixture was precipitated in 100 mL of ethanol (EtOH) and was recovered by filtrated. The product was parched at 60°C for 2 hours. Finally, the solid product was extracted with 0.05 M H₂SO₄/EtOH at 70°C for 8 hours to remove the template.

3.2.2 NR/HMS-SH containing alginate bead (AL:NR/HMS-SH)

The AL:NR/HMS-SH was prepared via sol-gel method. Firstly, 1% of alginate powder was dissolved in DI water to obtain a homogenous solution. Then, 10% of NR/HMS-SH powder was added into the viscous solution. The mixture was stirred until the solution was homogenous. After that, the mixture solution was dropped into 0.5 M calcium chloride (CaCl₂) solution. The beads were washed in DI water, and allowed to dry.

3.3 CHARACTERIZATION OF ADSORBENT

Table 3. 1 Characterization of NR/HMS-SH containing alginate bead

Parameters	Measurement
Porous structure	X-Ray Diffractometer
N ₂ adsorption-desorption isotherm	Surface area analyzer
Surface functional groups	Fourier Transform Infrared Spectrometer (FT-IR)
Sulfur analyzer	Elemental analyzer
Surface charge density	Titration
Material morphology	Scanning Electron Microscopy (SEM)

3.4 ANALYTICAL METHOD

3.4.1 Determination of HANs, THMs, and halogenated ketone

According to EPA method 551.1, 5 g of anhydrous sodium sulfate was added in 25 mL sample solution in glass vial. Then, adding 2.5 mL of methyl *tert*-butyl ether (MTBE) into the solution, and shaken for 2 min. After standing the solution for 3 min, 0.5 mL of organic layer was transferred into 2 mL glass vial. The sample concentration was analyzed by GC/ECD according to the EPA method 551.1(1990).

The gas chromatograph condition and parameters were conducted by setting the flow rate of helium carrier gas at 25 cm/sec, and the nitrogen gas was used as a make-up gas. The column was fused silica capillary column (HP-1, 30 m x 0.32 mm i.d. x 0.25 μ m film thickness). The injection temperature was set at 200°C with splitless mode, and the maintained detector temperature was at 300°C.

3.4.2 Determination of HAAs

According to EPA method 552.2, 25 μ L of surrogate standard (30 mg/L of 2,3-dibromopropionic acid in MTBE) was added into 15 mL of sample solution in 40 mL glass vial. After that, 0.5 mL of concentrated sulfuric acid, and 4 g of anhydrous sodium sulfate were added in the sample solution respectively. The sample was added with 1.5 g copper sulfate pentahydrate ($\text{CuSO}_4 \cdot 5\text{H}_2\text{O}$) and 2.5 mL MTBE. Then, the solution was shaken for 2 min, and standing for 5 min. Transfer 1.625 mL of organic layer into 2 mL of 10% H_2SO_4 /Methanol in glass vial. The solution was boiled in water bath at 50°C for 2 h, and then was cooled at 4°C for 3 min. The solution was added with 5 mL of saturated sodium bicarbonate (NaHCO_3), and shaken for 2 min. The sample was vented to release carbon dioxide and stand for 5 min. For 0.5 mL of organic layer was transferred to 2 mL glass vial. The sample concentration was analyzed by GC/ECD according to the EPA method 552.2 (1990).

The gas chromatograph condition and parameters were conducted by setting the helium carrier gas velocity at 25 cm/sec, and the nitrogen gas was used as a make-up gas. The used column was fused silica capillary column (VF-X, 30 m x 0.32 mm i.d. x 0.10 μ m film thickness). The injection temperature was set at 200°C with splitless mode, and the maintained detector temperature was at 290°C.

3.5 FRACTIONATION OF NATURAL ORGANIC MATTER (NOM)

The water from water supply system (Bangkok Metropolitan Authority's area) was fractionated into two parts including hydrophilic and hydrophobic groups. The collected water was adjusted pH by sulfuric acid at pH 2, and fractionated by filtrating through resin (DAX-8) with 20 mL/min of flow rate. The first part of water that was released from the column is hydrophilic NOM. After that, the remaining hydrophobic NOM was eluted by 25 mL of 0.1 N of NaOH and 125 mL of 0.01 N with 200 mL/hour of flow rate. The filtrated hydrophilic and hydrophobic NOM were measure the dissolved organic carbon values by using the total organic carbon (TOC) analyzer.

3.6 ADSORPTION EXPERIMENTALS

The adsorption of DBPs was conducted under batch condition. Stock solutions of DBPs were prepared in phosphate buffer for remaining pH of solutions and ionic strength. Adding 50 mL of HANs solution and 0.025 g of adsorbent in a 125 mL Erlenmeyer flask covered with a glass stopper. The slurry was shaken at 200 rpm at room temperature. The solid was removed by filtration through nylon syringe filter with pore size 0.45 mm, then was analyzed by GC/ECD according to EPA method 551.1 and 552.2 (1990).

3.6.1 Adsorption kinetic study

The Adsorption kinetic of DBPs was conducted by varying adsorption time from 0 to 24 hours. DCAN was a model of HANs, DCAA was a model of HAAs, TCM was a model of THMs, and TCA was a model of HK in this study. The

experiments were studied in batch condition. The initial concentration of DBPs was 200 $\mu\text{g/L}$ at pH7 and ionic strength was set at 10 mM by adjusting with phosphate buffer. The sample was shaken at 120 rpm at room temperature, and then the solution was separated by filtration through nylon syringe filter with pore size 0.45 μm . The remained concentration was analyzed by GC/ECD according to the EPA method 551.1 and 552.2.

3.6.2 Adsorption isotherm study

The adsorption isotherm was conducted by varying the initial concentration of DBPs from 50 to 700 $\mu\text{g/L}$. The ionic strength of the solution was fixed at 10 mM by adjusting with phosphate buffer at pH 7. The sample was shaken at 120 rpm at room temperature. The contact time was following the kinetic studied, and then the solution was separated by filtration through nylon syringe filter with pore size 0.45 μm . The remained concentration was analyzed by GC/ECD according to the EPA method 551.1 and 552.2.

3.6.3 Selectivity of adsorption

The experiment was conducted under batch condition by adding four types of DBPs including dichloroacetic acid, dichloroacetonitrile, trichloroacetonitrile and 1,1,1-trichloroacetone into the solution. The initial concentrations of the solutions were varied from 50 to 700 $\mu\text{g/L}$. The ionic strength of the solution was fixed at 10 mM by adjusting with phosphate buffer at pH 7. The sample was shaken at 120 rpm at room temperature for 15 hours. Then the solution was separated by filtration through

nylon syringe filter with pore size 0.45 μm . The remained concentration was analyzed by GC/ECD according to the EPA method 551.1 and 552.2.

3.6.4 Effect of NOM on DCAN adsorption

The experiment was conducted by adding DCAN into tap water, hydrophilic NOM and hydrophobic NOM. The initial concentrations of DCAN were varied from 50 to 700 $\mu\text{g/L}$. The sample was shaken at 120 rpm at room temperature. The contact time was following the kinetic studied, and then the solution was separated by filtration through nylon syringe filter with pore size 0.45 μm . The remained concentration was analyzed by GC/ECD according to the EPA method 551.1 and 552.2.

3.6.5 Fixed bed adsorption study

The experimental was conducted by passing the synthesized contaminated water through glass column with 2.5 cm diameter, and 10 cm and 13 cm length. The flow rate was controlled by peristaltic pump at 0.78 mL/min. The collected sample concentration was analyzed by GC/ECD according to the EPA method 551.1 and 552.2.

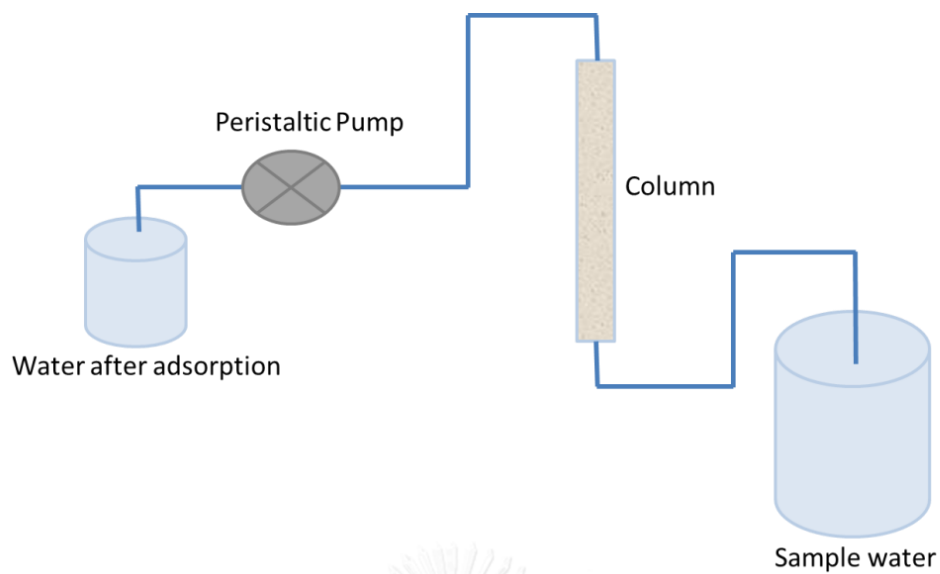


Figure 3.1 The fixed bed adsorption experiment



CHAPTER 4

RESULTS AND DISCUSSION

4.1 MATERIAL CHARACTERIZATION

The synthesized thiol- functionalized mesoporous composites based on natural rubber and hexagonal mesoporous silica containing with alginate bead adsorbent (AL:NR/HMS-SH) was characterized the physical and chemical properties by using several techniques.

4.1.1 X-Ray Diffraction

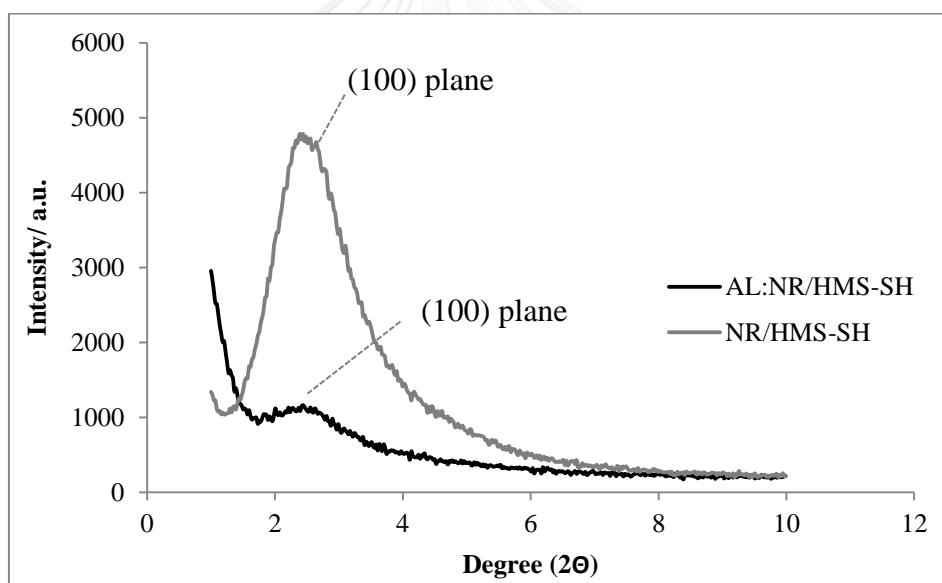


Figure 4.1 XRD pattern of AL:NR/HMS-SH

The XRD pattern of AL:NR/HMS-SH was showed in Figure 4.1. It indicated that the sample exhibited a diffraction peak at 2θ about 2.3° which refer to the (100) plane of hexagonal unit cell in the synthesized composite. Moreover, when combined alginate with the synthesized material found that intensity of 2θ diffraction peak was

lower than pure NR/HMS-SH compound. It can indicate that structure orders of the composite were decreased due to preventing of added alginate compound.

4.1.2 Surface area and pore structure by N₂ adsorption-desorption isotherm

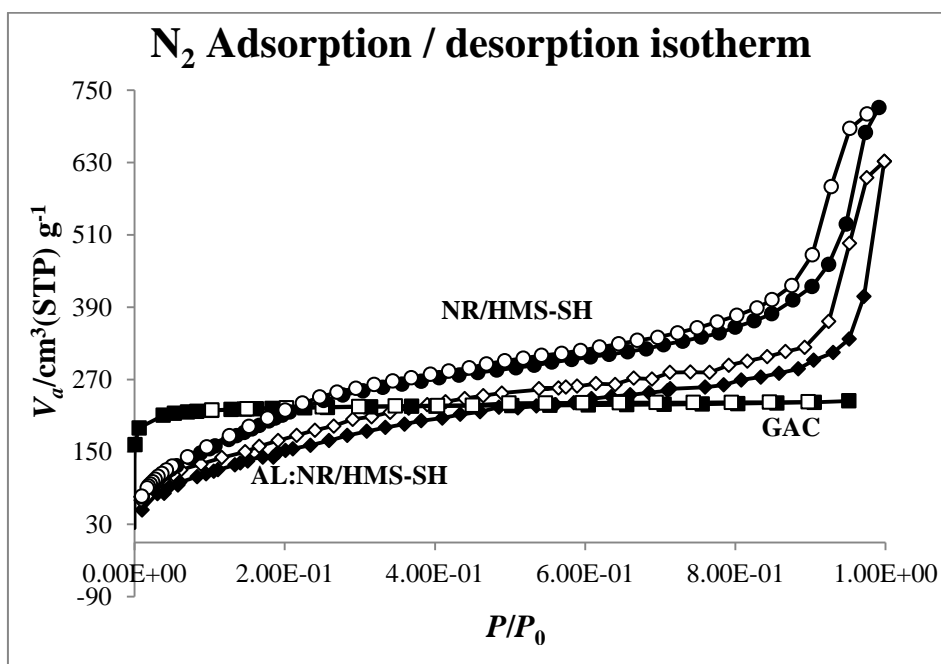


Figure 4.2 N₂ adsorption-desorption isotherms of NR/HMS-SH, AL:NR/HMS-SH and GAC. Closed and opened symbols presented N₂ adsorption and N₂ desorption respectively.

The N₂ adsorption-desorption isotherms of NR/HMS-SH, AL:NR/HMS-SH and granular activated carbon (GAC) as shown in Figure 4.2 were used to investigate the BET surface area, pore size and pore volume of each materials. The surface area, pore volume, and pore diameter of adsorbents were calculated by Brunauer-Emmett-Teller (BET) equation. The relationship between amount of adsorbed gas on particle at a given gas phase pressure resulted in isotherm to analyze the physical characteristics of the porous materials. According to IUPAC classification that showed in Figure 4.3 as below, the N₂ adsorption-desorption isotherm of NR/HMS-SH and AL:NR-HMS-SH were type IV isotherm that was used to determine the

mesoporous structure. It was generated by the capillary condensation of the adsorbate (N_2) in mesoporous materials. Moreover, NR/HMS-SH exhibited that the first region of curve was similar as type II which can indicate to formation of monolayer followed by multilayer adsorption. However, AL:NR/HMS-SH showed the lower BET surface area than NR/HMS-SH due to adding of alginate that might affect to the order structure of its surface. In addition, the N_2 adsorption-desorption isotherm of GAC were type I that was used to determine the adsorption on monolayer adsorption.

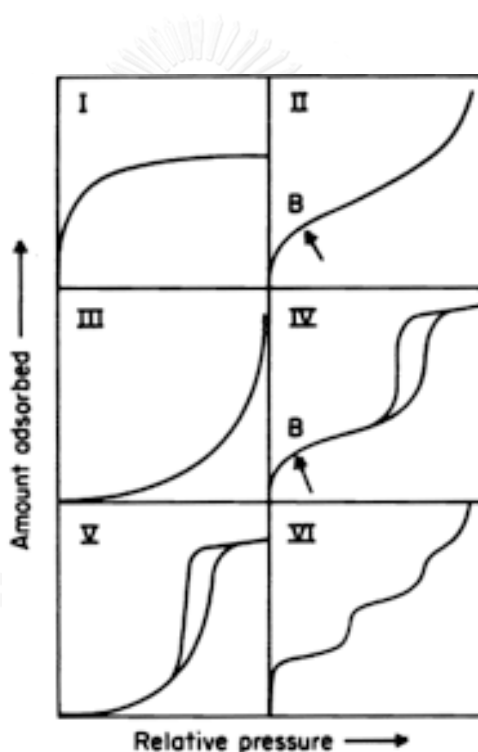


Figure 4.3 Types of isotherm shapes by IUPAC classification

Table 4.1 Mean pore diameter, pore volume, and BET surface area of AL:NR/HMS-SH and GAC.

Adsorbents	Functional group	Mean pore diameter (nm)	V_P ($mm^3 g^{-1}$)	S_{BET} ($m^2 g^{-1}$)
AL:NR/HMS-SH	Silanol, thiol	3.12	435.40	598.10
GAC	Carboxyl, phenyl and oxygen-containing groups	1.92	362.27	757.04

4.1.3 Surface functional group by FT-IR

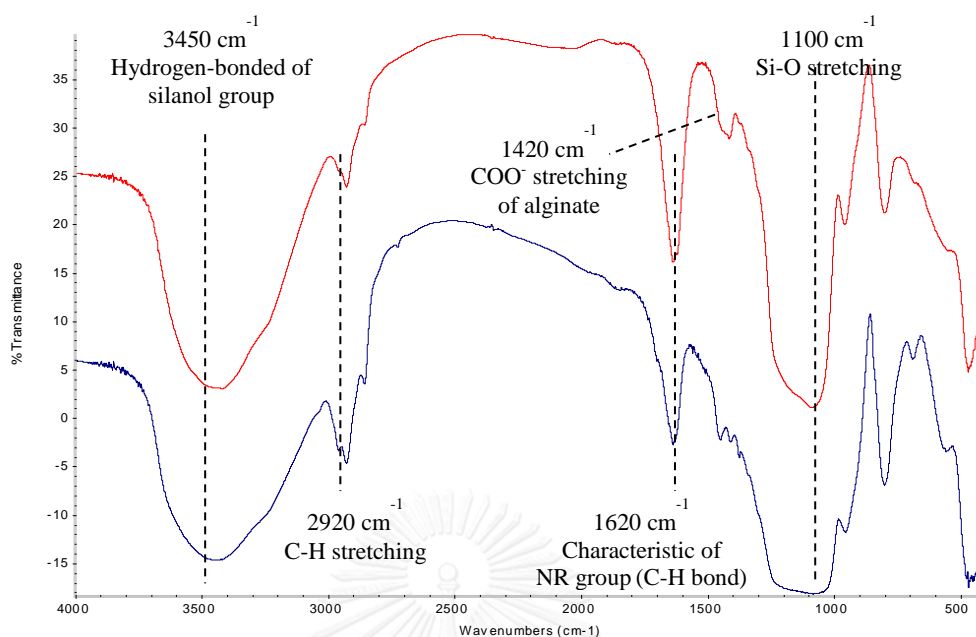


Figure 4.4 FTIR spectra of AL:NR/HMS-SH

The FT-IR analysis of the AL:NR/HMS-SH was shown in Figure 4.4. It exhibited the strong band of Si-O stretching vibration at 1100 cm^{-1} , and O-H stretching vibration of free silanol groups on the surface around 3450 cm^{-1} . The COO^- stretching of alginate was presented around 1420 cm^{-1} . Moreover, the bands at 1620 , and 2920 cm^{-1} were observed as C-H stretching of NR structure. In this case, S-H stretching of thiol-functionalized group on this material which occur the peak around $2490\text{ -}2580\text{ cm}^{-1}$ cannot show the peak; it might be caused by interfering of the broad peak of hydroxyl group. However, the present of thiol group in this synthesized material can confirm by CHNS elemental analyzer.

4.1.4 CHNS Elemental analyzer

The CHNS elemental analyzer was used to determine the amount of sulfur on the material surface to confirm the thiol-functionalized (-SH) of adsorbent. The data in table 4.2 showed the sulfur content on synthesized material was 5.53 (%w/w) which can confirm there were S-H groups on this adsorbent surface.

Table 4.2 Sulfur content of AL:NR/HMS-SH

% Carbon	% Hydrogen	% Sulfur
14.65	3.00	5.53

4.1.5 Scanning electron microscopy (SEM)

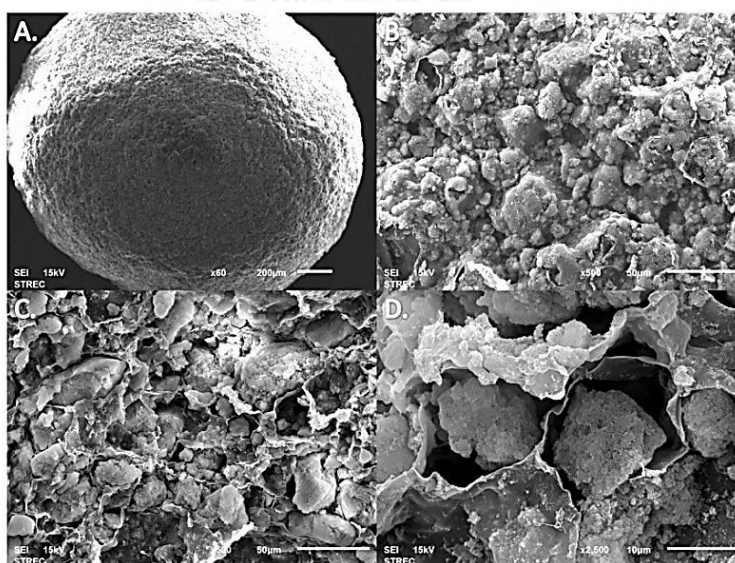


Figure 4.5 (A, B) show SEM images of AL: NR/HMS-SH (60x and 500x), and(C, D) show SEM images of cross-sectional view of AL: NR/HMS-SH (500x and 2500x)

The Figure 4.5A showed overall SEM images of AL:NR/HMS-SH that had spherical shape with 1.5 cm diameter. The surface area of the adsorbent was represented in Figure 4.5B that indicated the small spherical grain of silica particles distributed on the adsorbent surface. Moreover, Figure 4.5C and 4.5D showed SEM

images of cross-section view of AL:NR/HMS-SH. They revealed that there were the small particles of NR/HMS-SH dispersed into the hole of alginate sheet.

4.1.6 Surface charge density

The point of zero charge (pH_{zpc}) of synthesized material and GAC were investigated by using acid-base titration method. The surface of synthesized adsorbent was protonated at low pH caused to the positive surface charge, while it was negative surface charge at high pH due to their proton leaving by hydroxide. According to Figure 4.6, the pH_{zpc} of AL:NR/HMS-SH and GAC were 5.81 and 6.98 respectively.

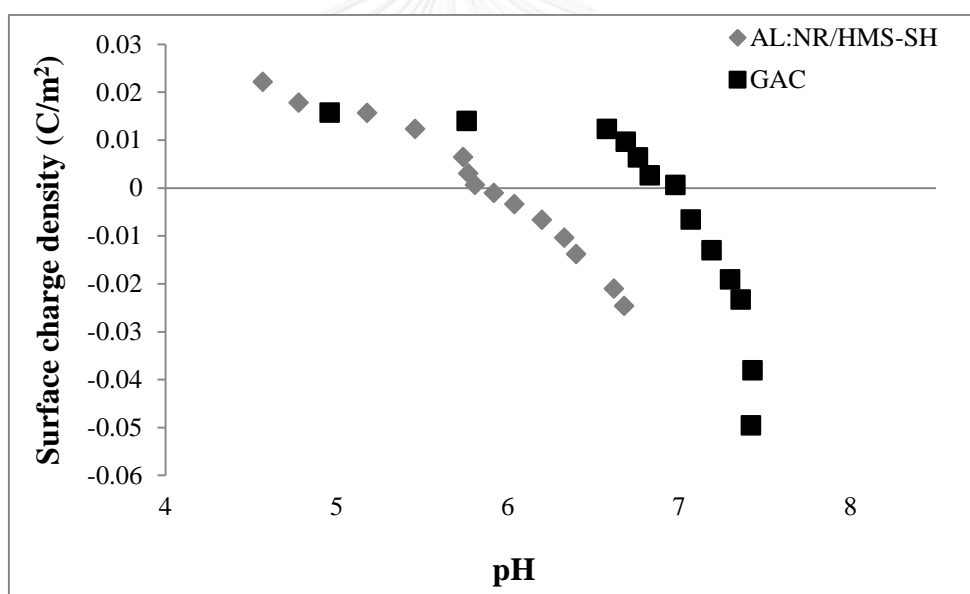


Figure 4.6 Surface charge density of AL:NR/HMS-SH and GAC

4.2 ADSORPTION OF DBPs ON NR/HMS-SH CONTAINING ALGINATE BEAD AND GAC

4.2.1 Adsorption kinetic

The adsorption kinetic can estimate the rate of adsorbate which be adsorbed on adsorbent and rate limiting step of the adsorption. Moreover, the kinetic parameters such as rate constant, and the amount of adsorbate at any time or at equilibrium can help to predict and design the adsorption process.

The kinetic models including pseudo-first-order and pseudo-second-order models were applied to investigate the adsorption mechanism. The pseudo-first-order model and the pseudo-second-order model can be represented as equation (4.2.1) and (4.2.2) respectively.

$$q_t = q_e(1 - \exp^{-k_1 t}) \quad (4.2.1)$$

$$q_t = \frac{q_e^2 k_2 t}{1 + q_e k_2 t} \quad (4.2.2)$$

where q_t and q_e are the amount of adsorbate ($\mu\text{g/g}$) that be adsorbed at time t (hour) and at equilibrium respectively, k_1 is the pseudo-first order rate constant, and k_2 is pseudo-second order rate constant.

Moreover, the initial adsorption rate, h ($\mu\text{g/g}^{-1} \text{h}^{-1}$) and the half-life time, $t_{1/2}$ (h) of the pseudo-second order model can be determined following equation (4.2.3) and (4.2.4) respectively.

$$h = k_2 q_e^2 \quad (4.2.3)$$

$$t_{1/2} = \frac{1}{k_2 q_e} \quad (4.2.4)$$

In case of quantitative comparison between the different models in fitting to the data, a normalized standard deviation Δq (%) was calculated as equation (4.2.5)

$$\Delta q = 100 \times \sqrt{\frac{\sum \left[\frac{q_{exp} - q_{cal}}{q_{exp}} \right]^2}{N-1}} \quad (4.2.5)$$

where N is a number of data points, q_{exp} and q_{cal} ($\mu\text{g/g}$) are the experiment value and the calculation value of adsorption capacities, respectively.

4.2.1.1 Adsorption kinetic of dichloroacetonitrile (DCAN)

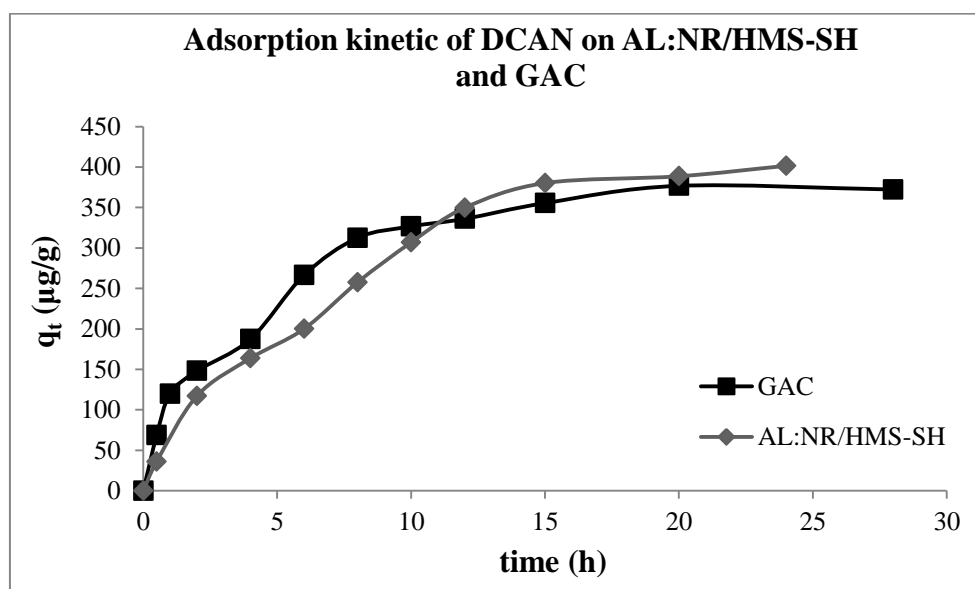


Figure 4.7 Kinetics adsorption of DCAN on AL:NR/HMS-SH and GAC at $200 \mu\text{g L}^{-1}$ (pH 7 and IS 10 mM)

Kinetic curves of DCAN adsorption on AL:NR/HMS-SH and GAC were shown in Figure 4.7. It resulted that the adsorption of DCAN on GAC reached equilibrium about 20 hours while AL:NR/HMS-SH reached the equilibrium at approximately 15 hours. Moreover, it found that the kinetic curves of both adsorbents had multi step of adsorption process. This might be associated to their wide pore size distribution and various functionalized on the surface. According to the adsorption kinetic data, the adsorption capacity of DCAN on AL:NR/HMS-SH showed high adsorption capacity nearby with GAC.

Table 4.3 Parameters of dichloroacetonitrile (DCAN) kinetic adsorption on AL:NR/HMS-SH and GAC using the pseudo-first order and pseudo-second order kinetic models

Adsorbents	$q_{e,exp}$ ($\mu\text{g g}^{-1}$)	Pseudo-first-order				Pseudo-second-order					
		$q_{e,cal}$ ($\mu\text{g g}^{-1}$)	k_1 (h^{-1})	R^2	Δq (%)	$q_{e,cal}$ ($\mu\text{g g}^{-1}$)	k_2 ($\text{g } \mu\text{g}^{-1}\text{h}^{-1}$)	h ($\mu\text{g g}^{-1}\text{h}^{-1}$)	$t_{1/2}$ (h)	R^2	Δq (%)
AL:NR/HMS-SH	380.19	420.73	0.1856	0.9335	21.34	555.56	0.0002	66.67	8.33	0.9746	8.95
GAC	355.40	343.16	0.2418	0.9866	19.74	416.67	0.0007	129.87	3.21	0.9922	11.47

According to the kinetic parameters, the correlation coefficients (R^2) of both models had high values and were not significantly different as shown in table 4.3. Therefore, the normalized standard deviation (Δq) calculations of pseudo-first-order model compared with pseudo-second-order model were used to determine the data fitting. The Δq value of pseudo-second models of GAC and the synthesized adsorbent were less than the pseudo-first-order model. Therefore, the adsorptions of DCAN on both adsorbents were suitable to describe by using pseudo-second-order model that determined to the chemisorption to explain the adsorption process. Moreover, this result indicated that the initial rate adsorption (h) of DCAN adsorption on GAC was higher than adsorption on synthesized adsorbent due to the higher adsorption affinity of DCAN. It might be because of the higher surface area and the complicated functional group on GAC surface.

4.2.1.2 Adsorption kinetic of trichloromethane (TCM)

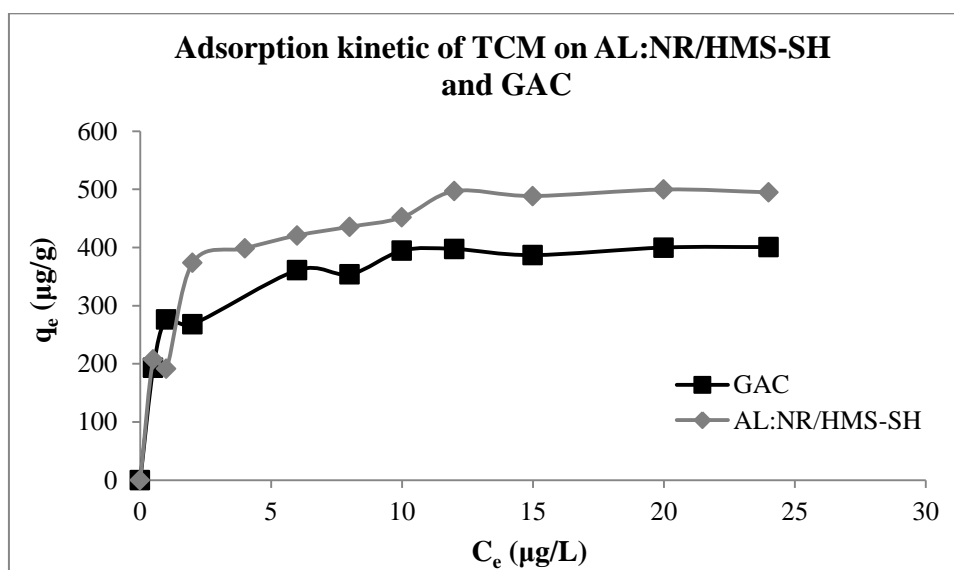


Figure 4.8 Kinetics adsorption of TCM on AL:NR/HMS-SH and GAC at $200 \mu\text{g L}^{-1}$ (pH 7 and IS 10 mM)

As shown in Figure 4.8, the kinetic curves for TCM adsorption showed adsorption of TCM on GAC reached equilibrium about 10 hours while the synthesized adsorbent reached the equilibrium at approximately 12 hours. Moreover, kinetic curves of TCM adsorption on both adsorbents showed multi step of adsorption process same as adsorption of DCAN.

Table 4.4 Parameters of TCM kinetic adsorption on AL:NR/HMS-SH and GAC using the pseudo-first order and pseudo-second order kinetic models

Adsorbents	$q_{e,exp}$ ($\mu\text{g g}^{-1}$)	Pseudo-first-order			Pseudo-second-order				
		$q_{e,cal}$ ($\mu\text{g g}^{-1}$)	k_1 (h^{-1})	R^2	$q_{e,cal}$ ($\mu\text{g g}^{-1}$)	k_2 ($\text{g } \mu\text{g}^{-1}\text{h}^{-1}$)	h ($\mu\text{g g}^{-1}\text{h}^{-1}$)	$t_{1/2}$ (h)	R^2
AL: NR/HMS-SH	496.92	317.10	0.2166	0.8737	526.32	0.0019	526.32	1	0.9963
GAC	394.52	178.54	0.2179	0.8757	416.67	0.0030	520.84	0.79	0.9986

The kinetic parameters of TCM on both mesoporous material containing in alginate bead and GAC were shown in table 4.4 as below. The correlation coefficients (R^2) of pseudo-second models of GAC and the synthesized adsorbent were higher than the pseudo-first-order model. Therefore, the adsorptions of TCM on both adsorbents were suitable to explain with pseudo-second-order model same as DCAN adsorption.

When considering the initial rate adsorption (h) of TCM on both adsorbents found that the synthesized adsorbent was nearly with GAC. However, they had higher adsorption affinity than DCAN adsorption. This might be associated to the higher hydrophobicity or less water solubility of TCM structure than DCAN.

4.2.1.3 Adsorption kinetic of 1, 1, 1,-trichloroacetone (TCA)

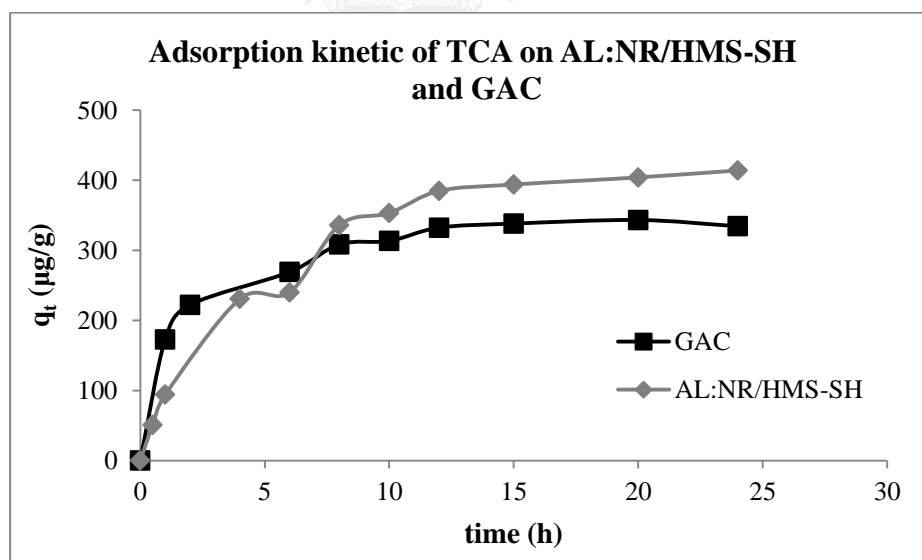


Figure 4.9 Kinetics adsorption of TCA on AL:NR/HMS-SH and GAC at $200 \mu\text{g L}^{-1}$ (pH 7 and IS 10 mM)

Kinetic curves for TCA adsorption on the synthesized material and GAC showed the adsorption of TCA on both GAC and AL:NR/HMS-SH reached equilibrium about 12 hours as presented in Figure 4.9.

Table 4.5 presented the kinetic parameters of TCA on both adsorbents resulted that the R^2 of pseudo-second-order models of GAC and the synthesized adsorbent were higher than the pseudo-first-order model. Thus, the adsorptions of TCA on both adsorbents were suitable to explain with pseudo-second-order model like adsorption of DCAN and TCM. When regarding the initial rate adsorption (h) of TCA on both adsorbents found that the adsorption on GAC had higher affinity compared with the synthesized material. This might be associated to higher surface area and complexity of activated carbon surface.

Table 4.5 Parameters of 1, 1, 1-trichloroacetone (TCA) kinetic adsorption on AL:NR/HMS-SH and GAC using the pseudo-first order and pseudo-second order kinetic models

Adsorbents	$q_{e,exp}$ ($\mu\text{g g}^{-1}$)	Pseudo-first-order			Pseudo-second-order				
		$q_{e,cal}$ ($\mu\text{g g}^{-1}$)	k_1 (h^{-1})	R^2	$q_{e,cal}$ ($\mu\text{g g}^{-1}$)	k_2 ($\text{g } \mu\text{g}^{-1}\text{h}^{-1}$)	h ($\mu\text{g g}^{-1}\text{h}^{-1}$)	$t_{1/2}$ (h)	R^2
AL:NR/HMS-SH	353.11	477.09	0.2663	0.8047	588.24	0.0002	60.24	9.76	0.9640
GAC	332.28	244.55	0.2650	0.9512	357.14	0.0029	370.37	0.96	0.9961

Moreover, when comparing the initial rate adsorption and half time of three DBPs on the same adsorbent resulted that the adsorption on AL:NR/HMS-SH showed the higher adsorption affinity on TCM followed by DCAN and TCA respectively. In the same way, GAC showed the highest adsorption efficiency on TCM. However, it displayed the higher initial rate adsorption on TCA than DCAN.

This might cause of the higher hydrophobicity (less water solubility) of TCM than DCAN (water solubility 7.95g/L and 33.5 g/L respectively followed USEPA,

2001&2004) that can be good adsorbed on AL:NR/HMS-SH which had hydrophobicity surface. However, TCA also had low water solubility (7.45 g/L followed USEPA, 2004); it presented in lower adsorption capacity on AL:NR/HMS-SH. According to the negative surface charge of adsorbent at pH7 solution, the presented of H-atom in TCM and DCAN molecules which can produce positive dipole can interact with negative charge of adsorbent surface with ion-dipole electrostatic interaction.

4.2.1.4 Adsorption kinetic of dichloroacetic acid (DCAA)

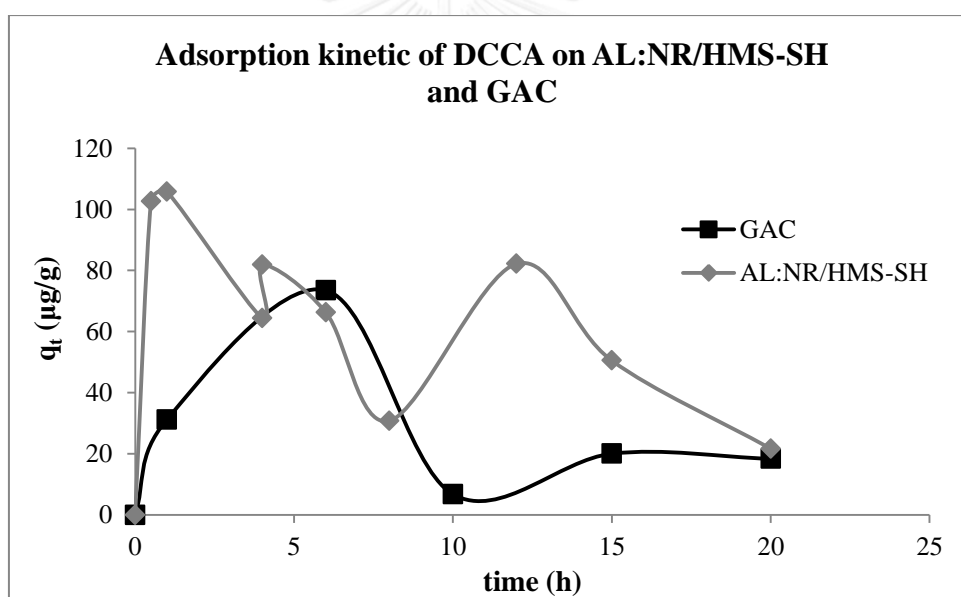


Figure 4.10 Kinetics adsorption of DCAA on AL:NR/HMS-SH and GAC at $200 \mu\text{g L}^{-1}$ (pH 7 and IS 10 mM)

According to kinetic curve for DCAA adsorption on the synthesized material and GAC that presented in Figure 4.10, they appeared the indeterminate adsorption capacity of DCAA on both adsorbents. This might because of DCAA cannot be adsorbed on the adsorbents steadily due to the surface characteristics of adsorbents such as the hydrophobicity of AL:NR/HMS-SH and GAC which might showed the

poorly adsorption for DCAA due to its very soluble. Moreover, the surface of these both adsorbents displayed the negative charge in pH 7 solution (pH_{zcp} of AL:NR/HMS-SH and GAC are 5.81 and 6.98 respectively) that might affected to the adsorption for DCAA which had low pK_a ($\text{pK}_a=1.26$) and displayed negative charge after its dissociation in water.

4.2.2 Intraparticle diffusion

The adsorption process of solid-liquid adsorption included three steps: (1) the film diffusion (2) intraparticle diffusion or pore diffusion and (3) adsorption process. The intraparticle diffusion model was developed by Weber and Morris used to analyze the kinetic data to examine the rate limiting step in adsorption process. The intraparticle diffusion equation can be defined as shown in equation (4.2.6)

$$q_t = k_{iP}t^{0.5} + C \quad (4.2.6)$$

where q_t is the amount of adsorbate ($\mu\text{g/g}$) at time t (hour), k_{iP} is the intraparticle diffusion rate constant ($\mu\text{g g}^{-1} \text{h}^{-0.5}$), and C is the interception which can be determined by plotting q_t and $t^{0.5}$.

4.2.2.1 Intraparticle diffusion model of DCAN adsorption

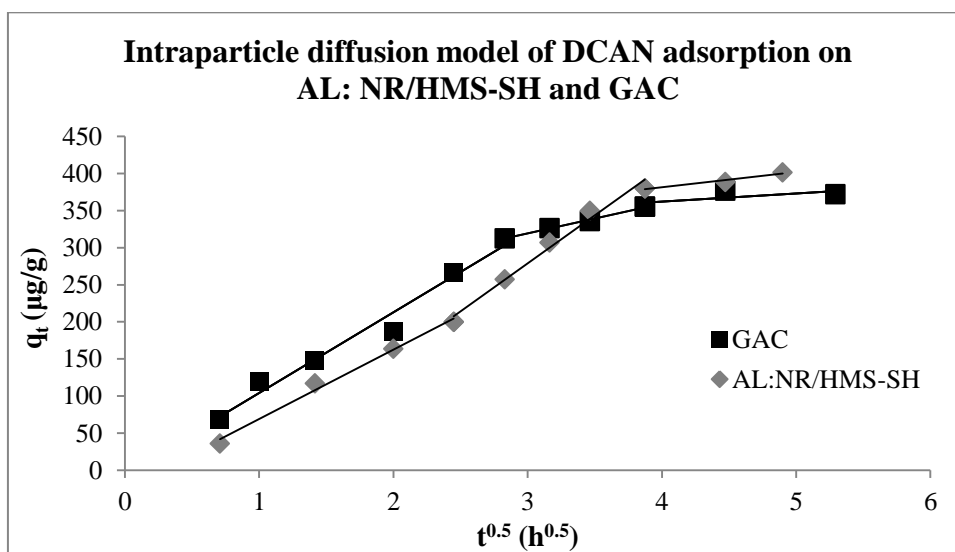


Figure 4.11 Plot of intraparticle diffusion model of DCAN adsorption on AL:NR/HMS-SH and GAC

According to the fitting curves as showed in Figure 4.11, they presented the multiple step of adsorption. The first step presented the external mass transfer in the boundary layer which can be indicated the rate constant from the slope of first region; the second step showed the diffusion of DCAN into internal surface of adsorbent which can be determined the rate constant from the second region of the curves; and the final step was the adsorption of DCAN on internal site of adsorbent which can be ignored due to its very rapidly occurred. Therefore, the rate controlling step of the adsorption can be the film diffusion and/or intraparticle diffusion step. Furthermore, when comparing the rate constant of each region on both adsorbents found that rate of AL:NR/HMS-SH was lower than GAC in the first region but it had higher rate on the second regime. It might because of the adsorption of DCAN on GAC was better than AL:NR/HMS-SH on boundary layer due to its higher surface area. However, on the internal diffusion step AL:NR/HMS-SH showed the higher rate of adsorption than GAC that might be the effect of their higher pore size and pore volume.

Table 4.6 Kinetic parameters of DCAN adsorption on AL:NR/HMS-SH and GAC using the intraparticle diffusion model.

Adsorbent	1 st step			2 nd step		
	k_{ip1} ($\mu\text{g g}^{-1} \text{h}^{-0.5}$)	Intercept (C_1)	R^2	k_{ip2} ($\mu\text{g g}^{-1} \text{h}^{-0.5}$)	Intercept (C_2)	R^2
AL:NR/HMS-SH	93.49	-24.38	0.9906	129.47	-109.67	0.9827
GAC	108.65	-4.53	0.9757	40.33	198.25	0.9942

4.2.2.2 Intraparticle diffusion model of TCM adsorption

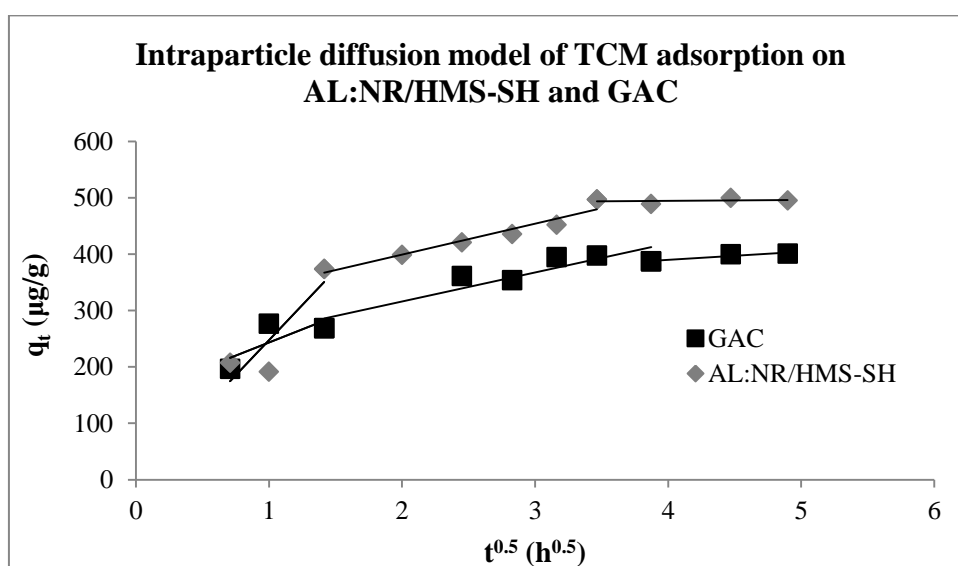


Figure 4.12 Plot of intraparticle diffusion model of TCM adsorption on NR/HMS-SH containing alginate bead and GAC

The intraparticle diffusion models of TCM adsorption on AL:NR/HMS-SH and GAC were presented in Figure 4.12 they revealed multi-linearity that refer to the multiple step of adsorption. The mechanism of each step can describe same as the adsorption mechanism of DCAN. When considering the rate of each step on TCM adsorption found that the rates of film diffusion step were higher than the internal diffusion step on both adsorbents. This might because of the low water solubility of TCM that can be better adsorbed on external surface of AL:HMS-SH and GAC which had high hydrophobic surface.

Table 4.7 Kinetic parameters of TCM adsorption on AL:NR/HMS-SH and GAC using the intraparticle diffusion model

Adsorbent	1 st step			2 nd step		
	k_{iP1} ($\mu\text{g g}^{-1} \text{h}^{-0.5}$)	Intercept (C_1)	R^2	k_{iP2} ($\mu\text{g g}^{-1} \text{h}^{-0.5}$)	Intercept (C_2)	R^2
AL:NR/HMS-SH	247.81	-0.20	0.9320	54.76	289.84	0.9396
GAC	203.44	26.69	0.8859	51.50	212.94	0.8432

4.2.2.3 Intraparticle diffusion model of TCA adsorption

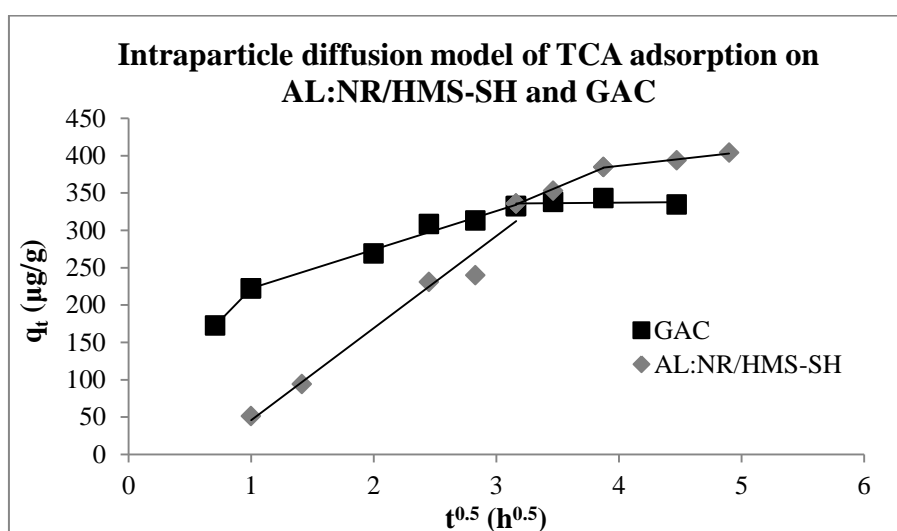


Figure 4.13 Plot of intraparticle diffusion model of TCA adsorption on AL:NR/HMS-SH and GAC

According to Figure 4.13, the intraparticle diffusion model of TCA adsorption on AL:NR/HMS-SH and GAC pointed to multi-linearity that refer to the multiple step of adsorption. The mechanism of each step can also describe same as the adsorption mechanism of DCAN and TCM. The data revealed that adsorption rates of the first step of both adsorbents were less than the second step. It can indicate that the adsorption of TCA can occur in the internal part of adsorbent better than external surface of adsorbent.

Table 4.8 Kinetic parameters of TCA adsorption on AL:NR/HMS-SH and GAC using the intraparticle diffusion model

Adsorbent	1 st step			2 nd step		
	k_{iP1} ($\mu\text{g g}^{-1} \text{h}^{-0.5}$)	Intercept (C_1)	R^2	k_{iP2} ($\mu\text{g g}^{-1} \text{h}^{-0.5}$)	Intercept (C_2)	R^2
AL:NR/HMS-SH	63.58	-2.85	0.9660	122.35	-77.55	0.9690
GAC	50.88	172.99	0.9212	67.59	137.74	0.9009

4.2.3 Adsorption isotherm model

According to adsorption isotherm model; Linear, Langmuir, and Freundlich isotherm models were applied to investigate the correlation with the experimental data. The Linear, Langmuir, and Freundlich isotherm models can be determined as equation (4.2.7), (4.2.8) and (4.2.9) respectively.

$$q = K_p C_e \quad (4.2.7)$$

$$\frac{1}{q_e} = \frac{1}{K_L q_m C_e} + \frac{1}{q_m} \quad (4.2.8)$$

$$\ln q_e = \ln k_f + \frac{1}{n} \ln C_e \quad (4.2.9)$$

where q_e is the amount of adsorbate at equilibrium ($\mu\text{g /L}$), C_e is the adsorbate concentration at equilibrium, K_p is the Linear constant ($\text{L}/\mu\text{g}$), q_m is the maximum adsorption capacity ($\mu\text{g/g}$), K_L is the Langmuir constant ($\text{L}/\mu\text{g}$), k_f is the Freundlich constant, and n is the adsorption intensity.

4.2.3.1 Adsorption isotherm model of HANs

According to the isotherm parameters that showed in Figure 4.14 and Table 4.9, MCAN adsorption on the synthesized adsorbent did not show the adsorption efficiency while the adsorption on GAC presented the linear adsorption which fitted to Linear isotherm model by considering the high correlation coefficient value (R^2) and the less amount of normalized standard deviations (Δq). It means that the amount of adsorbent surface was showed to be corresponding to the adsorbed molecules. Moreover, the figure presented the adsorption of DCAN and TCAN on the synthesized material and GAC. The data exhibited the best fitted with Freundlich isotherm model according to the fewer amounts of normalized standard deviations (Δq). It revealed that the adsorption process occur on heterogeneous surface of adsorbent. Moreover, n value can determine the nonlinearity degree between concentration of solution and adsorption. If $n=1$, the adsorption is linear; if n less than one, the adsorption is chemical process; and if n more than one, the adsorption is physical process. Thus, the DCAN adsorptions on AL:NR/HMS-SH and GAC were physical process and they had a good adsorption due to the n value within 1-10 range; whereas the TCAN adsorptions on both materials were chemical process. However, in some of these case Langmuir isotherm model might not suitable to describe the adsorption process due to the calculation parameters resulted in the invalid value on linear fitting calculation.

When comparison the adsorption capacities of each HANs on same adsorbent found that the adsorptions of TCAN on both AL:NR/HMS-SH and GAC showed the higher efficiencies than DCAN and MCAN respectively. This might be the effect of number of substituted Cl-atom in each HAN species that caused to the water

solubility of them. According to the USEPA (2004) database, TCAN which had three Cl atoms showed the less water solubility than DCAN and MCAN which had less number of Cl-atom (0.715 g/L, 33.5 mg/L and 100 g/L, respectively).

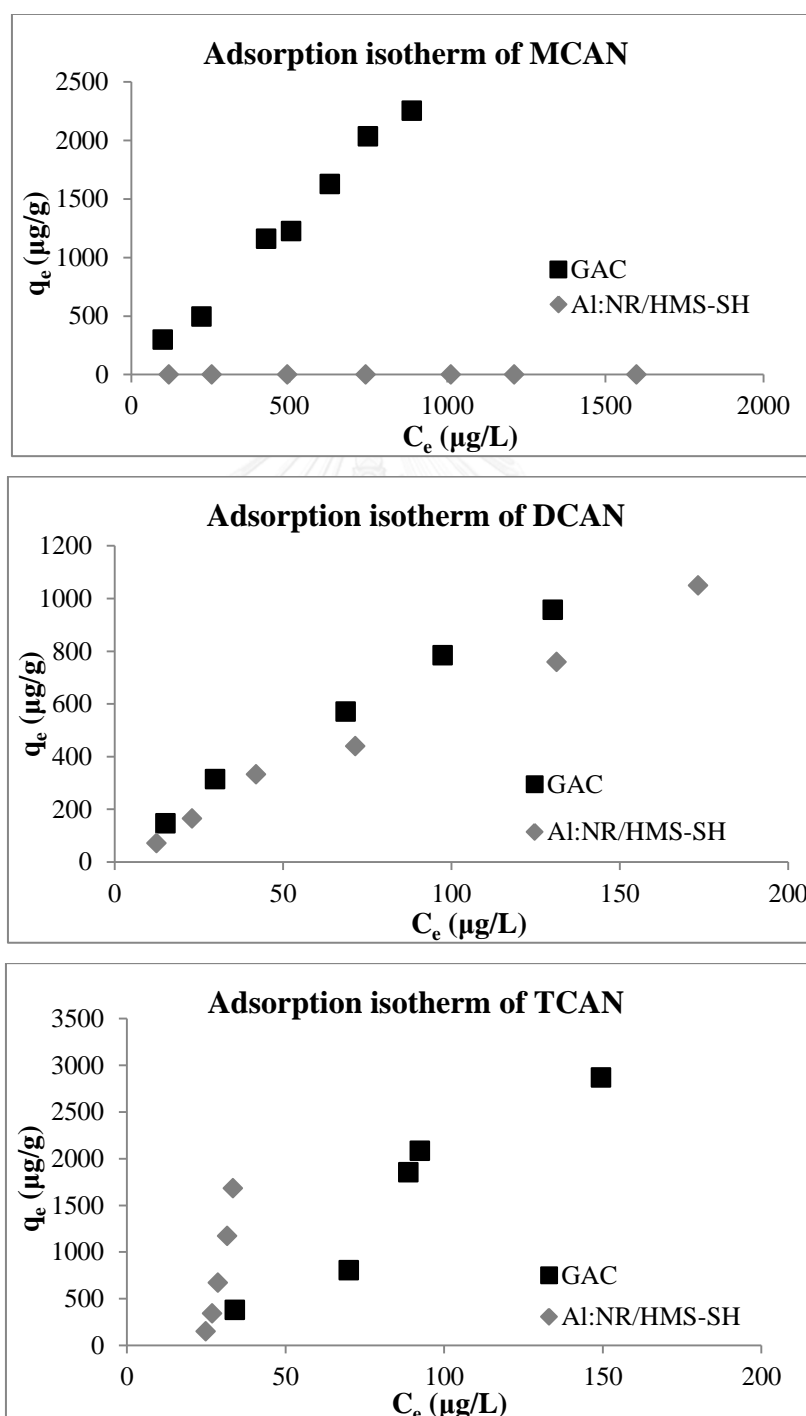


Figure 4.14 Isotherms adsorption of MCAN, DCAN and TCAN on Al:NR/HMS-SH and GAC (pH 7 and IS 10 mM)

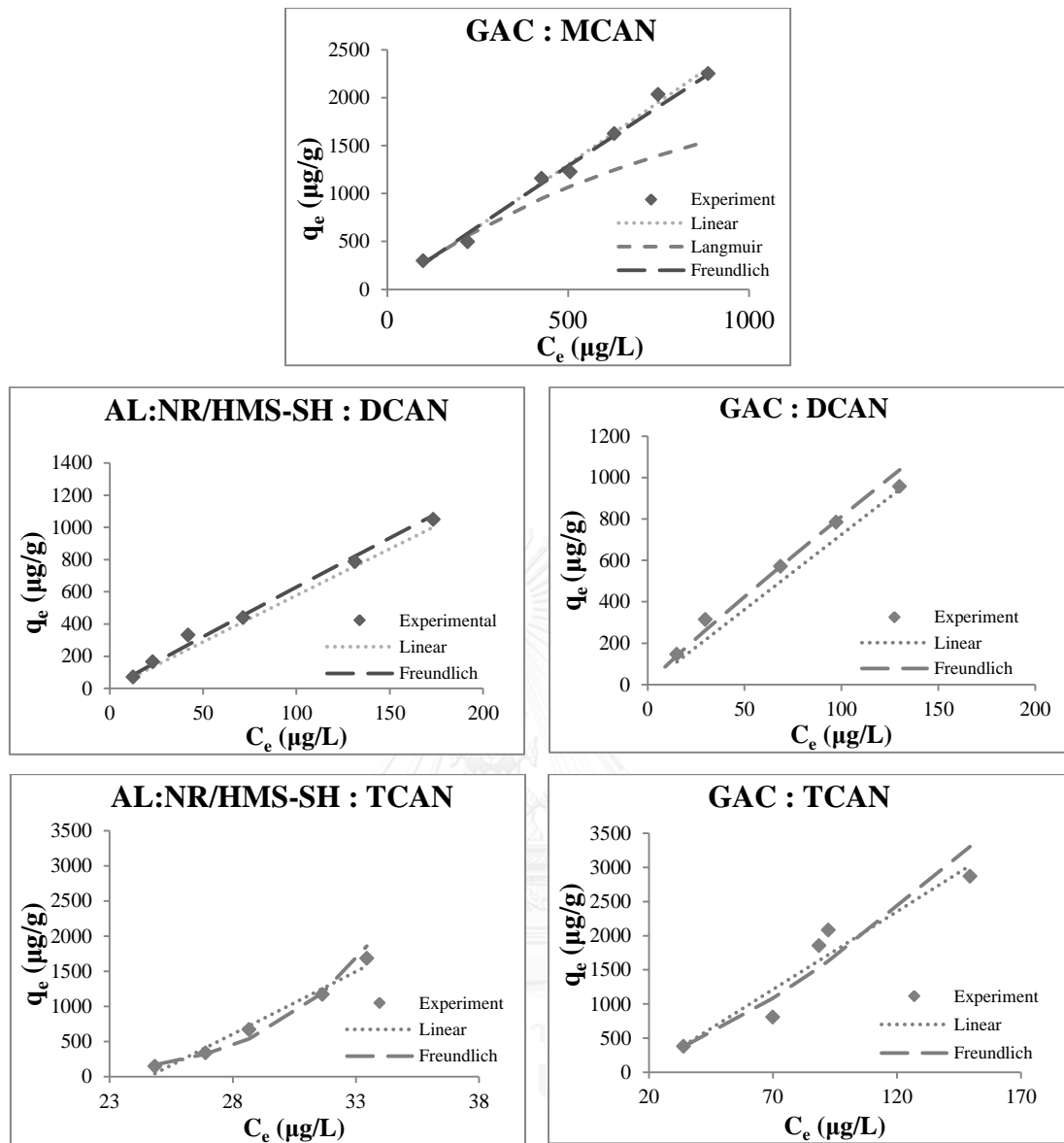


Figure 4.15 Comparison of the MCAN, DCAN and TCAN adsorption experimental data and the data from predicted model on AL:NR/HMS-SH and GAC at pH 7 with IS 10 mM

Table 4.9 Parameters of HANs isotherm adsorption on AL:NR/HMS-SH and GAC

Isotherm	HANs		
	MCAN	DCAN	TCAN
AL:NR/HMS-SH			
Linear	-		
K_p		5.78	177.52
R^2		0.9918	0.9761
Δq (%)		15.23	36.46
Langmuir	-	-	-
q_m ($\mu\text{g g}^{-1}$)			
K_L ($\text{L } \mu\text{g}^{-1}$)			
R^2			
Δq (%)			
Freundlich	-		
n		1.0280	0.1249
K_F ($\mu\text{g g}^{-1}$)		7.15	1.71×10^{-9}
R^2		0.9834	0.9792
Δq (%)		12.59	13.59
GAC			
Linear			
K_p	2.61	7.25	22.82
R^2	0.9911	0.9893	0.9094
Δq (%)	9.55	15.75	27.40
Langmuir		-	-
q_m ($\mu\text{g g}^{-1}$)	10000		
K_L ($\text{L } \mu\text{g}^{-1}$)	2.98		
R^2	0.9744		
Δq (%)	23.16		
Freundlich			
n	1.0310	1.0714	0.6807
K_F ($\mu\text{g g}^{-1}$)	3.10	11.03	2.11
R^2	0.9856	0.9881	0.9252
Δq (%)	9.41	10.78	23.40

4.2.3.2 Adsorption isotherm model of TCM

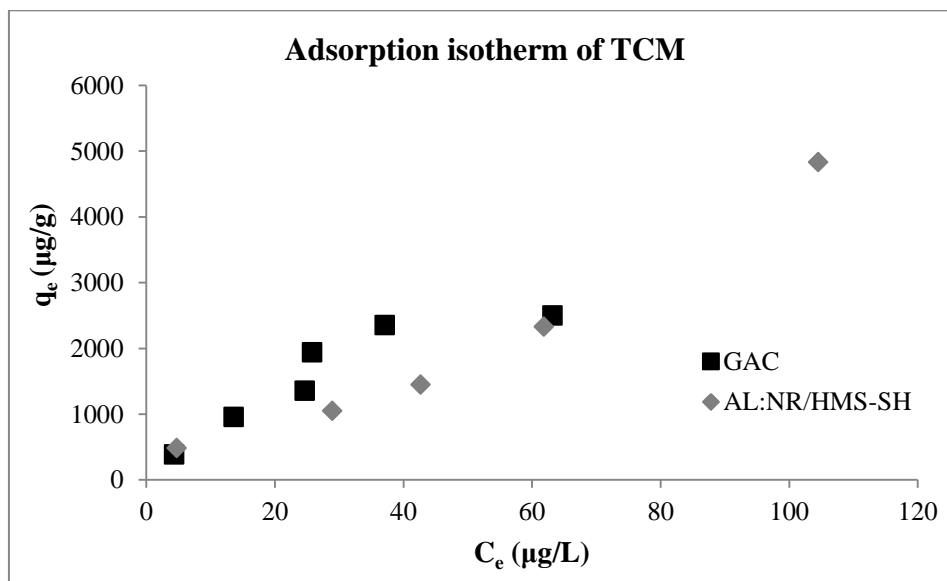


Figure 4.16 Isotherms adsorption of TCM on AL:NR/HMS-SH and GAC (pH 7 and IS 10 mM)

As the isotherm parameters that presented in Figure 4.16 and Table 4.10, the adsorption of TCM on AL:NR/HMS-SH showed the adsorption isotherm data that fitted to Freundlich isotherm model while the adsorption on GAC displayed the data was fitted to Langmuir isotherm model. The result revealed that the adsorption of TCM on synthesized material occurred on multilayer adsorption of the surface followed the concept of Freundlich isotherm model while the adsorption on GAC occurred on homogeneous surface of adsorbent and can be defined on monolayer surface. In addition, the adsorption of TCM on both materials exhibited the nearly amount of capacity.

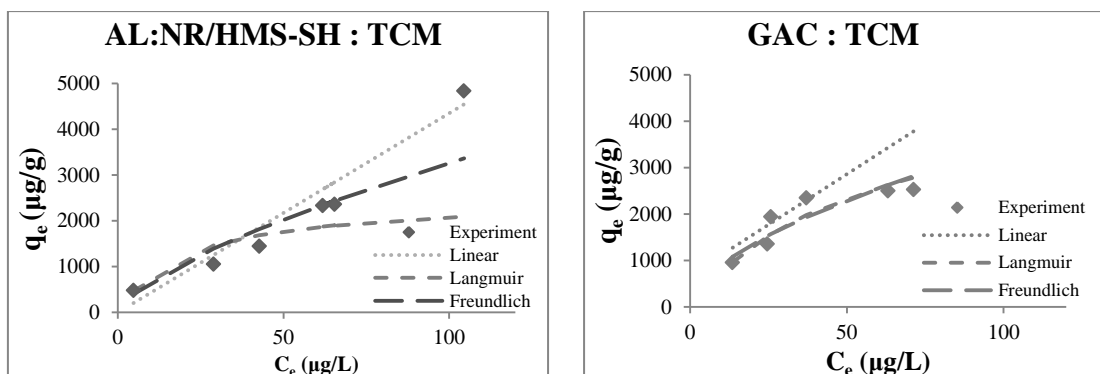


Figure 4.17 Comparison of the TCM adsorption experimental data and the data from predicted model on AL:NR/HMS-SH and GAC at pH 7 with IS 10 mM

Table 4.10 Parameters of TCM isotherm adsorption on NR/HMS-SH containing in alginate bead and GAC

Isotherm	AL:NR/HMS-SH	GAC
Linear		
K_p	44.50	36.36
R^2	0.9604	0.8119
Δq (%)	32.20	31.01
Langmuir		
q_m ($\mu\text{g g}^{-1}$)	2500	5000
K_L ($\text{L } \mu\text{g}^{-1}$)	123.46	98.04
R^2	0.9193	0.9907
Δq (%)	34.03	13.41
Freundlich		
n	1.4463	1.3503
K_F ($\mu\text{g g}^{-1}$)	136.65	140.31
R^2	0.8998	0.9518
Δq (%)	24.24	14.15

4.2.3.3 Adsorption isotherm model of TCA

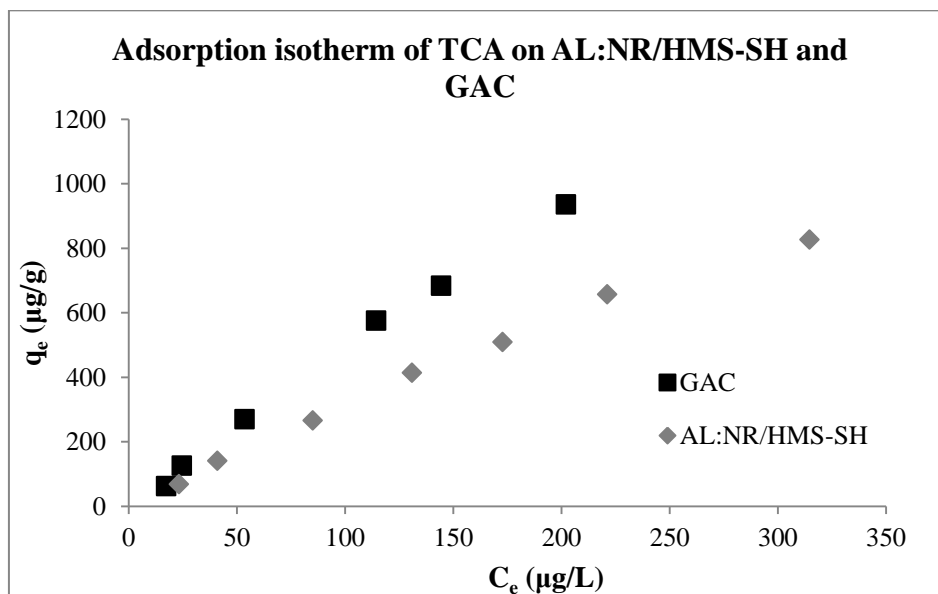


Figure 4.18 Isotherms adsorption of TCA on AL:NR/HMS-SH and GAC (pH 7 and IS 10 mM)

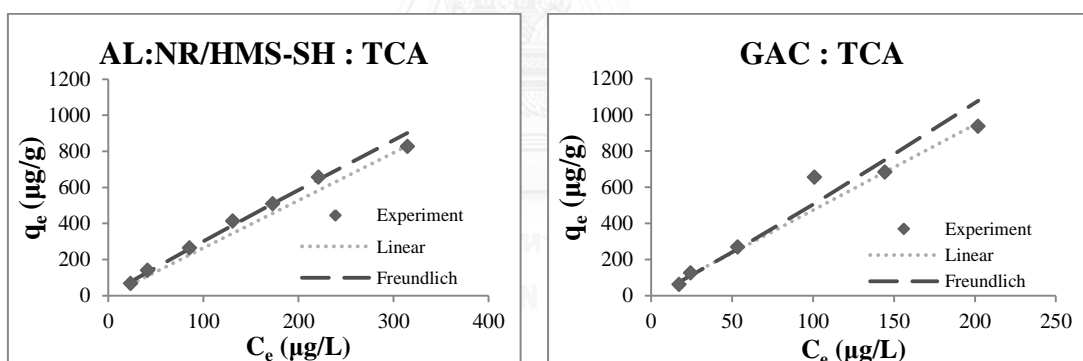


Figure 4.19 Comparison of the TCM adsorption experimental data and the data from predicted model on AL:NR/HMS-SH and GAC at pH 7 with IS 10 mM

The adsorption isotherm parameters of 1, 1, 1,-trichloroacetone (TCA) on AL:NR/HMS-SH and GAC were shown in Figure 4.18 and Table 4.11, they revealed that the adsorption of TCA on both synthesized adsorbent and GAC presented the data that best fitted with Freundlich isotherm model by regarding R^2 and Δq value. It can indicate that the adsorption of TCA appeared on heterogeneous surface of both adsorbent. Nevertheless, Langmuir isotherm model might not suitable to describe the

adsorption of TCA on these two materials. They showed the parameters from calculation on Langmuir equation that resulted in the invalid value. This might due to the adsorption mechanisms that were not occurred follow the Langmuir adsorption isotherm model.

Table 4.11 Parameters of TCA isotherm adsorption on AL:NR/HMS-SH and GAC

Isotherm	AL:NR/HMS-SH	GAC
Linear		
K_p	2.64	4.68
R^2	0.9885	0.9963
Δq (%)	15.31	14.35
Langmuir		
q_m ($\mu\text{g g}^{-1}$)	-	-
K_L ($\text{L } \mu\text{g}^{-1}$)	-	-
R^2	-	-
Δq (%)	-	-
Freundlich		
n	1.0502	0.9384
K_F ($\mu\text{g g}^{-1}$)	3.77	3.63
R^2	0.9939	0.9829
Δq (%)	7.07	14.07

4.2.3.4 Adsorption isotherm model of HAAs

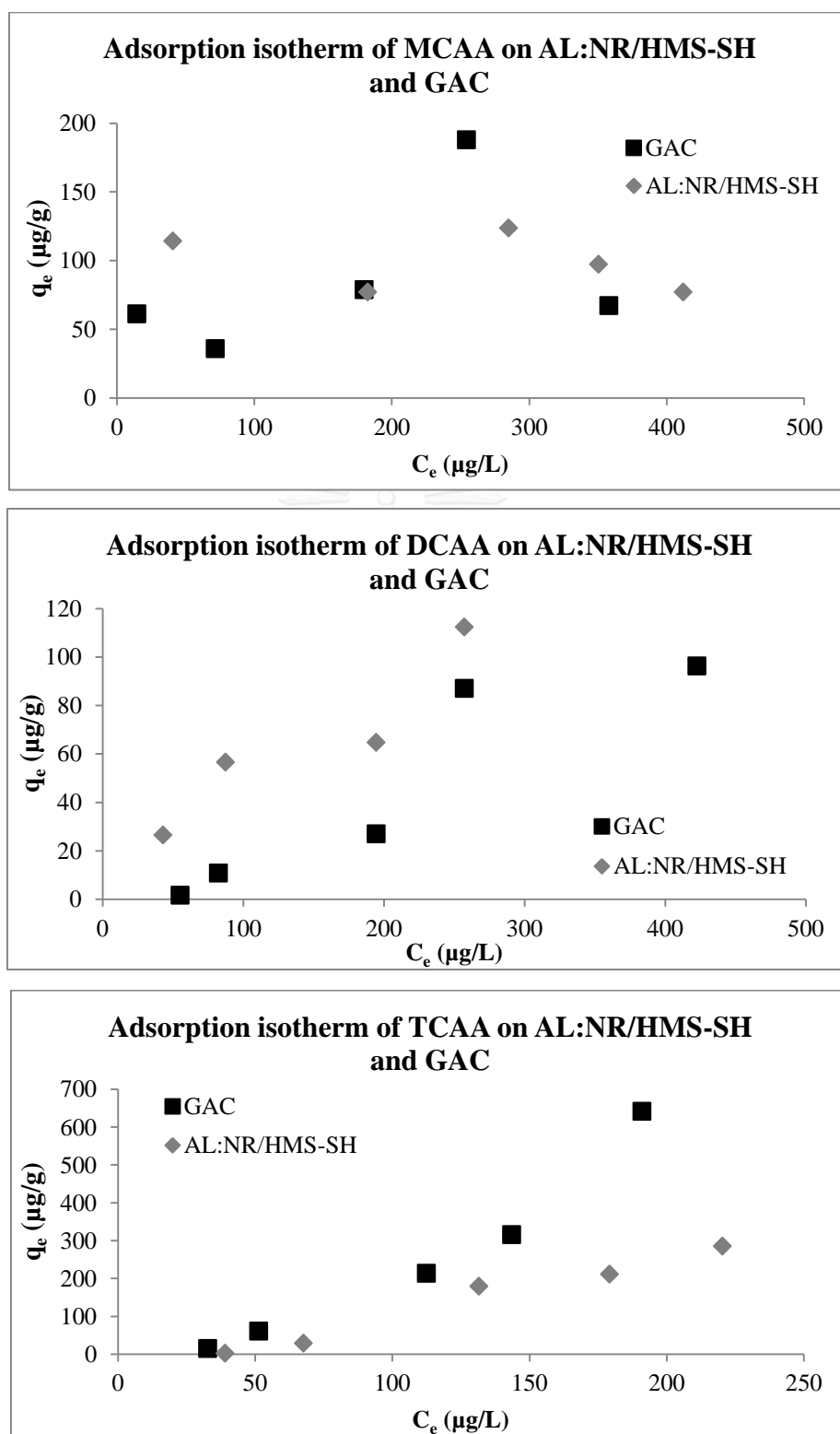


Figure 4.20 Isotherms adsorption of CAA, DCAA and TCAA on AL:NR/HMS-SH and GAC (pH 7 and IS 10 mM)

Table 4.12 Parameters of HAAs isotherm adsorption on AL:NR/HMS-SH and GAC

Isotherm	HAAs		
	MCAA	DCAA	TCAA
AL:NR/HMS-SH			
Linear	-		
K_p		0.3376	1.5922
R^2		0.8643	0.9750
Δq (%)		40.26	44.12
Langmuir	-	-	-
q_m ($\mu\text{g g}^{-1}$)			
K_L ($\text{L } \mu\text{g}^{-1}$)			
R^2			
Δq (%)			
Freundlich	-		
n		1.5092	0.3801
K_F ($\mu\text{g g}^{-1}$)		2.24	0.00029
R^2		0.9304	0.9452
Δq (%)		27.90	49.37
GAC			
Linear	-		
K_p		0.2762	3.7023
R^2		0.8613	0.9347
Δq (%)		73.50	127.17
Langmuir	-	-	-
q_m ($\mu\text{g g}^{-1}$)			
K_L ($\text{L } \mu\text{g}^{-1}$)			
R^2			
Δq (%)			
Freundlich	-		
n		0.5107	0.4999
K_F ($\mu\text{g g}^{-1}$)		0.001	0.017
R^2		0.9230	0.9836
Δq (%)		46.90	18.20

According to the isotherm parameters that showed in Figure 4.20 and Table 4.12, the adsorption of monochloroacetic acid (MCAA) on both the synthesized adsorbent and GAC appeared the data that cannot calculate to determine the adsorption isotherm model due to their indeterminate information. However, the adsorption isotherm of DCAA and TCAA on both adsorbents showed the data fitting with Freundlich isotherm model excepted the adsorption of TCAA on AL:NR/HMS-SH which showed the best fitted with Linear isotherm model. It means that most of all adsorption were multilayer adsorption of the adsorbents surface follow Freundlich model. Moreover, n values of all adsorption were less than one; means that the adsorptions were chemical adsorption and might be unfavorable adsorption. When comparing the adsorption capacities of these three HAAs on same adsorbent, it found that TCAA had higher adsorption capacities on both adsorbent due to its less water solubility than DCAA (water solubility of TCAA and DCAA are 13 g/L and 86,3 g/L respectively followed WHO, 2004&2005).

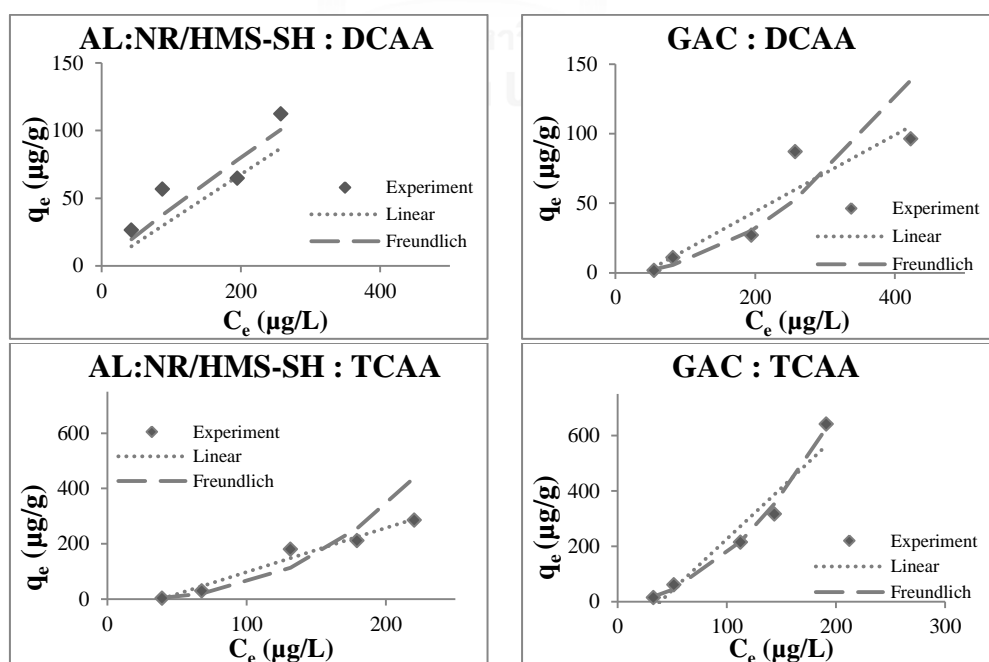


Figure 4.21 Comparison of the HAAs adsorption experimental data and the data from predicted model on AL:NR/HMS-SH and GAC at pH 7 with IS 10 mM

4.3 SELECTIVITY OF ADSORPTION

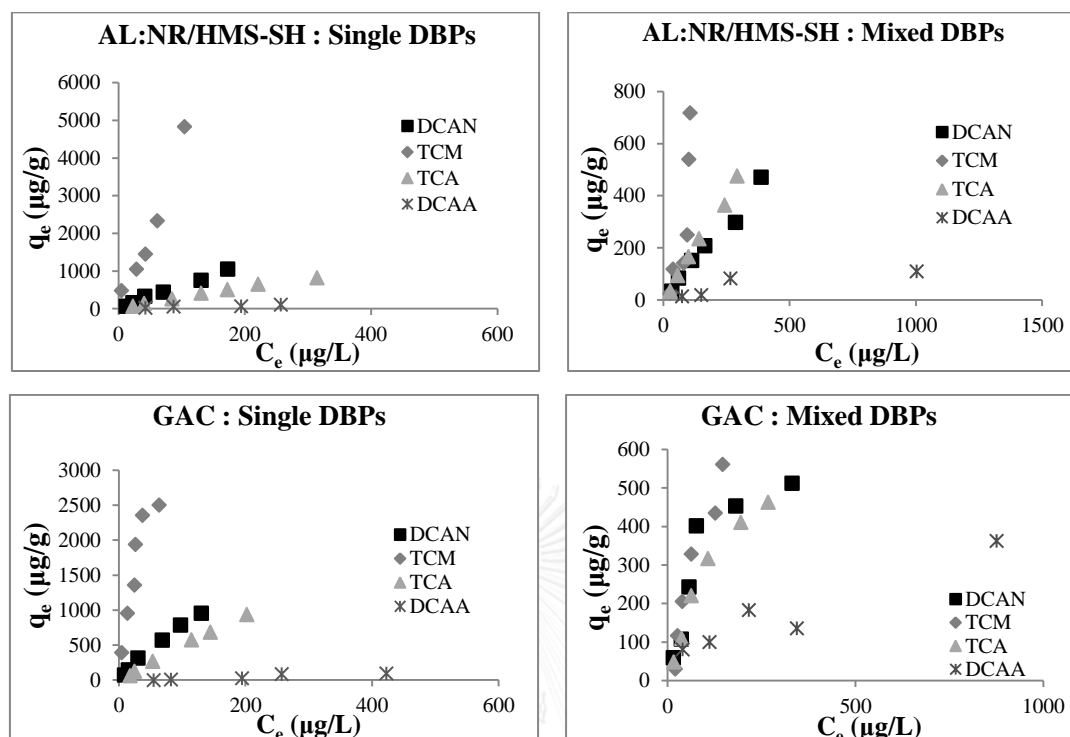


Figure 4.22 Adsorption isotherms of four-DBPs as a single solute and mixed solute on AL:NR/HMS-SH and GAC at pH 7 with IS 10 mM

As the previous information showed that there were various species of DBPs occurred in the real water supply system as mixture. Therefore, this research wanted to study the selectivity adsorption of each species of DBPs on AL:NR/HMS-SH and GAC when they are among other competitive DBPs. Figure 4.22 showed the adsorption isotherms of four types of DBPs on synthesized adsorbent and GAC in the mixed solution. The results presented that the appearance of other species had effects to the adsorption efficiencies of each species by reducing their adsorption capacities except the adsorption of DCAA. However, the enhanced of DCAA capacity had very low amount correlating with other species. When comparing the adsorption capacities of other three species (except DCAA) found that TCM were best adsorbed on both adsorbents follow by DCAN and TCA. This might cause of the hydrophobicity of

adsorbate molecules especially TCM that can be adsorbed on the synthesized adsorbent which had high hydrophobicity surface. However, for DCAN and TCA which can be adsorbed on AL:NR/HMS-SH with high capacity but lower than TCM it might due to their molecular dipole.

4.4 EFFECT OF NOM ON DBPS ADSORPTION

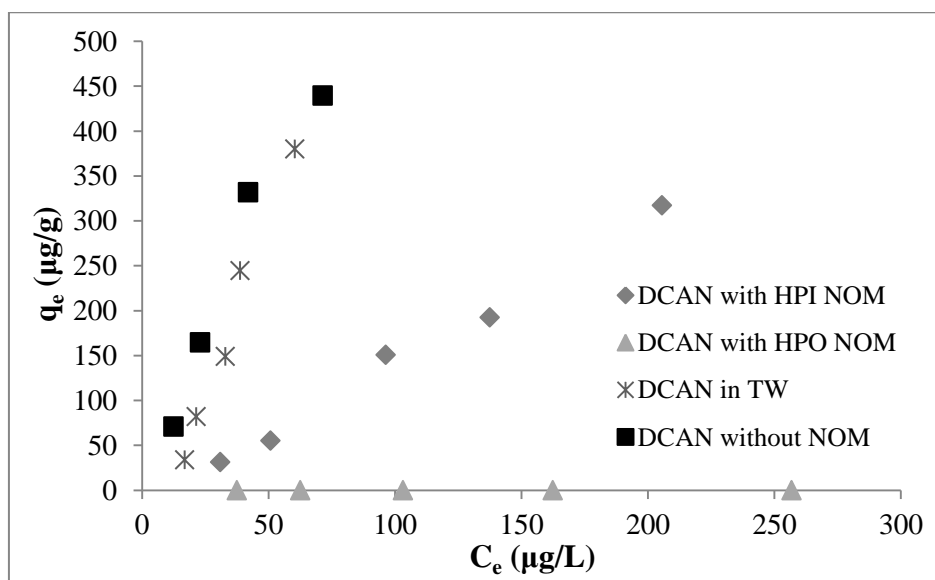


Figure 4.23 Effect of NOM on DCAN adsorption capacity on AL:NR/HMS-SH

Figure 4.23 showed the adsorption capacities of DCAN in presence of HPI and HPO NOM, in Tab water (TW), and adsorption on DCAN without adding natural organic matter in the system. The results revealed that the adsorption of DCAN in tab water resulted in the less adsorption capacity than non-adding NOM condition but not significantly different. It related to TOC values of tab water before and after adsorption that showed the decreased value after adsorption. However, the amounts of TOC between both conditions were not highly different. In addition, the ionic strength of each solution in this experiment was not equal due to the pH adjusted by very

concentrate of acidic and hydroxide in adding HPI and HPO NOM solutions. Therefore the adsorption capacity of DCAN on without NOM condition and in tap water cannot be compared with adding HPI and HPO conditions.

Furthermore, the results presented that the adsorption capacity of DCAN with HPO NOM was lower than HPI NOM. This related to the decreased TOC of adding HPO condition than adding HPI NOM condition. It might be because of the adsorption competition between DCAN and HPO NOM on synthesized adsorbent which had hydrophobic surface. Moreover, HPO NOM might be able to block adsorbent pore caused to the decreasing of active sites on adsorbent surface due to the lower adsorption capacity of DCAN.

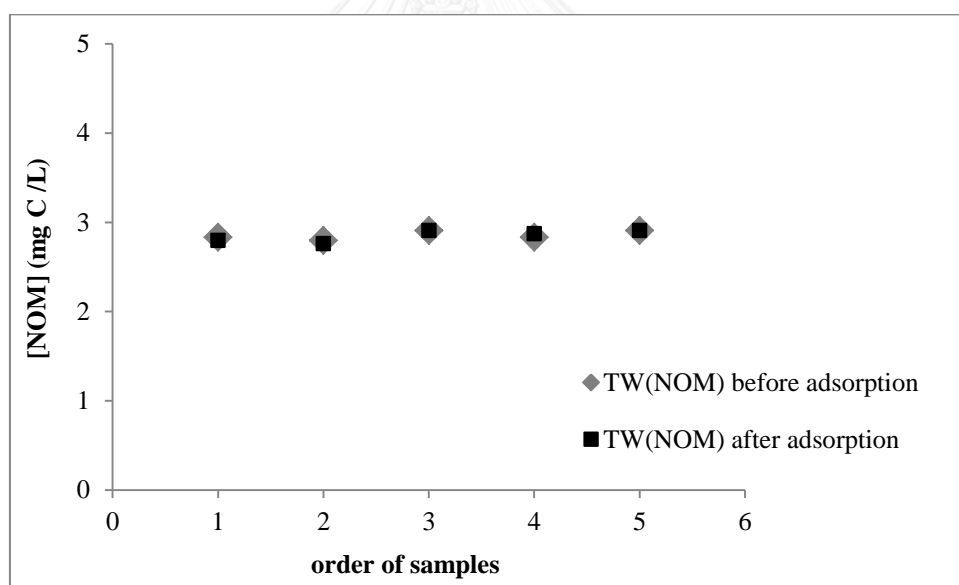


Figure 4.24 Concentration of NOM in Tab water before and after adsorption of DCAN on AL:NR/HMS-SH

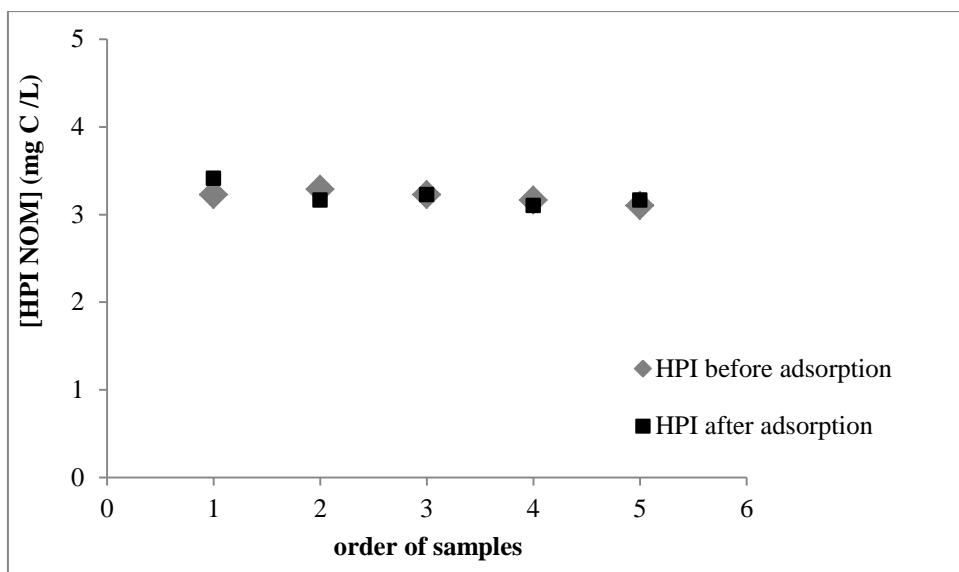


Figure 4.25 Concentration of hydrophilic NOM before and after adsorption of DCAN on AL:NR/HMS-SH

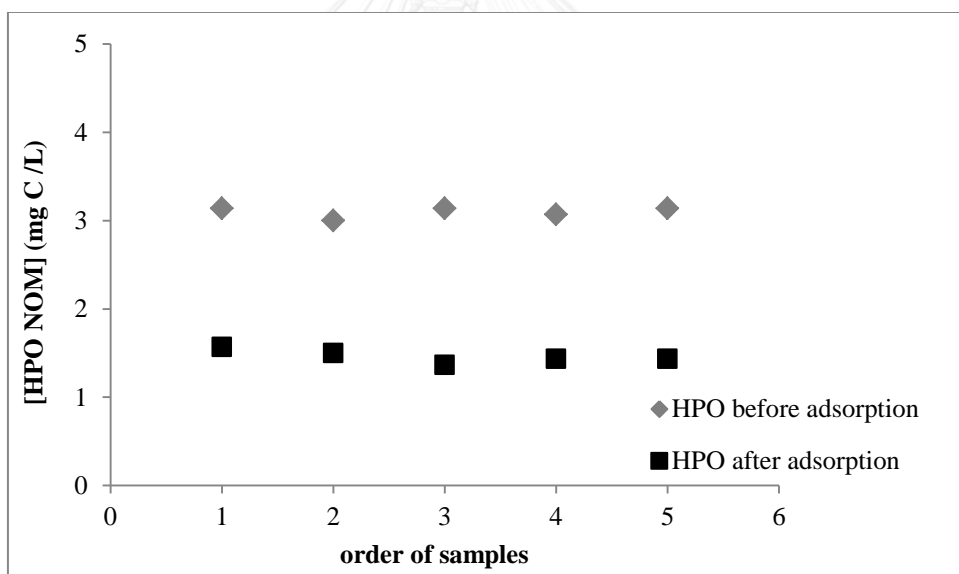


Figure 4.26 Concentration of hydrophobic NOM before and after adsorption of DCAN on AL:NR/HMS-SH

4.5 ADSORPTION ON FIXED BED CONDITION

4.5.1 Effect of bed volume

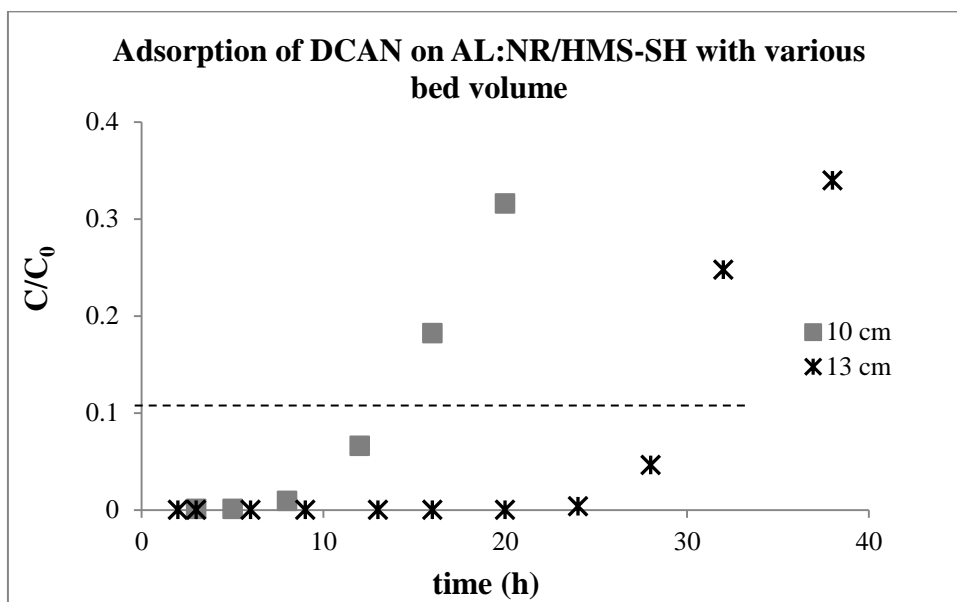


Figure 4.27 Breakthrough curve of DCAN adsorption on AL:NR/HMS-SH with various bed volume

This experiment was done by varying the bed volume of adsorbent. Breakthrough concentration was designed at 10% of removal. The breakthrough curves of two initial concentrations were showed in Figure 4.27. It revealed that the breakthrough time at breakthrough concentration increased with increasing of bed volume. Moreover, the raising of bed depth from 10 cm to 13 cm increased the breakthrough capacities from 256.81 to 372.35 cm/cm². This might because of the higher of bed volume means that it had more available sorption sites for particles to be adsorbed, moreover it found that the breakthrough capacity of DCAN adsorption increased by increasing of bed volume. Moreover, Table 4.13 presented the Thomas model parameters that indicated the higher maximum solid phase concentration with increased of column depth. However, it presented the decreasing of Thomas rate constant with more bed volume.

Table 4.13 Parameters of various bed volume of AL:NR/HMS-SH for DCAN adsorption in fixed bed condition

Bed depth (cm)	Breakthrough time (h)	Capacity of breakthrough (cm/cm ²)	Weight of Adsorbent (g)
10	14	256.81	9.3721
13	29	372.35	13.3895

Table 4.14 Parameters of the breakthrough curve models for DCAN adsorption on NR/HMS-SH containing in alginate bead in fixed bed condition

Breakthrough curve Models	Bed depth	
	10 cm	13 cm
Thomas model	8.35×10^{-5}	7.68×10^{-5}
K_{TH} (mL μg^{-1} min ⁻¹)	2,900.49	3589.69
q_0 ($\mu\text{g g}^{-1}$)	0.9501	0.8071
R^2		

CHAPTER 5

CONCLUSIONS

5.1 CONCLUSIONS

According to the adsorption kinetic study of each species of DBPs including haloacetonitrile, trihalomethane, halogenated ketone, and haloacetic acid on thiol-functionalized hexagonal mesoporous silicates based on natural rubber (NR/HMS-SH) containing alginate bead adsorbent comparing with granular activated carbon (GAC) found that the data of all kinetic adsorption were suitable to describe by the pseudo-second-order model excepted the adsorption kinetic of DCAA that appeared the indeterminate adsorption capacity of DCAA on both adsorbents. The adsorption rate and capacity of TCM showed higher amount than DCAN and TCA respectively. Moreover, the results indicated that the adsorption of each DBP reached the equilibrium longer than GAC at nearly time. The adsorption of TCM showed higher adsorption rate and capacity than DCAN and TCA respectively on both AL:NR/HMS-SH and GAC.

Considering the intraparticle model of the adsorptions, they presented multilinearity that can intimate to the multiple step of adsorption, and showed the rate controlling step of the adsorption that can be the film diffusion and/or intraparticle diffusion step. As the results of DBPs adsorption isotherm, they revealed the fitted data to various isotherm models relying on the characteristic of each DBP on adsorbents surface. When comparing the adsorption capacity of each species of DBPs on AL:NR/HMS-SH resulted that the lower water solubility DBPs such as TCAN, TCM and TCA had higher adsorption capacity than the lower water solubility DBPs.

Furthermore, the adsorption capacities of each DBP on synthesized adsorbent were nearly with GAC at lower amount excepted the adsorption of TCAN and TCM which showed the higher efficiency on AL:NR/HMS-SH adsorbent.

Moreover, the study found that the presented of other DBP species in the same solution affected to the adsorption efficiencies of each DBPs comparing with the adsorption of the single solution by decreasing their adsorption capacities.

Furthermore, the research resulted that the adsorption of DCAN had lower efficiency when there was HPO NOM appeared in the system more than the appearance of HPI NOM. It might because of the effect of competitive between HPO NOM and DCAN on active sites of adsorbent surface.

Finally, the adsorption study in the fixed bed condition by varying the bed volume found that the higher bed depth increased breakthrough time and breakthrough capacity due to the increasing of the sorption site for particle to be adsorbed.

5.2 RECOMMENDATIONS

5.2.1 This synthesized adsorbent should be investigated and improved the stability.

5.2.2 The adsorption experiments should be prepared with the adsorption on HMS-SH containing alginate beads (without natural rubber).

5.2.3 The adsorption experiment on the fixed bed condition should be studied by investigated more variant such as more various bed depth and varying flow rate

REFERENCES

- 551.1, E. M. (1990). Determination of Chlorination Disinfection Byproducts, Chlorinated solvents, and Halogenated Pesticides/Herbicides in Drinking Water by Liquid-Liquid Extraction and Gas Chromatography with Electron-capture Detection. *National Exposure Research Laboratory, Office of Research and Development, U.S. Environmental Protection Agency, Cincinnati, OHIO.*
- 552.2, E. M. (1990). Determination of Haloacetic Acids and Dalapon in Drinking Water by Liquid-Liquid Extraction, Derivatization and Gas Chromatography with Electron-capture Detection. *National Exposure Research Laboratory, Office of Research and Development, U.S. Environmental Protection Agency, Cincinnati, OHIO.*
- Ahmad, A. A., & Hameed, B. H. (2010). Fixed-bed adsorption of reactive azo dye onto granular activated carbon prepared from waste. *Journal of Hazardous Materials, 175*(1–3), 298-303.
- Ates, N., et al. (2009). Removal of disinfection by-product precursors by UF and NF membranes in low-SUVA waters. *Journal of Membrane Science, 328*(1–2), 104-112.
- Athens, G. L., et al. (2009). Functionalization of mesostructured inorganic–organic and porous inorganic materials. *Current Opinion in Colloid & Interface Science, 14*(4), 281-292.
- Bibby, A., & Mercier, L. (2002). Mercury(II) Ion Adsorption Behavior in Thiol-Functionalized Mesoporous Silica Microspheres. *Chemistry of Materials, 14*(4), 1591-1597.
- Bohart, G. S., & Adams, E. Q. (1920). SOME ASPECTS OF THE BEHAVIOR OF CHARCOAL WITH RESPECT TO CHLORINE.1. *Journal of the American Chemical Society, 42*(3), 523-544.
- Bond, T., et al. (2011). Treatment of disinfection by-product precursors. *Environmental Technology, 32*(1), 1-25.
- Bond, T., et al. (2011). Occurrence and control of nitrogenous disinfection by-products in drinking water – A review. *Water Research, 45*(15), 4341-4354.
- Chu, W., et al. (2011). Impacts of drinking water pretreatments on the formation of nitrogenous disinfection by-products. *Bioresource Technology, 102*(24), 11161-11166.
- Desta, M., B., (2013). Batch Sorption Experiments: Langmuir and Freundlich Isotherm Studies for the Adsorption of Textile Metal Ion onto Teff Straw Agricultural Waste. *Journal of Thermodynamics 2013.*

- Feretti, D., et al. (2012). Ground and Surface Water for Drinking: A Laboratory Study on Genotoxicity Using Plant Tests. *Journal of Public Health Research*, 1(1), 31-37.
- Fryxell, G. E., et al. (1999). Design and Synthesis of Selective Mesoporous Anion Traps. *Chemistry of Materials*, 11(8), 2148-2154.
- Gopal, K., et al. (2007). Chlorination byproducts, their toxicodynamics and removal from drinking water. *Journal of Hazardous Materials*, 140(1-2), 1-6.
- Hou, Y., et al. (2012). Carbonaceous and nitrogenous disinfection by-product formation in the surface and ground water treatment plants using Yellow River as water source. *J Environ Sci (China)*, 24(7), 1204-1209.
- Hsin Hsin Tung, R. F. U., Yuefeng F. Xie. (2006). HAA removal by GAC adsorption. *American Water Works Association*, 107-112.
- Hua, G., & Reckhow, D. A. (2007). Characterization of Disinfection Byproduct Precursors Based on Hydrophobicity and Molecular Size. *Environmental Science & Technology*, 41(9), 3309-3315.
- Huang, Y. (2009). Functionalization of mesoporous silica nanoparticles and their applications in organo-, metallic and organometallic catalysis.
- Jayhyun Park, H. K., and Jaikoo Park. (2012). Characteristics of Thiol-Functionalized Mesoporous Silica and Its Application to Silver and Cadmium Ion Removal. *International Journal of Environmental Science and Development*, 3(2), 81-85.
- Jerry A. Leenheer, A. D. a. P., & Westerhoff. (2007). DISSOLVED ORGANIC NITROGEN FRACTIONATION. *Annals of Environmental Science*, 1, 45-56.
- Kim, H.-C., & Yu, M.-J. (2005). Characterization of natural organic matter in conventional water treatment processes for selection of treatment processes focused on DBPs control. *Water Research*, 39(19), 4779-4789.
- Kim, H., et al. (2002). Formation of disinfection by-products in chlorinated swimming pool water. *Chemosphere*, 46(1), 123-130.
- Kim, J., & Kang, B. (2008). DBPs removal in GAC filter-adsorber. *Water Research*, 42(1-2), 145-152.
- Kim, T. Y., et al. (2008). Adsorption equilibrium of copper ion and phenol by powdered activated carbon, alginate bead and alginate-activated carbon bead. *Journal of Industrial and Engineering Chemistry*, 14(6), 714-719.

- Kleiser, G., & Frimmel, F. H. (2000). Removal of precursors for disinfection by-products (DBPs) — differences between ozone- and OH-radical-induced oxidation. *Science of The Total Environment*, 256(1), 1-9.
- Lee, K. Y., & Mooney, D. J. (2012). Alginate: Properties and biomedical applications. *Progress in Polymer Science*, 37(1), 106-126.
- Lee, W., & Westerhoff, P. (2005). Dissolved Organic Nitrogen Measurement Using Dialysis Pretreatment. *Environmental Science & Technology*, 39(3), 879-884.
- Lee, W., et al. (2007). Dissolved Organic Nitrogen as a Precursor for Chloroform, Dichloroacetonitrile, N-Nitrosodimethylamine, and Trichloronitromethane. *Environmental Science & Technology*, 41(15), 5485-5490.
- Liangming Wei, N. H. a. Y. Z. (2010). Synthesis of Polymer—Mesoporous Silica Nanocomposites. *Materials*, 3, 4066-4079.
- Lin, S., et al. (2013). Silver nanoparticle-alginate composite beads for point-of-use drinking water disinfection. *Water Research*, 47(12), 3959-3965.
- Lin, Y.-B., et al. (2005). Removal of organic compounds by alginate gel beads with entrapped activated carbon. *Journal of Hazardous Materials*, 120(1-3), 237-241.
- Marhaba, T. F., & Van, D. (2000). The variation of mass and disinfection by-product formation potential of dissolved organic matter fractions along a conventional surface water treatment plant. *Journal of Hazardous Materials*, 74(3), 133-147.
- Muellner, M. G., et al. (2007). Haloacetonitriles vs. Regulated Haloacetic Acids: Are Nitrogen-Containing DBPs More Toxic? *Environmental Science & Technology*, 41(2), 645-651.
- Nuntang, S., et al. (2014). Novel mesoporous composites based on natural rubber and hexagonal mesoporous silica: Synthesis and characterization. *Materials Chemistry and Physics*, 143(3), 1199-1208.
- Nuntang, S., et al. (2014). Organosulfonic acid-functionalized mesoporous composites based on natural rubber and hexagonal mesoporous silica. *Materials Chemistry and Physics*, 147, 583-593.
- Park, H. G., et al. (2007). Activated carbon-containing alginate adsorbent for the simultaneous removal of heavy metals and toxic organics. *Process Biochemistry*, 42(10), 1371-1377.
- Park, J., et al. (2012). Characteristics of Thiol-Functionalized Mesoporous Silica and Its Application to Silver and Cadmium Ion Removal. *International Journal of Environmental Science and Development*, 3(2), 81-85.

- Plazinski, W., et al. (2013). Modeling of sorption kinetics: the pseudo-second order equation and the sorbate intraparticle diffusivity. *Adsorption*, 19, 1055–1064.
- Plewa, M. J., et al. (2004). Halonitromethane Drinking Water Disinfection Byproducts: Chemical Characterization and Mammalian Cell Cytotoxicity and Genotoxicity. *Environmental Science & Technology*, 38(1), 62-68.
- Prarat, P., et al. (2011). Adsorption characteristics of haloacetonitriles on functionalized silica-based porous materials in aqueous solution. *Journal of Hazardous Materials*, 192(3), 1210-1218.
- Prarat, P., et al. (2013). Removal of haloacetonitriles in aqueous solution through adsolubilization process by polymerizable surfactant-modified mesoporous silica. *Journal of Hazardous Materials*, 244–245(0), 151-159.
- Punyapalakul, P., et al. (2009). Effects of crystalline structures and surface functional groups on the adsorption of haloacetic acids by inorganic materials. *Journal of Hazardous Materials*, 171, 491–499.
- Tang, L.-C., et al. (2013). Mechanical properties and fracture behaviors of epoxy composites with multi-scale rubber particles. *Materials Chemistry and Physics*, 141(1), 333-342.
- Tung, H.-h., & Xie, Y. F. (2006). Disinfection By-Product Removal by Point of Use Carbon Filter. *Water Conditioning & Purification*.
- Ueno, H., et al. (1996). Disinfection by-products in the chlorination of organic nitrogen compounds: By-products from kynurenine. *Chemosphere*, 33(8), 1425-1433.
- Uyak, V., et al. (2007). Disinfection by-products precursors removal by enhanced coagulation and PAC adsorption. *Desalination*, 216(1–3), 334-344.
- Wang, Z., et al. (2012). Influence of Bacterial Extracellular Polymeric Substances on the Formation of Carbonaceous and Nitrogenous Disinfection Byproducts. *Environmental Science & Technology*, 46(20), 11361-11369.
- Wei, X., et al. (2013). Occurrence of Regulated and Emerging Iodinated DBPs in the Shanghai Drinking Water. *PLoS ONE*, 8(3), e59677.
- Y.S Ho, G. M. (1999). Pseudo-second order model for sorption processes. *Process Biochemistry*, 34(5), 451–465.
- Zehra Yigit, H. I., Guven Seydioglu, and Vedat Uyak. (2009). Enhanced Coagulation of Disinfection By-Products Precursors in Porsuk Water Resource, Eskisehir. *World Academy of Science, Engineering and Technology*, 30, 1648-1651.

- Zhao, Y., et al. (2013). Disinfection byproduct precursor removal by enhanced coagulation and their distribution in chemical fractions. *Journal of Environmental Sciences*, 25(11), 2207-2213.
- Zhe XU, et al. (2013). Mathematically modeling fixed-bed adsorption in aqueous systems. *Journal of Zhejiang University-SCIENCE A (Applied Physics & Engineering)*, 14(3), 155-176.
- Zou, H., et al. (2008). Polymer/Silica Nanocomposites: Preparation, Characterization, Properties, and Applications. *Chemical Reviews*, 108(9), 3893-3957.



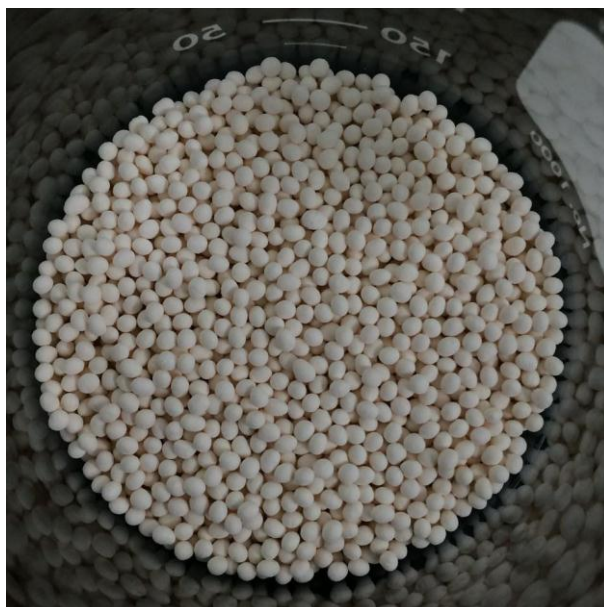




APPENDIX A
ADSORBENT SYNTHESIS AND CHARACTERIZATION

จุฬาลงกรณ์มหาวิทยาลัย
CHULALONGKORN UNIVERSITY

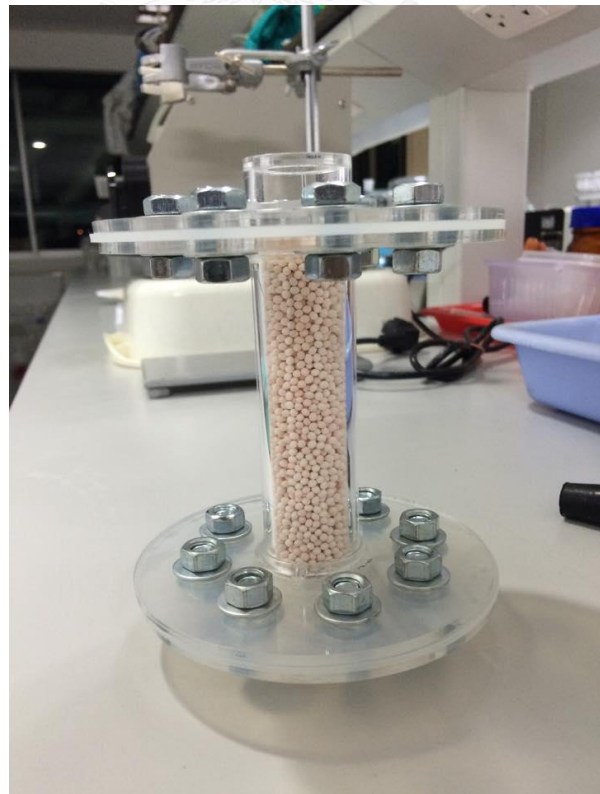
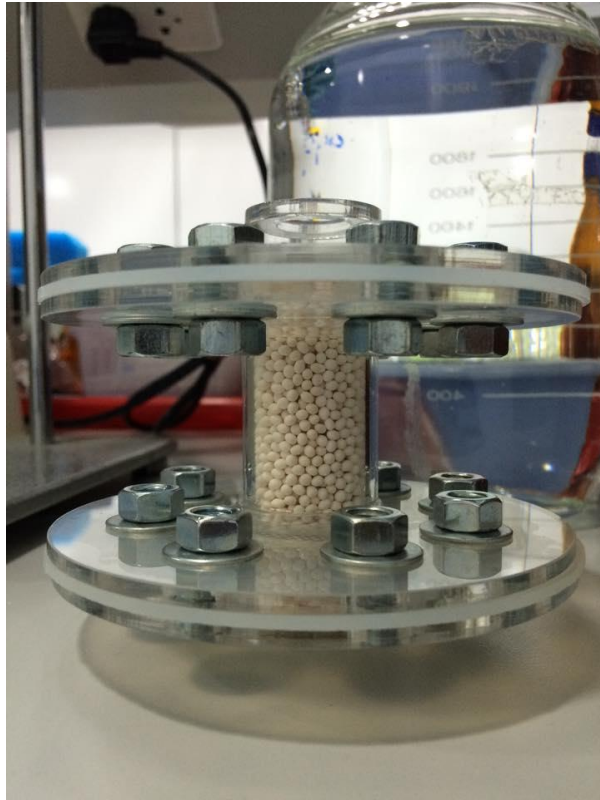
1. AL:NR/HMS-SH

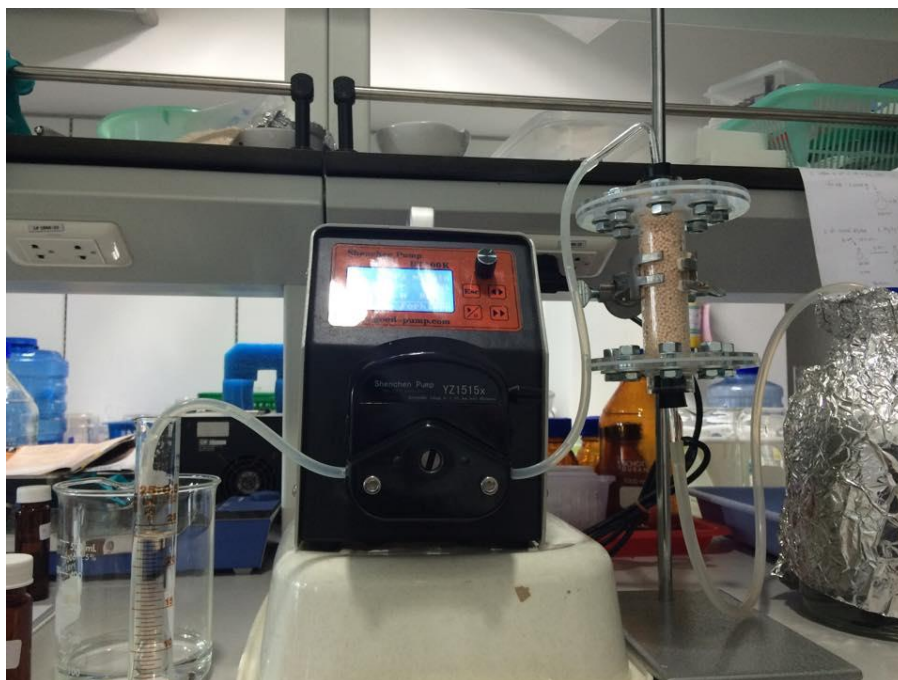


2. AL:NR/HMS-SH character after adsorption

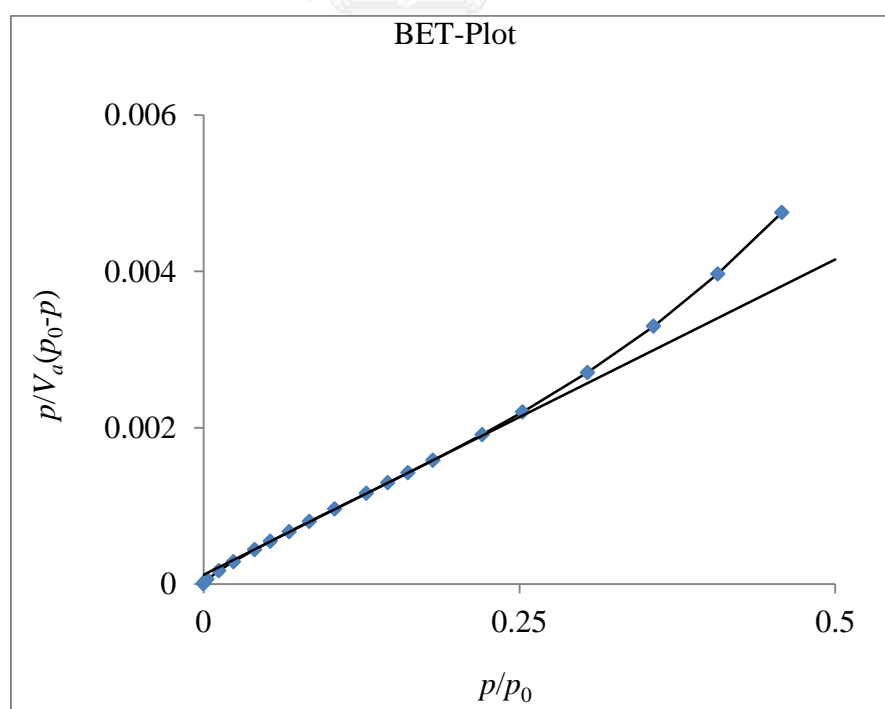


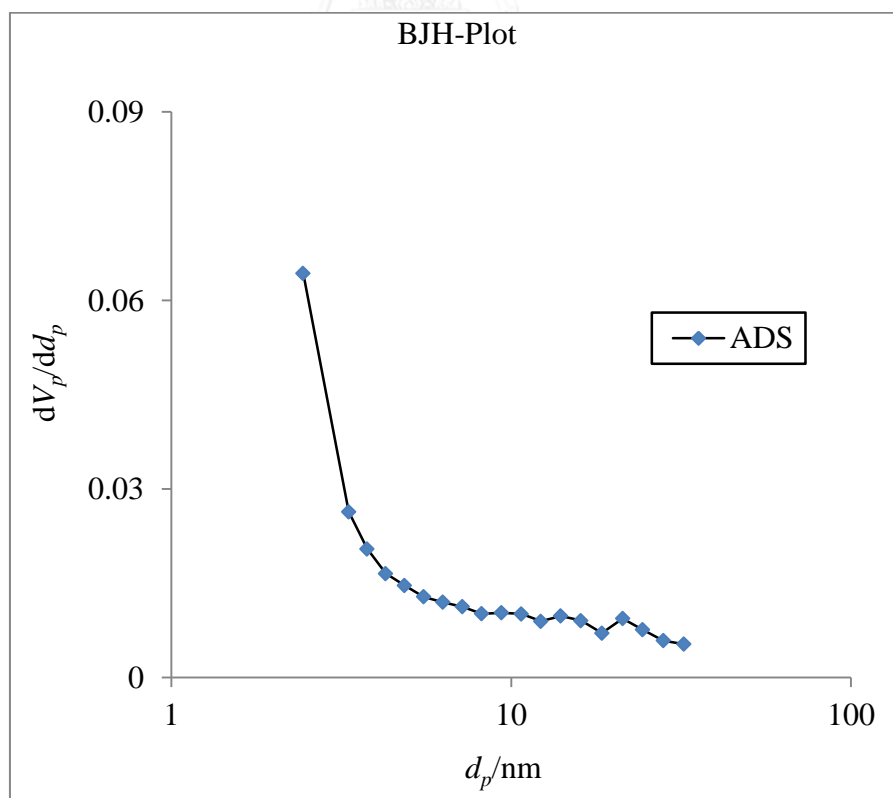
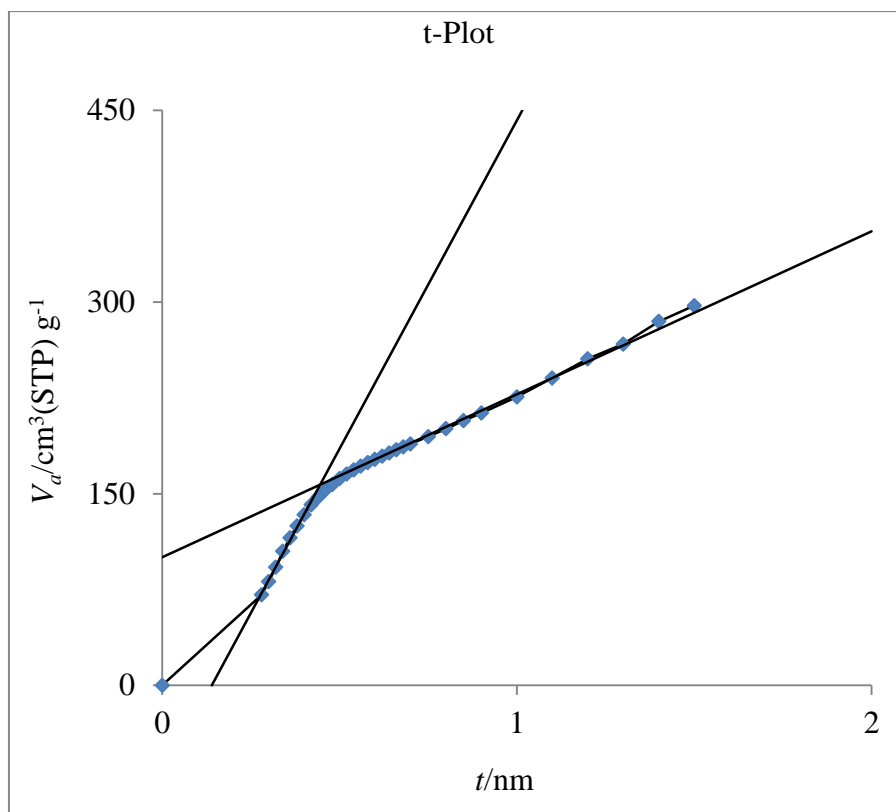
3. Fixed bed column experiment

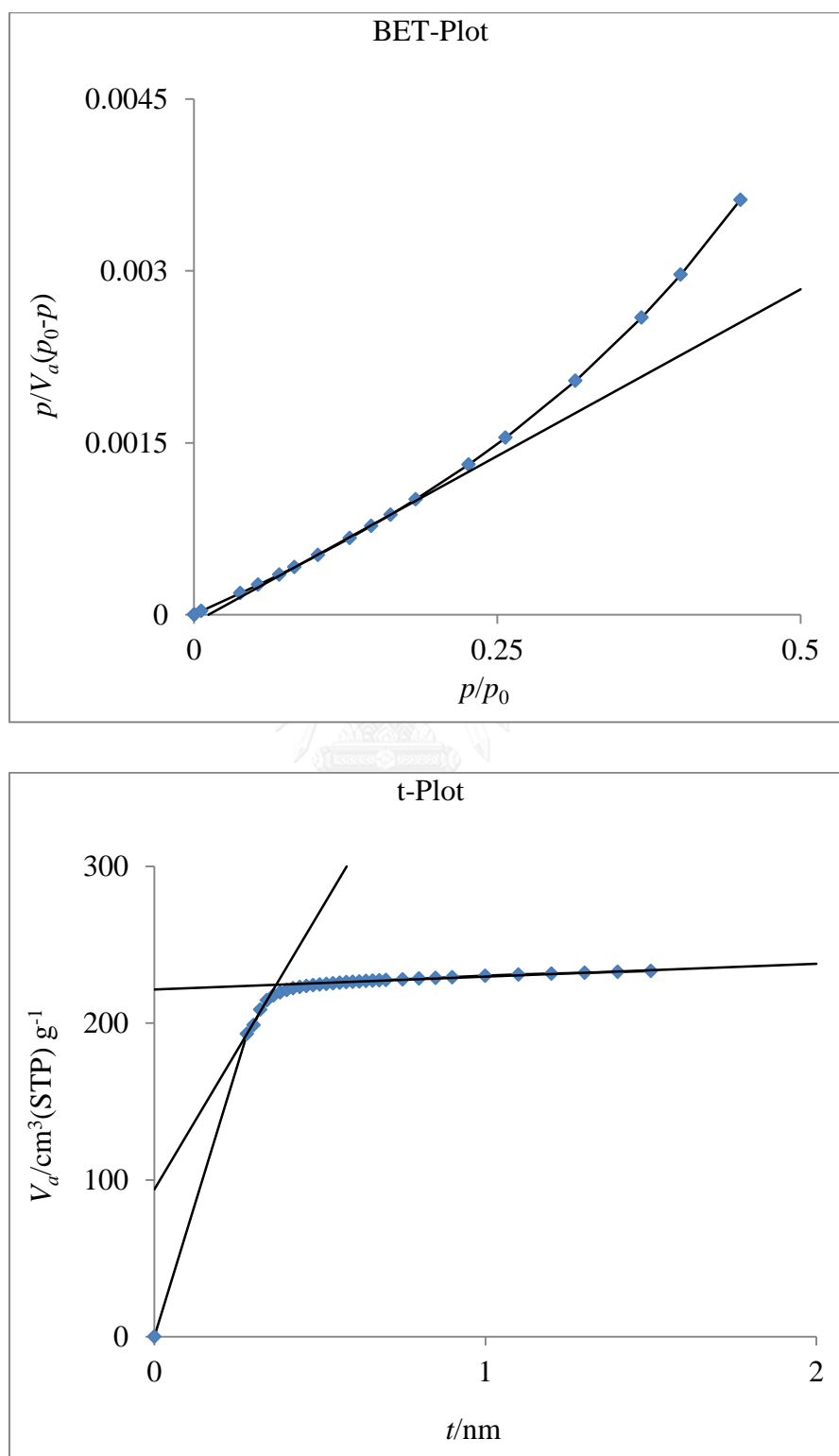


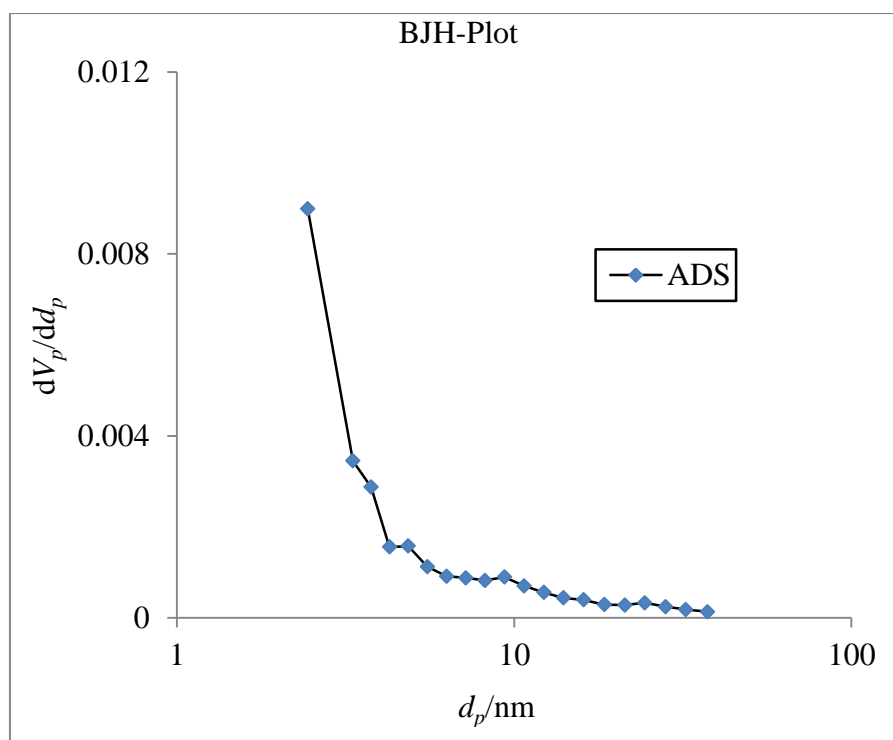


4. N₂ adsorption-desorption isotherm of AL:NR/HMS-SH





5. N₂ adsorption-desorption isotherm of GAC



6. Surface charge density investigation by Acid-Base titration

Table 1.1 The calculation data from surface charge density of AL:NR/HMS-SH

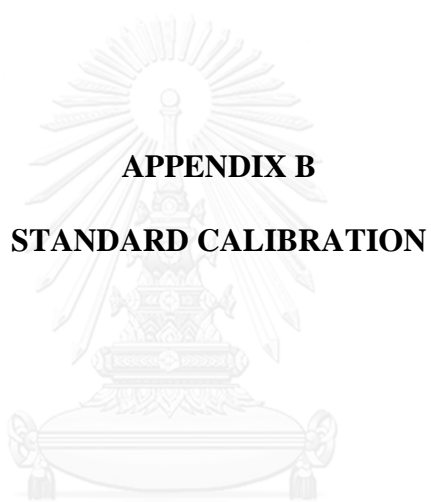
Sample	pH	Surface charge (C/m ²)
1	4.57	0.022156855
2	4.78	0.017798395
3	5.18	0.015639256
4	5.46	0.012292066
5	5.74	0.006419229
6	5.77	0.003042098
7	5.81	0.000625023
8	5.92	-0.001045302
9	6.04	-0.003407503
10	6.2	-0.006697311
11	6.33	-0.010404244
12	6.4	-0.013834088
13	6.62	-0.02102399
14	6.68	-0.024666966

Table 1.2 The calculation data from surface charge density of GAC

Sample	pH	Surface charge (C/m ²)
1	4.96	0.01571184
2	5.76	0.01395892
3	6.58	0.012276383
4	6.69	0.009638096
5	6.76	0.006384228
6	6.83	0.002612311
7	6.98	0.00061407
8	7.07	-0.006579938
9	7.19	-0.01299541
10	7.3	-0.019101477
11	7.36	-0.023324535
12	7.43	-0.038059234
13	7.42	-0.049571378

7. TOC that released from AL:NR/HMS-SH at time t

Time (h)	TOC (mg/L)
0.5	1.181
1	1.089
2	1.018
4	1.606
8	1.090
12	1.335
18	2.093
24	1.719



APPENDIX B

STANDARD CALIBRATION

จุฬาลงกรณ์มหาวิทยาลัย
CHULALONGKORN UNIVERSITY

Analysis concentration of DBPs by Gas Chromatography (GAC) with Electron Capture Detector (ECD)

Laboratory Equipment and chemical reagent

1. Gas Chromatography with Electron capture detector (GC/ECD)
2. Stock solution of each DBPs including MCAN, DCAN, TCAN, TCM, TCA, MCAA, DCAA, and TCAA
3. Phosphate buffer IS 10 mM
4. Volumetric flask
5. Micropipette
6. Deionized water

Preparation of DBPs stock solution at 500 ppm

Table1 the preparation of stock DBPs at 500 ppm

DBPs	Volume of DBPs (μL)	Total volume (mL)
MCAN	4.2	10
DCAN	3.7	10
TCAN	3.5	10
TCM	3.4	10
TCA	3.7	10
MCAA	3.1	10
DCAA	3.2	10
TCAA	3.1	10

DBPs at volume that showed on above table were dissolved in deionized water by using micropipette adding DI water to adjust the volume.

After that, dilute the stock 500 ppm of DBPs to 1 ppm with DI water in 100 mL of volumetric flask by calculation from equation 1 as below.

$$C_1V_1 = C_2V_2 \quad (1)$$

Example Preparation of DBP at 1 mg/L from stock solution 500 mg/L in 100 mL of volumetric flask

$$C_1V_1 = C_2V_2$$

$$500 \text{ mg/L} \times V_1 = 1 \text{ mg/L} \times 100 \text{ mL}$$

$$V_1 = 0.2 \text{ mL}$$

Therefore, pipetted stock solution of DBP 0.2 mL into 100 mL of volumetric flask and adjusted volume of solution by phosphate buffer 10 mM until final volume was 100 mL.

Then, preparation of DBP standard concentration (in ppb unit) by diluting from the stock 1 ppm of DBP in 25 mL of volumetric flask by calculation from equation 1.

Table 2 volume of stock DBP 1 ppm to prepare standard concentration

Concentration of DBPs (ppb)	Volume of stock 1 ppm (mL)
1	0.025
5	0.125
25	0.625
50	1.250
100	2.50
150	3.75
200	5.00
250	6.25

GC analytical condition

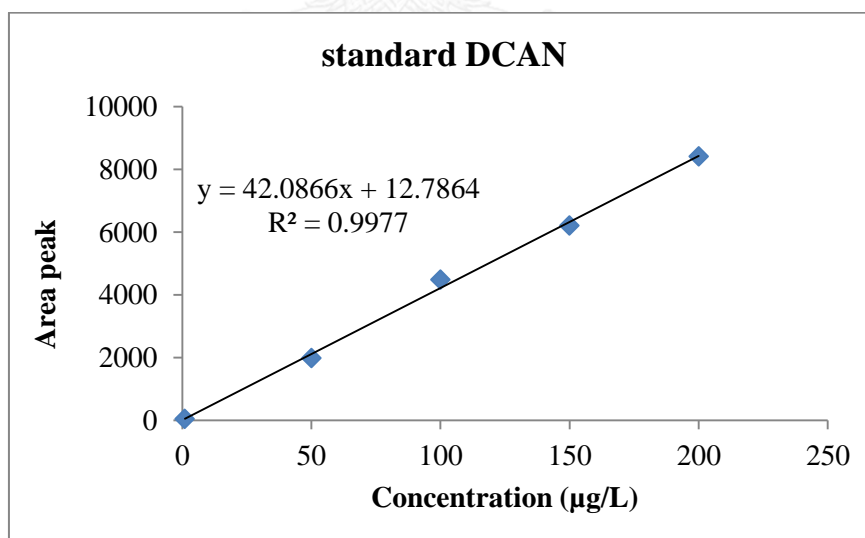
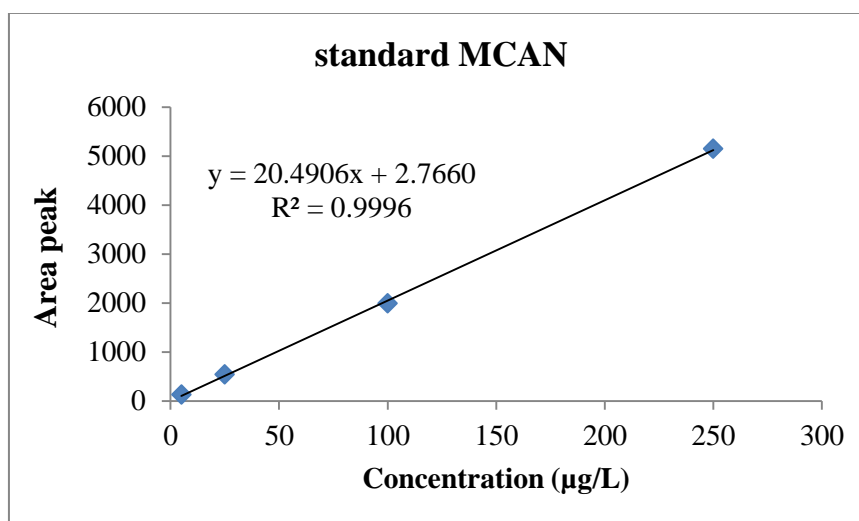
The gas chromatography condition was performed as follows: the velocity of Helium-carrier gas was 25 cm/sec and used N₂ gas as a make-up gas. The column was fused silica capillary column (VF-X Varian, 30 m x 0.32 mm i.d. x 0.10 μm film thickness). The inject temperature was set at 200 °C with splitless mode. The detector temperature was maintained at 300 °C. The temperature of column oven was programmed as follow; (1) set initial temperature at 35°C for 7 min, (2) ramping to 55°C with rate at 5°C/min, and (3) ramping to 110°C with rate at 7.5°C/min.

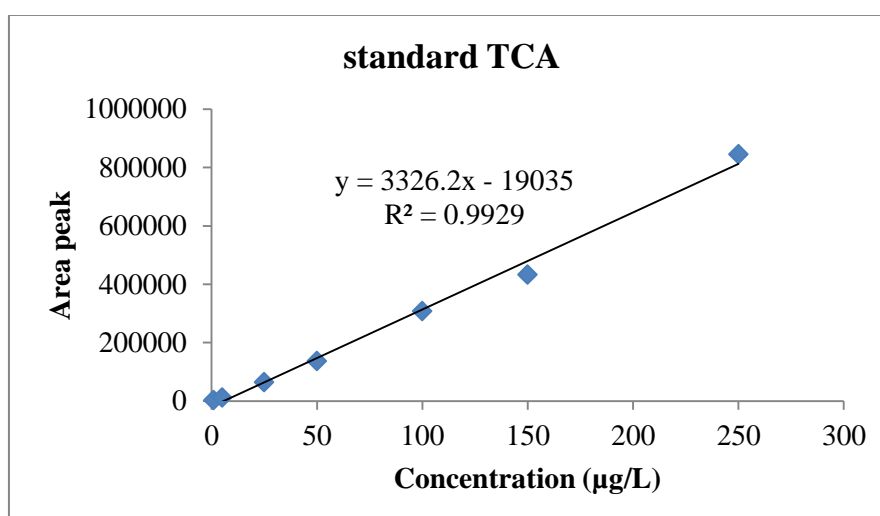
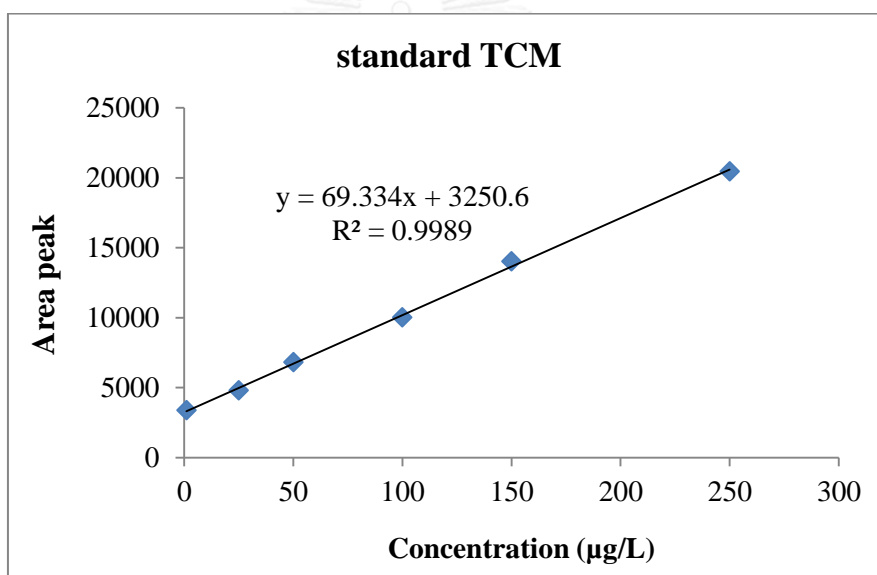
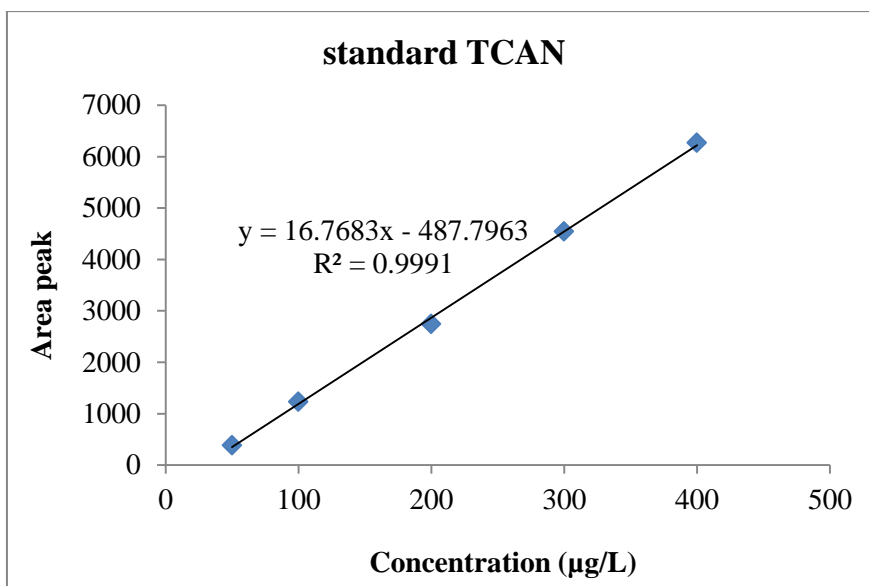
Table3 Retention time of each DBP on VF-X Varian column

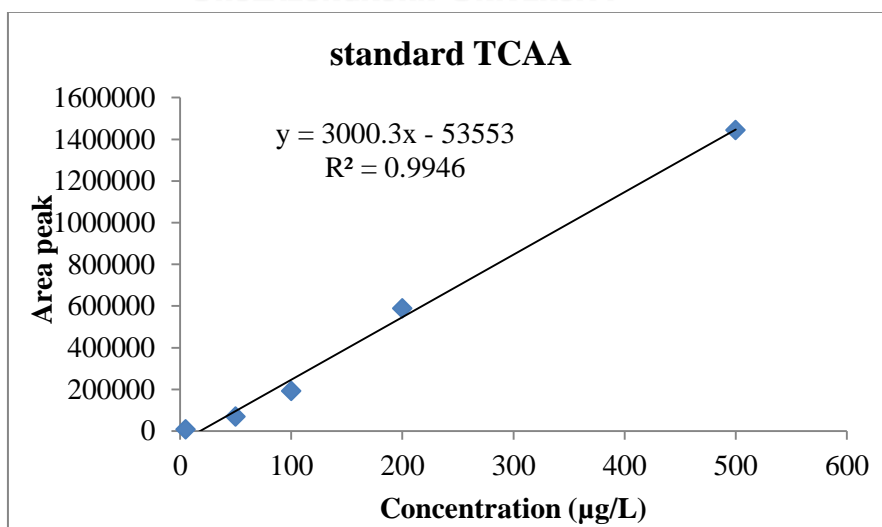
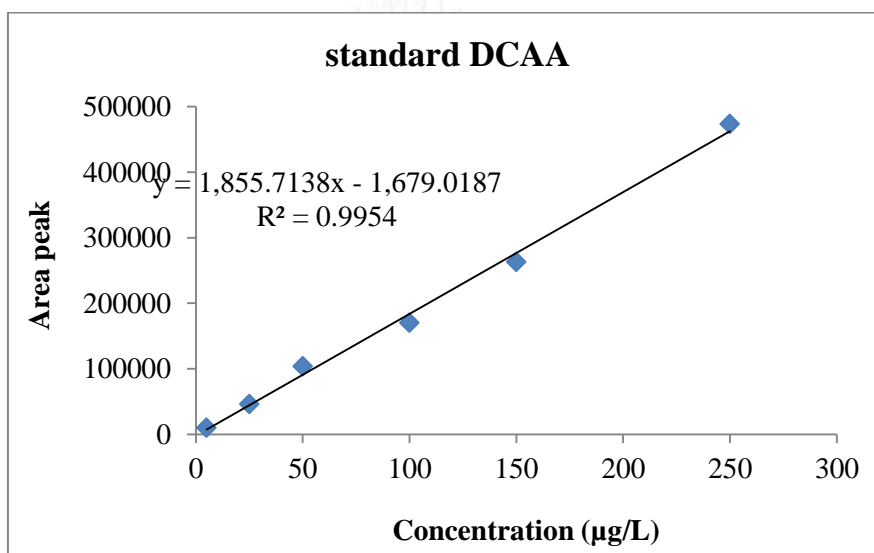
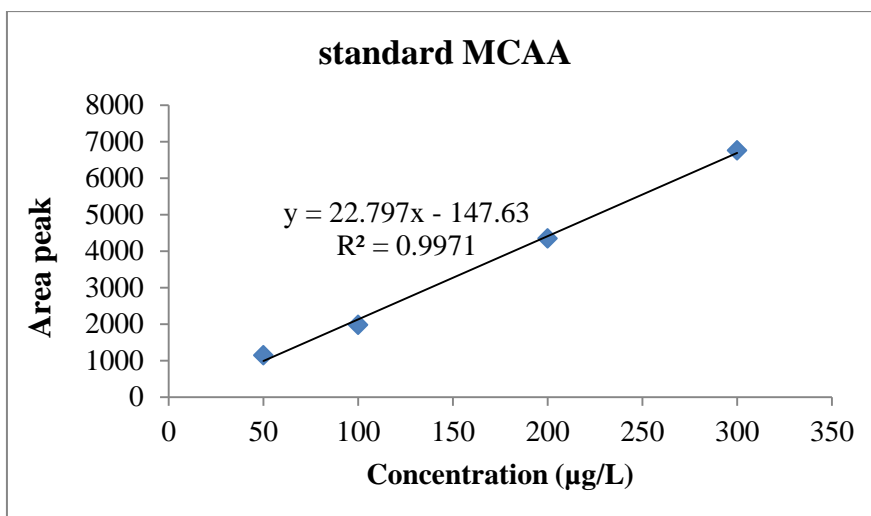
DBPs	Retention time
MCAN	3.410
DCAN	4.091
TCAN	3.128
TCM	2.858
TCA	6.942
MCAA	4.585
DCAA	7.192
TCAA	8.446

Standard curve

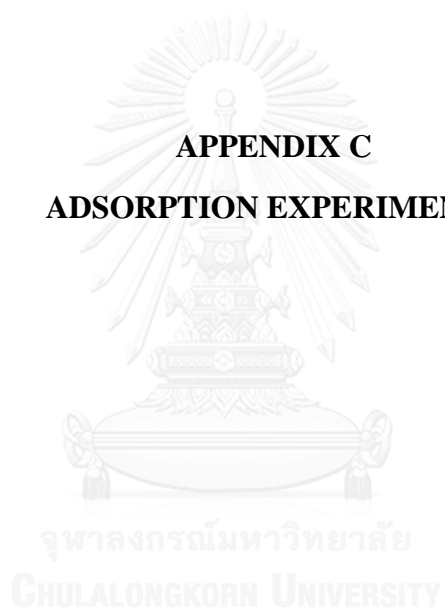
The concentrations of standard solution of DBPs were analyzed by GC/ECD with VF-X column. Standard curve was plotted between peak area and concentration of standard solution of DBP.







APPENDIX C
ADSORPTION EXPERIMENTS



1. Adsorption kinetic study

Table 1.1 Data from adsorption kinetic of DCAN, TCM, TCA, and DCAA on AL:NR/HMS-SH at pH 7 and IS 10 mM

DCAN		TCM		TCA		DCAA	
Time (h)	q_t ($\mu\text{g/g}$)	Time (h)	q_t ($\mu\text{g/g}$)	Time (h)	q_t ($\mu\text{g/g}$)	Time (h)	q_t ($\mu\text{g/g}$)
0	0.00	0	0.00	0	0.00	0	0.00
0.5	35.94	0.5	207.54	0.5	50.99	0.5	102.64
2	117.09	1	191.42	1	93.95	1	105.79
4	163.72	2	373.73	4	230.63	4	64.43
6	200.03	4	398.69	6	239.72	4	81.87
8	257.56	6	420.82	8	335.96	6	66.28
10	306.88	8	435.74	10	353.11	8	30.796
12	349.65	10	451.97	12	384.64	12	82.18
15	380.19	12	496.92	15	393.78	15	50.52
20	388.59	15	488.60	20	403.95	20	21.69
24	401.50	20	499.77	24	413.92		

Table 1.2 Data from adsorption kinetic of DCAN, TCM, TCA, and DCAA on GAC at pH 7 and IS 10 mM

DCAN		TCM		TCA		DCAA	
Time (h)	q_t ($\mu\text{g/g}$)	Time (h)	q_t ($\mu\text{g/g}$)	Time (h)	q_t ($\mu\text{g/g}$)	Time (h)	q_t ($\mu\text{g/g}$)
0	0	0	0.00	0	0.00	0	0.00
0.5	68.56	0.5	193.43	1	172.59	1	31.20
1	119.79	1	276.68	2	222.06	6	73.51
2	148.05	2	268.42	6	269.12	10	6.77
4	187.40	6	361.06	8	308.51	15	20.04
6	266.32	8	353.82	10	313.24	20	18.36
8	312.54	10	394.52	12	332.28	24	9.50
10	326.64	12	397.52	15	338.07	28	5.15
12	335.97	15	386.97	20	343.19	36	56.45
15	355.40	20	399.97	24	334.33		
20	376.79	24	400.81				
28	372.22						

Figure 1.1 showed adsorption kinetic of DCAN, TCM, TCA, and DCAA on AL:NR/HMS-SH at pH 7 and IS 10 mM

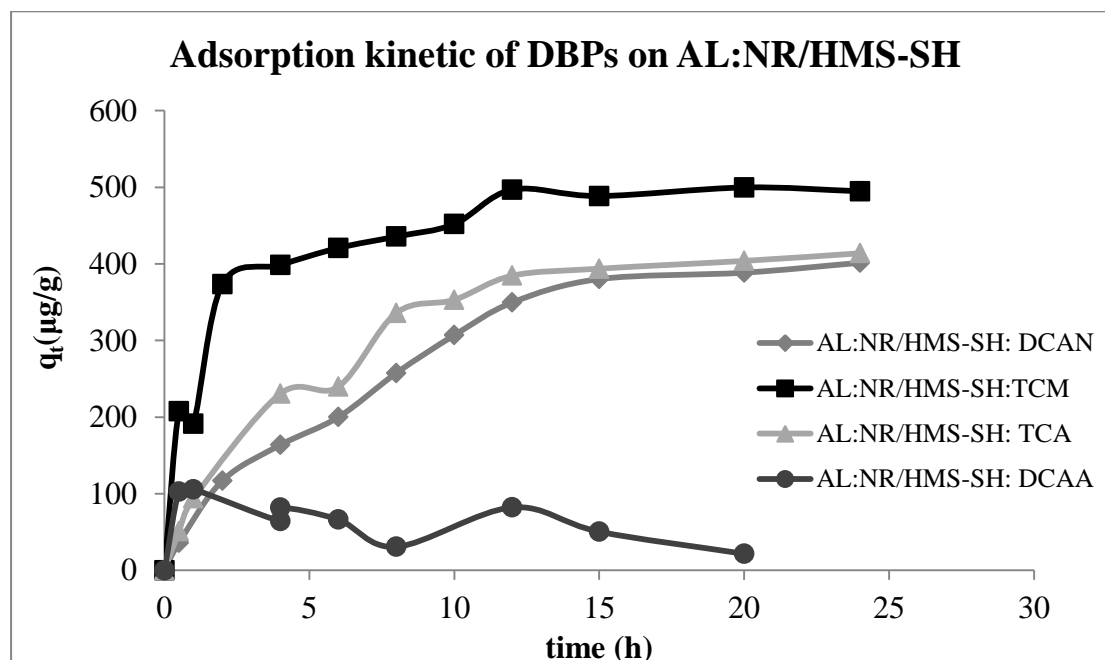


Figure 1.2 showed adsorption kinetic of DCAN, TCM, TCA, and DCAA on GAC at pH 7 and IS 10 mM

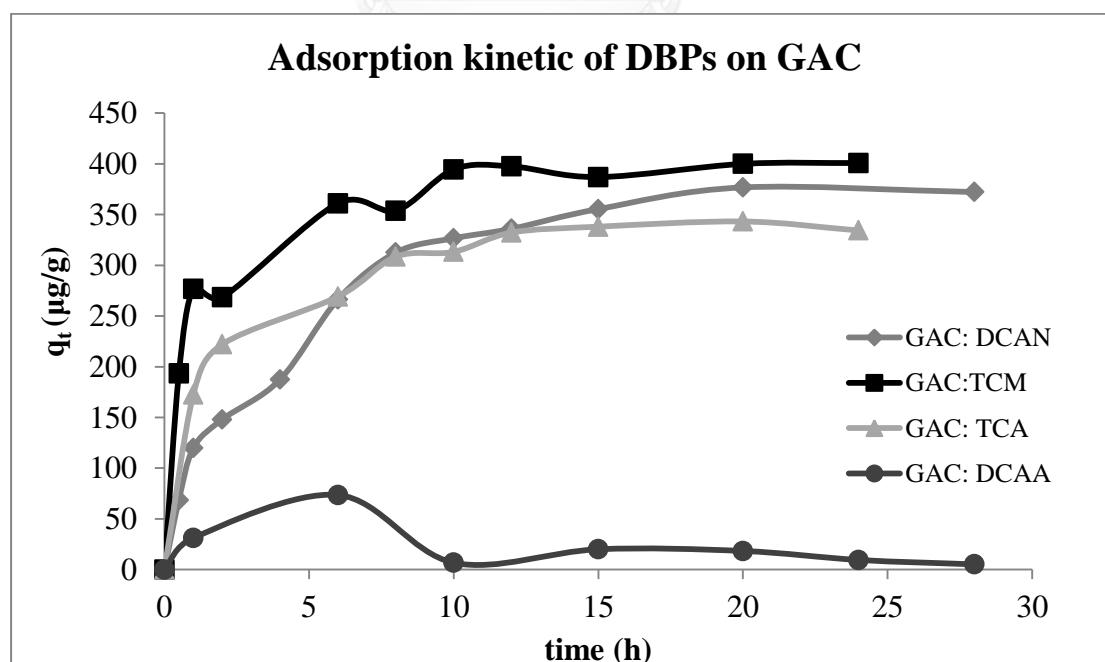
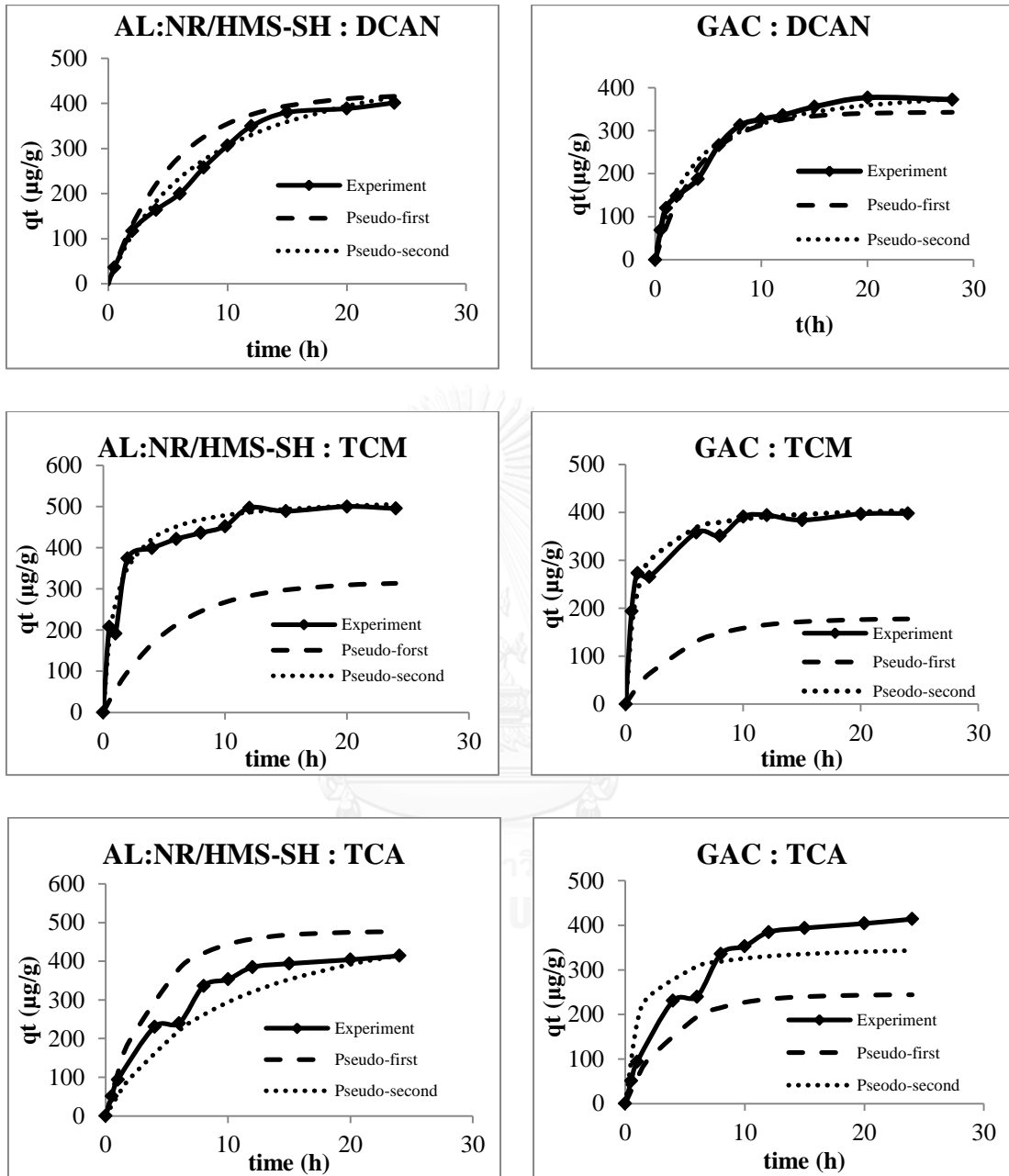


Figure 1.3 Comparison data from kinetic experiments of each DBPs and data from predicted model



2. Adsorption isotherm study

Table 2.1 Data from adsorption isotherm of three-HANs, TCM, TCA, and three-HAAs on AL:NR/HMS-SH in single solution at pH 7 and IS 10 mM

MCAN			DCAN			TCAN		
C_0 ($\mu\text{g/L}$)	C_e ($\mu\text{g/L}$)	q_e ($\mu\text{g/g}$)	C_0 ($\mu\text{g/L}$)	C_e ($\mu\text{g/L}$)	q_e ($\mu\text{g/g}$)	C_0 ($\mu\text{g/L}$)	C_e ($\mu\text{g/L}$)	q_e ($\mu\text{g/g}$)
115.81	118.82	0	50.00	12.46	70.84	88.94	24.84	149.08
245.73	254.99	0	100.00	22.96	164.61	177.64	26.89	341.05
474.84	493.36	0	200.00	41.99	331.94	303.57	28.67	670.50
720.05	741.95	0	300.00	71.44	439.54	475.44	36.21	1045.79
967.45	1011.79	0	500.00	117.20	787.65	1500.61	63.48	3044.77
1230.05	1211.52	0	700.00	173.28	1049.25	88.94	24.84	149.08
TCM			TCA			MCAA		
C_0 ($\mu\text{g/L}$)	C_e ($\mu\text{g/L}$)	q_e ($\mu\text{g/g}$)	C_0 ($\mu\text{g/L}$)	C_e ($\mu\text{g/L}$)	q_e ($\mu\text{g/g}$)	C_0 ($\mu\text{g/L}$)	C_e ($\mu\text{g/L}$)	q_e ($\mu\text{g/g}$)
250.00	4.73	484.73	50.00	23.25	68.24	47.25	0	0
500.00	28.91	1051.54	100.00	41.05	141.04	91.54	40.76	114.36
750.00	42.70	1449.39	200.00	85.13	265.90	217.44	182.46	77.04
1000.00	65.48	2359.91	300.00	130.91	414.44	345.64	285.01	123.74
1200.00	61.86	2332.26	400.00	172.77	509.48	393.73	350.32	97.34
DCAA			TCAA					
C_0 ($\mu\text{g/L}$)	C_e ($\mu\text{g/L}$)	q_e ($\mu\text{g/g}$)	C_0 ($\mu\text{g/L}$)	C_e ($\mu\text{g/L}$)	q_e ($\mu\text{g/g}$)			
55.08	42.84	15.47	40.47	39.14	2.85			
87.45	112.33	0	81.59	67.71	29.30			
194.58	222.42	0	213.61	131.56	179.93			
257.10	352.73	0	287.57	179.23	211.60			
422.61	449.48	0	351.32	220.40	285.85			

Table 2.2 Data from adsorption isotherm of three-HANs, TCM, TCA, and three-HAAs on GAC in single solution at pH 7 and IS 10 mM

MCAN			DCAN			TCAN		
C_0 ($\mu\text{g/L}$)	C_e ($\mu\text{g/L}$)	q_e ($\mu\text{g/g}$)	C_0 ($\mu\text{g/L}$)	C_e ($\mu\text{g/L}$)	q_e ($\mu\text{g/g}$)	C_0 ($\mu\text{g/L}$)	C_e ($\mu\text{g/L}$)	q_e ($\mu\text{g/g}$)
250.00	99.63	297.17	45.35	9.00	74.78	250.00	34.06	378.84
500.00	222.53	495.49	100.12	15.12	146.05	500.00	69.94	805.35
1000.00	426.94	1160.03	203.63	29.80	313.78	1000.00	88.67	1852.29
1200.00	506.02	1226.11	348.12	68.62	570.41	1200.00	92.35	2082.05
1500.00	628.24	1626.42	483.43	97.41	784.59	1750.00	149.50	2868.28
1750.00	749.42	2033.70	633.48	130.13	956.95			
2000.00	887.41	2252.19						
TCM			TCA			MCAA		
C_0 ($\mu\text{g/L}$)	C_e ($\mu\text{g/L}$)	q_e ($\mu\text{g/g}$)	C_0 ($\mu\text{g/L}$)	C_e ($\mu\text{g/L}$)	q_e ($\mu\text{g/g}$)	C_0 ($\mu\text{g/L}$)	C_e ($\mu\text{g/L}$)	q_e ($\mu\text{g/g}$)
200.00	4.33	391.35	50.00	17.37	62.99	40.47	39.14	2.85
500.00	13.57	957.53	100.00	24.49	125.84	81.59	67.71	29.30
750.00	24.67	1358.29	200.00	53.55	270.20	213.61	131.56	179.93
1000.00	25.81	1940.62	400.00	114.34	575.93	287.57	179.23	211.60
1200.00	37.09	2354.07	500.00	144.35	683.94	351.32	220.40	285.85
1500.00	63.21	2503.13	700.00	202.05	935.99			
1750.00	71.37	2528.06						
DCAA			TCAA					
C_0 ($\mu\text{g/L}$)	C_e ($\mu\text{g/L}$)	q_e ($\mu\text{g/g}$)	C_0 ($\mu\text{g/L}$)	C_e ($\mu\text{g/L}$)	q_e ($\mu\text{g/g}$)			
55.97	55.08	1.67	40.47	32.76	15.00			
87.45	82.34	10.78	81.60	51.30	60.83			
207.53	194.58	26.98	213.61	112.50	214.22			
303.77	257.11	87.05	287.57	143.58	315.78			
471.30	422.61	96.22	499.04	191.07	641.62			

Figure 2.1 Adsorption isotherm of three-HANs, TCM, TCA, and three-HAAs on AL:NR/HMS-SH in single solution at pH 7 and IS 10 mM

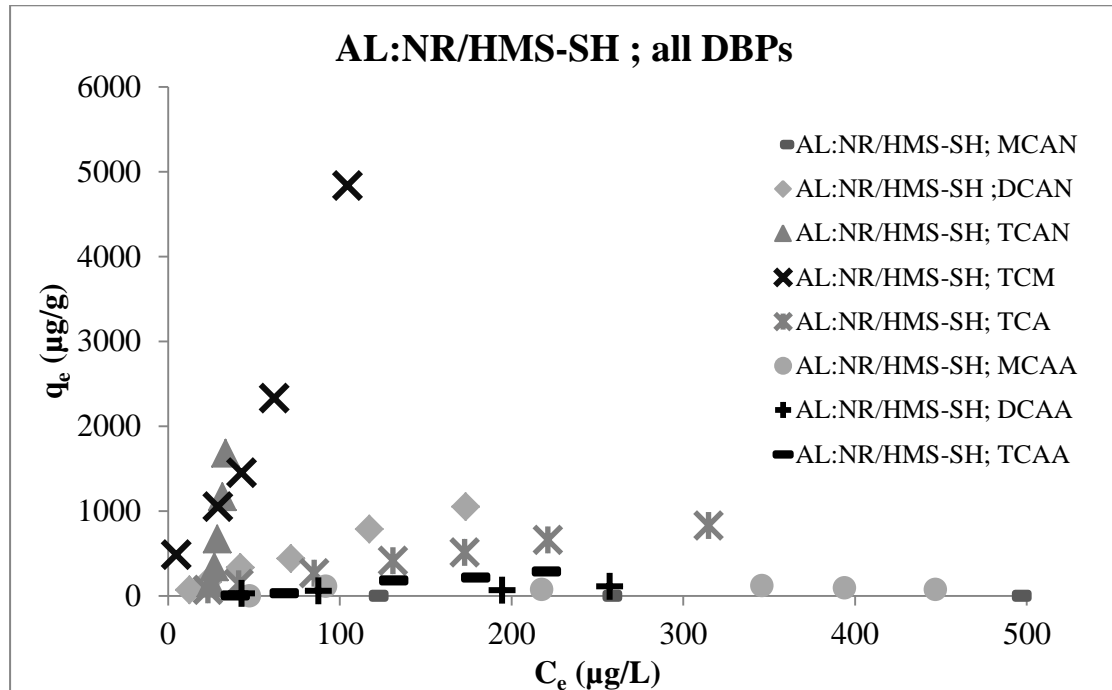
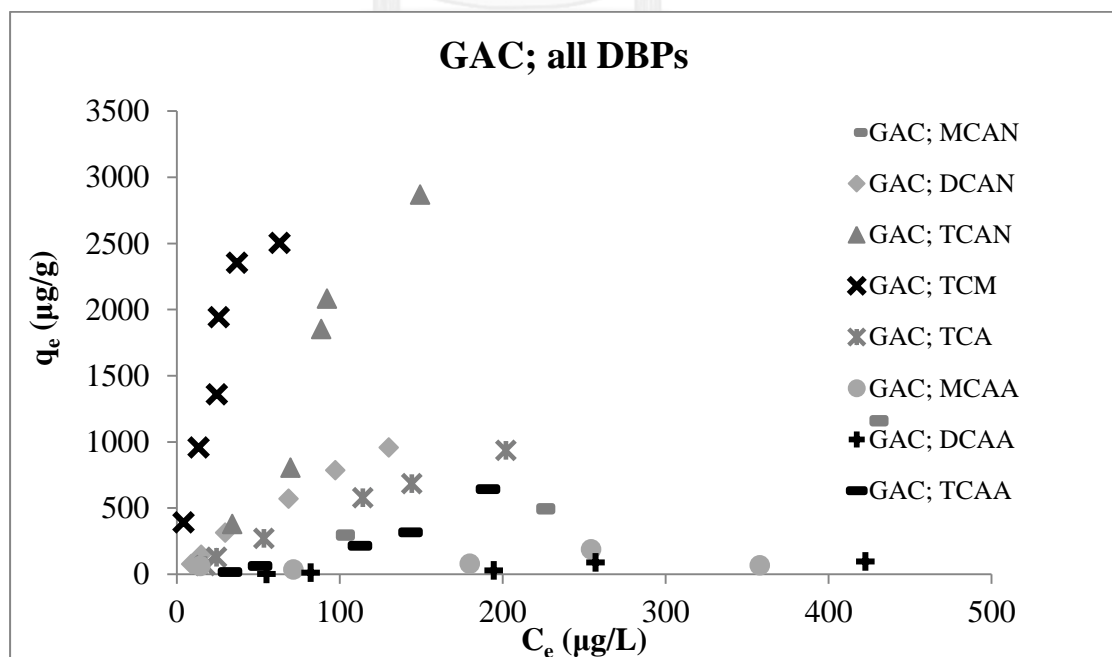


Figure 2.2 Adsorption isotherm of three-HANs, TCM, TCA, and three-HAAs on GAC in single solution at pH 7 and IS 10 mM



3. Selectivity of adsorption

Table 3.1 Data from adsorption isotherms of four DBPs on AL:NR/HMS-SH in mixed solution at pH 7 and IS 10 mM

DCAN			TCM			TCA		
C_0 ($\mu\text{g/L}$)	C_e ($\mu\text{g/L}$)	q_e ($\mu\text{g/g}$)	C_0 ($\mu\text{g/L}$)	C_e ($\mu\text{g/L}$)	q_e ($\mu\text{g/g}$)	C_0 ($\mu\text{g/L}$)	C_e ($\mu\text{g/L}$)	q_e ($\mu\text{g/g}$)
49.89	33.35	33.47	38.03	25.59	25.18	44.31	27.96	33.10
99.14	59.90	84.21	93.73	38.79	117.90	100.39	56.98	93.16
186.38	112.65	151.72	149.02	80.05	141.91	180.01	99.30	166.07
270.93	164.62	208.45	222.40	95.08	249.65	260.52	140.84	234.66
432.38	285.43	297.45	367.74	101.22	539.51	422.73	242.94	363.95
624.68	387.25	471.10	467.60	105.77	717.92	532.42	292.51	476.02
DCAA								
C_0 ($\mu\text{g/L}$)	C_e ($\mu\text{g/L}$)	q_e ($\mu\text{g/g}$)						
80.60	74.14	13.07						
158.72	150.08	18.53						
305.90	265.74	82.64						
1058.87	1003.48	109.90						

Table 3.2 Data from adsorption isotherms of four DBPs on GAC in mixed solution at pH 7 and IS 10 mM

DCAN			TCM			TCA		
C_0 ($\mu\text{g/L}$)	C_e ($\mu\text{g/L}$)	q_e ($\mu\text{g/g}$)	C_0 ($\mu\text{g/L}$)	C_e ($\mu\text{g/L}$)	q_e ($\mu\text{g/g}$)	C_0 ($\mu\text{g/L}$)	C_e ($\mu\text{g/L}$)	q_e ($\mu\text{g/g}$)
49.89	15.36	59.73	38.03	20.22	30.81	44.31	16.26	48.52
99.14	36.84	108.15	93.73	26.20	117.24	100.39	37.35	109.44
186.38	57.13	242.95	149.02	39.47	205.91	180.01	62.77	220.37
270.93	76.59	401.53	222.40	63.21	328.92	260.52	107.25	316.67
432.38	181.45	452.94	367.74	126.65	435.18	422.73	195.23	410.66
624.68	331.58	512.40	467.60	146.34	561.65	532.42	267.65	462.90
DCAA								
C_0 ($\mu\text{g/L}$)	C_e ($\mu\text{g/L}$)	q_e ($\mu\text{g/g}$)						
80.60	40.38	81.42						
158.72	112.01	100.25						
305.90	216.79	183.37						
414.15	344.70	136.19						
1058.87	876.04	362.75						

4. Effect of NOM on DCAN adsorption

Table 4.1 TOC of initial NOM, HPI and HPO NOM after fractionated #1 and #2

#1	DOC (mg/L)	DOC(mg/L)
Raw	2.759	2.759
HPI	2.731	2.731
HPO	2.456	0.246
HPI + HPI		2.977

#2	DOC (mg/L)	DOC(mg/L)
Raw	2.759	2.759
HPI	2.641	2.747
HPO	2.208	0.230
		2.977

Table 4.2 Mass balance calculation of NOM fractionation #1 and #2

Parameter #1	Fractionated water		HPI+HPO	Unfractionated water	% Diff
	HPI	HPO			
Mass DOC (mg)	13.66	1.23	14.88	13.80	7.31
%DOC mass	91.75	8.25	100	-	-
DOC (mg/L)	2.731	2.456	-	2.759	-
Cal Conc.	2.731	0.246	2.98	2.76	-
Dilution (100 ml)	100	10	-	-	-

Parameter #2	Fractionated water		HPI+HPO	Unfractionated water	% Diff
	HPI	HPO			
Mass DOC (mg)	13.21	1.10	14.31	13.80	3.59
%DOC mass	92.28	7.72	100	-	-
DOC (mg/L)	2.641	2.208	-	2.759	-
Cal Conc.	2.747	0.230	2.86	2.76	-
Dilution (100 ml)	104.01	10.40	-	-	-

Table 4.3 Data from adsorption isotherm of DCAN in NOM solution

DCAN in Tab water			DCAN with HPI NOM			DCAN with HPO NOM		
C_0 ($\mu\text{g/L}$)	C_e ($\mu\text{g/L}$)	q_e ($\mu\text{g/g}$)	C_0 ($\mu\text{g/L}$)	C_e ($\mu\text{g/L}$)	q_e ($\mu\text{g/g}$)	C_0 ($\mu\text{g/L}$)	C_e ($\mu\text{g/L}$)	q_e ($\mu\text{g/g}$)
30.85	16.93	33.95	43.54	30.99	31.53	35.53	37.49	0.00
54.29	21.42	82.17	73.29	50.78	55.47	59.96	62.59	0.00
94.07	32.91	149.18	156.96	96.34	150.78	113.95	103.24	0.00
133.70	38.80	244.60	214.90	137.54	192.44	156.56	162.41	0.00
214.63	60.40	379.89	333.14	205.59	317.28	255.73	256.79	0.00
30.85	16.93	33.95	43.54	30.99	31.53	35.53	37.49	0.00

Table 4.4 Data of organic carbon NOM in the solution before and after adsorption

TOC of Tab water		TOC of HPI NOM		TOC of HPO NOM	
Before adsorption (mg/L)	After adsorption (mg/L)	Before adsorption (mg/L)	After adsorption (mg/L)	Before adsorption (mg/L)	After adsorption (mg/L)
2.83	2.80	3.23	3.41	3.14	1.57
2.80	2.76	3.29	3.17	3.00	1.50
2.91	2.91	3.23	3.23	3.14	1.36
2.83	2.87	3.17	3.10	3.07	1.43
2.91	2.91	3.10	3.17	3.14	1.43
2.83	2.80	3.23	3.41	3.14	1.57

5. Adsorption of DCAN on fixed bed condition

Table 5.1 Data from adsorption of DCAN on fixed bed column at pH 7 and IS 10 mM

Bed depth 10 cm			Bed depth 13 cm		
Time (h)	C ($\mu\text{g/L}$)	C/C_0	Time (h)	C ($\mu\text{g/L}$)	C/C_0
Initial conc.	27.56	-	Initial conc.	24.73	-
0	0.38	0.014954	0	0.26	0.010589567
2	0.04	0.001553	1	0.072	0.002891604
3	0.03	0.000932	2	0.00	0.00
5	0.030	0.001101	3	0.00	0.00
8	0.25	0.009198	6	0.00	0.00
12	1.82	0.06602	9	0.00	0.00
16	5.03	0.182404	13	0.00	0.00
20	8.71	0.315896	16	0.00	0.00
24	8.99	0.326368	20	0.00	0.00
28	9.10	0.330164	24	0.09	0.003699091
34	9.67	0.350809	28	1.14	0.0461265
40	8.71	0.315872	32	6.12	0.247570268
46	8.93	0.324143	38	8.40	0.339787325
			42	9.31	0.37637886
			46	9.39	0.379652491
			52	9.71	0.392805674

VITA

Miss Dollaya Buaoui was born on May 17, 1991 in Saraburi province. She graduated Bachelor's degree of Science of Chemistry from Department of Chemistry, the Faculty of Science, Chulalongkorn University in 2012 . She continue studied Master degree in the International Program in Environmental Management, Chulalongkorn University in 2013.

